

**Cairo University
Faculty of Engineering**

Aerospace Engineering Department

4th Year, Second term

**AER 408 : Aerospace Guidance and Control Systems
Autopilot Project**

Submitted to:Dr.Osama
Eng.Hassan ali
Eng.

By:

Abrar abdelGwad	Sec:01	BN:02
Bahgat Ahmed	Sec:01	BN:23
rowida kamal eldin	Sec:01	BN:28
Famta khalil	Sec:02	BN:03
Mohamed Mansour	Sec:02	BN:20

Contents

1	Introduction	6
1.1	Autopilot in UAVs	6
1.1.1	Hardware	6
1.1.2	Software	7
1.2	Autopilot in a manned aircraft	8
1.3	How exactly does Autopilot work?	8
2	Airplane Equation of motion	8
2.1	Velocity of Aircraft in the fixed frame	9
2.2	Angular Velocity in body frame	9
2.3	Force equations	9
2.4	Moment equations	10
3	Linearized equation of motion	10
3.1	Linearized longitudinal equation	10
3.2	Linearized lateral equation	11
4	Algorithm of numerical solution for nonlinear system of differential equations	11
4.1	Runge-Kutta Method 4th Order	12
4.2	Algorithm flow chart	12
5	Results of nonlinear simulation	12
5.1	Comparison with the TA's results using his submitted data	13
5.1.1	Firstly: Aircraft Data	13
5.1.2	Secondly: Results with different inputs	14
6	Linearized equations of motion solution	20
6.1	Longitudinal motion	20
6.2	Longitudinal Approximations	21
6.2.1	Short Period Approximation	21
6.2.2	Long Period Approximation	21
6.2.3	Results (Using TA's airplane)	21
6.3	Lateral motion	61
6.3.1	Introduction (Lateral Modes)	61
6.3.2	Our new Airplane Data (Boeing 747)	65
6.4	Approximations	67
6.4.1	Three degrees of freedom :	67
6.4.2	Two degrees of freedom :	67
6.4.3	One degree of freedom	67
6.4.4	Transfer Functions	67
6.5	Response	68
6.6	Bode Plot & Root Locus	83
6.6.1	From Transfer Function of Aileron Input	83
6.6.2	From Transfer Function of Rudder Input	87
7	Autopilot	91
7.1	Autopilot longitudinal control	91
7.1.1	Level Flight	91
7.1.2	Flight Qualities	92
7.1.3	Thrust from Airspeed:	93
7.1.4	Elevator from pitch and pitch from Altitude:	94
7.2	1- Re design the controller implemented before:	96
7.3	Re-design of the pitch from altitude :	103
7.4	Re-design of the pitch from altitude (using SISO tool):	105

7.5	Implementing controller on nonlinear model	109
8	References	111

List of Tables

List of Figures

1	An autopilot already connected to all sensors and ready-to-use	6
2	The 9-dof Razor IMU,It contains also a triple-axis magnetometer to increase accuracy	7
3	GPS Module for UAV	7
4	Autopilot Control System	8
5	Solution Flow chart	12
6	Steady State (No inputs): ($\theta_0 = 2.7^\circ$)	14
7	Steady State (No inputs): ($\theta_0 = 10^\circ$)	15
8	For ($\delta_e = -5^\circ$)	16
9	For ($\delta_r = 5^\circ$)	17
10	For ($\delta_a = 5^\circ$)	18
11	For ($\delta_t = 20$)	19
12	21
13	22
14	22
15	23
16	23
17	24
18	24
19	25
20	25
21	26
22	26
23	27
24	27
25	28
26	28
27	29
28	29
29	30
30	30
31	31
32	31
33	32
34	32
35	33
36	33
37	34
38	34
39	35
40	35
41	36
42	36
43	37
44	37
45	38
46	38

47	.	39
48	.	39
49	.	40
50	.	40
51	.	41
52	.	41
53	.	42
54	.	42
55	.	43
56	.	43
57	.	44
58	.	44
59	.	45
60	.	45
61	.	46
62	.	46
63	.	47
64	.	47
65	.	48
66	.	48
67	.	49
68	.	49
69	.	50
70	.	50
71	.	51
72	.	51
73	.	52
74	.	52
75	.	53
76	.	53
77	.	54
78	.	54
79	.	55
80	.	55
81	.	56
82	.	56
83	.	57
84	.	57
85	.	58
86	.	58
87	.	59
88	.	59
89	.	60
90	.	60
91	.	61
92	Roll	62
93	Spiral	62
94	P	69
95	r	69
96	β	70
97	ϕ	70
98	P	71
99	r	71
100	β	71
101	ϕ	72

102	P	72
103	r	72
104	β	73
105	ϕ	73
106	P	73
109	ϕ	74
107	r	74
108	β	74
110	P	75
111	r	75
113	ϕ	76
112	β	76
114	P	77
115	r	77
116	β	78
117	ϕ	78
118	P	79
119	r	79
121	ϕ	80
120	β	80
122	P	81
123	r	81
124	β	82
125	ϕ	82
126	$\frac{\beta}{\delta_a}$	83
127	Rott locus for $\frac{\beta}{\delta_a}$	83
128	bode polt for $\frac{P}{\delta_a}$	84
129	Root locus For $\frac{P}{\delta_a}$	85
130	bode polt for $\frac{r}{\delta_a}$	85
131	Root locus For $\frac{r}{\delta_a}$	86
132	bode polt for $\frac{\phi}{\delta_a}$	86
133	Root locus for $\frac{\phi}{\delta_a}$	87
134	$\frac{\beta}{\delta_a}$	87
135	Rott locus for $\frac{\beta}{\delta_r}$	88
136	bode polt for $\frac{P}{\delta_r}$	88
137	Root locus For $\frac{P}{\delta_r}$	89
138	bode polt for $\frac{r}{\delta_r}$	89
139	Root locus For $\frac{r}{\delta_a}$	90
140	Bode plot for $\frac{\phi}{\delta_r}$	90
141	Root locus for $\frac{\phi}{\delta_r}$	91
142	Level Flight AP	92
143	damping and % O.S.	93
144	Thrust from airspeed	93
145	PID Controller	93
146	Thrust from Airspeed Response	94
147	Thrust from Airspeed characteristics	94
148	Elevator from pitch and pitch from Altitude control loop	94
149	Calculating PID for the θ loop	95
150	θ loop PID gains	95
151	θ loop response	95
152	Outer loop PID gains	96
153	Outer loop PID response	96
154	Outer loop response characteristics	96

155	97
156	98
157	98
158	99
159	99
160	100
161	101
162	101
163	102
164	102
165	104
166	104
167	105
168	The diplacement Autopilot using the velocity feedback	105
169	Simulink new full-model	105
170	SISO on inner most loop	106
171	SISO second inner loop	107
172	SISO second inner loop after adding complex zeros	107
173	SISO second inner loop after adding complex zeros and gain	108
174	SISO outer open loop	109
175	SISO second inner loop after adding complex zeros and gain	109

1 Introduction

An autopilot is a system used to make the airplane go on a certain flight path with little need to manual control from the pilot. Autopilots do not replace human operators but assist them in controlling aircraft by automating some pilots functions, allowing them to focus on broader aspects of operations such as monitoring the trajectory, weather and systems.

The common thought that the autopilot is only applied on UAVs (Unmanned Arial Vehicles), but it is also used in manned aircraft as a system not a pilot as there is in UAV. In the next section we will show the difference between autopilot in UAV and manned aircraft.

1.1 Autopilot in UAVs

1.1.1 Hardware

This part is the part with the processor and sensors to receive data during flight and processing it to decide the best command for the airplane.

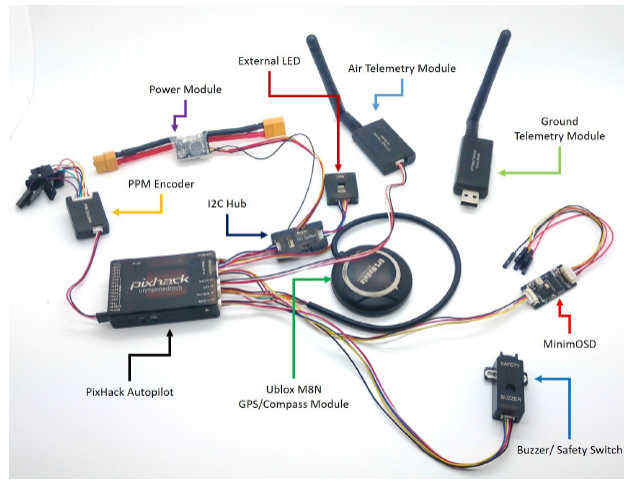


Figure 1: An autopilot already connected to all sensors and ready-to-use

The sensors will be integrated in the IMU (inertial measurement unit) which consists of a collection of gyroscopes and accelerometers. Gyroscopes detect changes in the orientation of airplane from a reference position during the whole flight while linear and angular accelerometers measure the non-gravitational accelerations of the airplane and also the rate by which the airplane rotates in any direction, we have 3 accelerometers for each axis (Rolling, pitching and yawing).

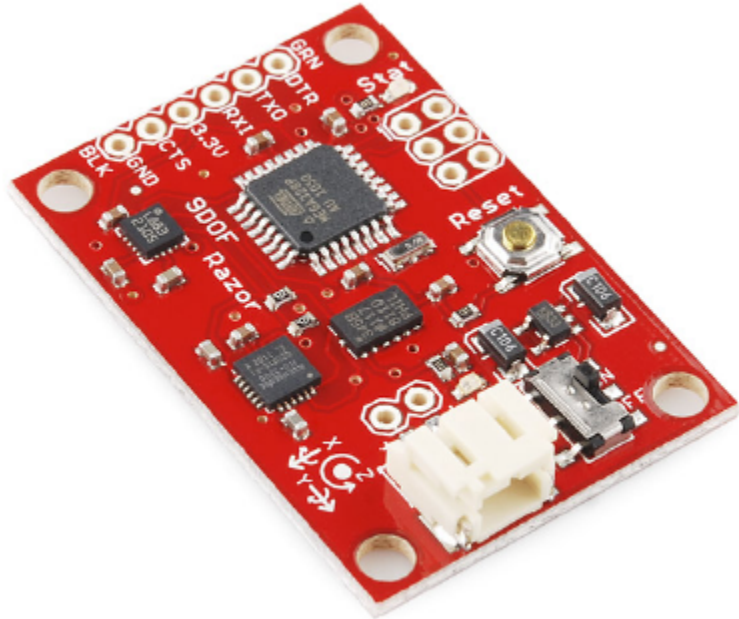


Figure 2: The 9-dof Razor IMU,It contains also a triple-axis magnetometer to increase accuracy

We will also need an airspeed sensor to measure the speed of the airplane and sensors for measuring the angle of attack and side slip angle. A GPS is also needed to locate the airplane during flight and to calculate the altitude of the airplane at every instant of flight.

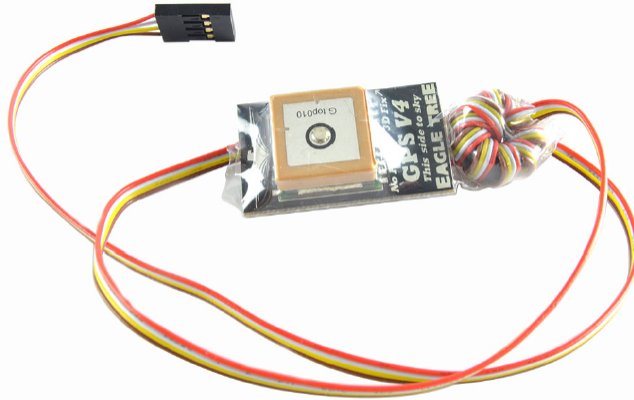


Figure 3: GPS Module for UAV

1.1.2 Software

That is the part were the computer is used to generate the code by which the processor will control the airplane and give suitable command to sustain a steady flight. By solving the airplane equations of motion we can predict the suitable motion for any disturbance that can occur during flight and counteract it so the airplane can return to a stable state, this process of detecting disturbances and continuously correcting it is what an autopilot do until the end of the mission. A telemetry can be used(optional) to connect the airplane to the ground control station, It consists of two part, a part connected to the airplane and another to the PC or tablet where you can control the airplane. The data from the airspeed sensors and angle are then used by Kalman Filter to correct the readings of the IMU to reduce the accumulated error in those readings

1.2 Autopilot in a manned aircraft

An autopilot is an example of a control system. Control systems apply an action based on a measurement and almost always have an impact on the value they are measuring. In the world of aircraft, the autopilot is more accurately described as the automatic flight control system (AFCS). An AFCS is part of an aircraft's avionics. The original use of an AFCS was to provide pilot relief during tedious stages of flight, such as high-altitude cruising. Advanced autopilots can do much more, carrying out even highly precise maneuvers, such as landing an aircraft in conditions of zero visibility. There are three levels of control in autopilots for smaller aircraft. A single-axis autopilot controls an aircraft in the roll axis only. A two-axis autopilot controls an aircraft in the pitch axis as well as roll. A three-axis autopilot adds control in the yaw axis and is not required in many small aircraft.

1.3 How exactly does Autopilot work?

Autopilot refers to a collection of systems that automate a plane's operations. The complex computer matrix tells your plane how to fly, including navigation, altitude, speed, and engine thrust, which controls the force by which the plane moves through the air. When these systems are engaged—after a human enters the flight destination information, autopilot culls data about the flight route, location, and navigation—the navigation harnesses the same GPS technology that's on your cell phone and spits out an optimized flight plan. This allows the pilot to remain hands-free for the duration of the flight. The system itself works on a negative feedback loop, which means it receives data from the aircraft's various mechanisms and responds by inhibiting a particular action in response to another action. For instance, the autopilot is set to maintain the aircraft in a level position. If the wings are no longer level, the autopilot receives data telling it that, and it activates to correct the problem. Once the wings are level, the loop closes and that communication essentially stops. This repeats with all of the functions of a plane in flight including steering, speed, altitude, and more. All of this is done without the pilot lifting a finger, although they are monitoring closely to mind for any issues or inconsistencies.

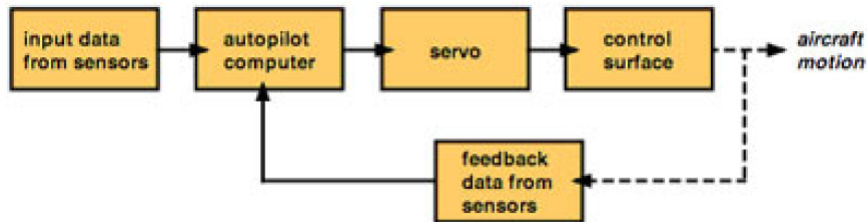


Figure 4: Autopilot Control System

2 Airplane Equation of motion

The rigid body equation of motion are obtained from newton's second law, which states that : The summation of all external forces acting on a body is equal to the time rate of change of the momentum of the body; and the summation of the external moments acting on the body is equal to the time rate of change of the moments of the momentum (angular momentum).

Newton's second law can be expressed in the following vector equation:

$$\sum F = \frac{d}{dt}(mv) \quad (1)$$

$$\sum M = \frac{d}{dt}(H) \quad (2)$$

where

mv :is the momentum and H :is the moment of momentum.

$$H = \sum r\delta m \times V_c + \sum [r \times (\omega \times r)] \delta m \quad (3)$$

If we express the angular velocity and position vector as:

$$\omega = p i + q j + r k \quad (4)$$

$$r = x i + y j + z k \quad (5)$$

then eqn(??)can be written in vector form as:

$$H = (p i + q j + r k) \sum (x^2 + y^2 + z^2) \delta m - \sum (x i + y j + z k) (px + qy + rz) \delta m \quad (6)$$

The equation of motion have been derived for an axis system fixed to the airplane. Unfortunately,the position and orientation of the airplane cannot be described relative to the moving body axis frame.

The position and orientation of the airplane can be defined in terms of a fixed frame of reference.

The orientation of the airplane can be described by three consecutive rotations,whose order is important.

1. Rotate the x_f, y_f, z_f frame about $0Z_f$ through the yaw angle ψ to the frame to x_1, y_1, z_1 .
2. Rotate the x_1, y_1, z_1 frame about $0Y_1$ through the pitch angle Θ to bringing the frame to x_2, y_2, z_2
3. Rotate the x_2, y_2, z_2 frame about $0x_2$ through the roll angle Φ to bringing the frame to x_3, y_3, z_3 ,the actual orientation of the body frame relative to the fixed frame.

Having defined the Euler angles ,one can determine the velocity components relative to the fixed reference frame.To accomplish this,let the velocity components along the x_f, y_f, z_f frame be $\frac{dx}{dt}, \frac{dy}{dt}, \frac{dz}{dt}$.

Finally we can get the absolute velocity in terms of the Euler angles and velocity components in the body frame:

2.1 Velocity of Aircraft in the fixed frame

$$\begin{bmatrix} \frac{dx}{dt} \\ \frac{dy}{dt} \\ \frac{dz}{dt} \end{bmatrix} = \begin{bmatrix} C_\theta C_\psi & S_\Phi S_\theta C_\psi - C_\Phi C_\psi & C_\Phi S_\theta c\psi + S_\Phi S_\psi \\ C_\theta S_\psi & S_\Phi S_\theta S_\psi + C_\Phi C_\psi & C_\Phi S_\theta S_\psi - S_\Phi C_\psi \\ -S_\theta & S_\theta C_\theta & C_\Phi C_\theta \end{bmatrix} \begin{bmatrix} u \\ v \\ w \end{bmatrix} \quad (7)$$

2.2 Angular Velocity in body frame

$$\begin{bmatrix} p \\ q \\ r \end{bmatrix} = \begin{bmatrix} 1 & 0 & -S_\theta \\ 0 & C_\Phi & C_\theta S_\Phi \\ 0 & -S_\Phi & C_\theta C_\Phi \end{bmatrix} \begin{bmatrix} \Phi \\ \Theta \\ \Psi \end{bmatrix} \quad (8)$$

2.3 Force equations

$$X - mgS_\theta = m(u + qw - rv) \quad (9)$$

$$Y + mgC_\theta S_\phi = m(v + ru + pw) \quad (10)$$

$$Z + mgC_\theta C_\phi = m(w + pv - qu) \quad (11)$$

2.4 Moment equations

$$L = I_x p \cdot - I_{xz} r \cdot + qr(I_z - I_y) - I_{xz} pq \quad (12)$$

$$M = I_y q \cdot + rq(I_x - I_z) + I_{xz}(p^2 - r^2) \quad (13)$$

$$N = -I_{xz} p \cdot + I_z r \cdot + pq(I_y - I_x) + I_{xz} qr \quad (14)$$

3 Linearized equation of motion

The equation developed in the previous section are non linear equation can be linearized using small disturbance theory,we assume that the motion of the airplane consists of small deviations about a steady flight condition.

Obviously ,this theory cannot be applied to problems in which large-amplitude motions are to be expected (e.g.,spinnong or stalled flight).However, in many cases the small -disturbance theory yields sufficient accuracy for practical engineering purposes.

All the variables in the equations of motion are replaced by a reference value plus a perturbation or disturbance:

$$\begin{aligned} u &= u_0 + \Delta u & v &= v_0 + \Delta v & w &= w_0 + \Delta w \\ p &= p_0 + \Delta p & q &= q_0 + \Delta q & r &= r_0 + \Delta r \\ X &= X_0 + \Delta X & Y &= Y_0 + \Delta Y & Z &= Z_0 + \Delta Z \\ M &= M_0 + \Delta M & N &= N_0 + \Delta N & L &= L_0 + \Delta L \\ \delta &= \delta_0 + \Delta \delta \end{aligned}$$

where:

$$\begin{aligned} \Delta X &= \frac{\partial X}{\partial u} \Delta u + \frac{\partial X}{\partial w} \Delta w + \frac{\partial X}{\partial \delta_e} \Delta \delta_e + \frac{\partial X}{\partial \delta_T} \Delta \delta_T \\ \Delta Y &= \frac{\partial Y}{\partial v} \Delta v + \frac{\partial Y}{\partial p} \Delta p + \frac{\partial Y}{\partial r} \Delta r + \frac{\partial Y}{\partial \delta_r} \Delta \delta_r \\ \Delta Z &= \frac{\partial Z}{\partial u} \Delta u + \frac{\partial Z}{\partial w} \Delta w + \frac{\partial Z}{\partial \dot{w}} \Delta \dot{w} + \frac{\partial Z}{\partial p} \Delta p + \frac{\partial Z}{\partial \delta_e} \Delta \delta_e + \frac{\partial Z}{\partial \delta_T} \Delta \delta_T \\ \Delta L &= \frac{\partial L}{\partial v} \Delta v + \frac{\partial L}{\partial p} \Delta p + \frac{\partial L}{\partial r} \Delta r + \frac{\partial L}{\partial \delta_r} \Delta \delta_r + \frac{\partial L}{\partial \delta_a} \Delta \delta_a \\ \Delta M &= \frac{\partial M}{\partial u} \Delta u + \frac{\partial M}{\partial w} \Delta w + \frac{\partial M}{\partial \dot{w}} \Delta \dot{w} + \frac{\partial M}{\partial q} \Delta q + \frac{\partial M}{\partial \delta_e} \Delta \delta_e + \frac{\partial M}{\partial \delta_T} \Delta \delta_T \\ \Delta N &= \frac{\partial N}{\partial v} \Delta v + \frac{\partial N}{\partial p} \Delta p + \frac{\partial N}{\partial r} \Delta r + \frac{\partial N}{\partial \delta_r} \Delta \delta_r + \frac{\partial N}{\partial \delta_a} \Delta \delta_a \end{aligned}$$

For convenience, the reference flight condition is assumed to be symmetric and the propulsive forces are assumed to remain constant .This implies that

$$v_0 = p_0 = q_0 = r_0 = \Phi_0 = \psi_0 = 0$$

Furthermore , if we initially align the x axis so that it is along the direction of the airplane's velocity ,then $w_0 = 0$

then finally we get:

3.1 Linearized longitudinal equation

$$\begin{bmatrix} \Delta \dot{u} \\ \Delta \dot{w} \\ \Delta \dot{q} \\ \Delta \dot{\theta} \end{bmatrix} = \begin{bmatrix} X_u & X_w & 0 & -g \\ Z_u & Z_w & u_0 & 0 \\ M_u + M_{\dot{w}} Z_u & M_w + M_{\dot{w}} Z_w & M_q + M_{\dot{w}} u_0 & 0 \\ 0 & 0 & 1 & 0 \end{bmatrix} \begin{bmatrix} \Delta u \\ \Delta w \\ \Delta q \\ \Delta \theta \end{bmatrix} + \begin{bmatrix} X_\delta & X_{\delta T} \\ Z_\delta & Z_{\delta T} \\ M_\delta + M_{\dot{w}} Z_\delta & M_{\delta T} + M_{\dot{w}} Z_{\delta T} \\ 0 & 0 \end{bmatrix} \begin{bmatrix} \Delta \delta \\ \Delta \delta_T \end{bmatrix}$$

3.2 Linearized lateral equation

$$\begin{aligned} & \cdot \left(\frac{d}{dt} - Y_v \right) \Delta v - Y_p \Delta p + [u_o - Y_r] \Delta r - g \cos \theta_o \Delta \varphi = Y_{\delta_r} \Delta \delta r \\ & - L_v \Delta v + \left(\frac{d}{dt} - L_p \right) \Delta p - \left(\frac{I_{xz}}{I_x} \frac{d}{dt} + L_r \right) \Delta r = L_{\delta_r} \Delta \delta r + L_{\delta_a} \Delta \delta a \\ & - N_v \Delta v - \left(\frac{I_{xz}}{I_z} \frac{d}{dt} + N_p \right) \Delta p + \left(\frac{d}{dt} - N_r \right) \Delta r = N_{\delta_r} \Delta \delta r + N_{\delta_a} \Delta \delta a \end{aligned}$$

4 Algorithm of numerical solution for nonlinear system of differential equations

1. By knowing the initial flight conditions, aircraft data, stability derivatives and inputs for control surfaces. We can substitute in the forces and moments equations and get their initial values.

Force equations:

$$\begin{aligned} X - mgS_\theta &= m(u \cdot + qw - rv) \\ Y + mgC_\theta S_\phi &= m(v \cdot + ru + pw) \\ Z \cdot + mgC_\theta C_\phi &= m(w \cdot + pv - qu) \end{aligned}$$

Moment equations:

$$\begin{aligned} L &= I_x p \cdot - I_{xz} r \cdot + qr(I_z - I_y) - I_{xz} pq \cdot \\ M &= I_y q \cdot + rq(I_x - I_z) + I_{xz}(p^2 - r^2) \\ N &= -I_{xz} p \cdot + I_z r \cdot + pq(I_y - I_x) + I_{xz} qr \cdot \end{aligned}$$

2. After calculating the initial values of the forces and moments, we can substitute in the equations of motion and get the initial values of $(u \cdot, v \cdot, w \cdot, p \cdot, q \cdot, r \cdot)$.

$$\begin{aligned} \dot{u} &= X/m - g \sin \theta + rv - qw \\ \dot{v} &= Y/m + g \cos \theta \sin \phi + pw - ru \\ \dot{w} &= Z/m + g \cos \theta \cos \phi + qu - pv \\ \dot{p} &= (I_{zz}L + I_{xz}N - \{I_{xz}(I_{yy} - I_{xx} - I_{zz})p + [I_{xz}^2 + I_{zz}(I_{zz} - I_{yy})]r\}q) / (I_{xx}I_{zz} - I_{xz}^2) \\ \dot{q} &= [M - (I_{xx} - I_{zz})pr - I_{xz}(p^2 - r^2)] / I_{yy} \\ \dot{r} &= (I_{xz}L + I_{xx}N - \{I_{xz}(I_{yy} - I_{xx} - I_{zz})r + [I_{xz}^2 + I_{xx}(I_{xx} - I_{yy})]p\}q) / (I_{xx}I_{zz} - I_{xz}^2) \end{aligned}$$

3. Apply the numerical integration 4th order Runge-Kutta to the obtained states to get the new velocities, angular rates which will be used as the input for the next step (step 1).

4.1 Runge-Kutta Method 4th Order

$$x(t + \Delta t) = x(t) + \Delta t \left(\frac{k_1}{6} + \frac{k_2}{3} + \frac{k_3}{3} + \frac{k_4}{6} \right)$$

The coefficients

$$k_1 = f(x(t), u(t))$$

$$k_2 = f\left(x(t) + \frac{\Delta t}{2} k_1, u(t + \frac{\Delta t}{2})\right)$$

$$k_3 = f\left(x(t) + \frac{\Delta t}{2} k_2, u(t + \frac{\Delta t}{2})\right)$$

$$k_4 = f(x(t) + \Delta t k_3, u(t + \Delta t))$$

4. Repeat the steps until the error converge.

After applying the previous algorithm, we got the response of the aircraft due to the change of any flight parameters.

4.2 Algorithm flow chart

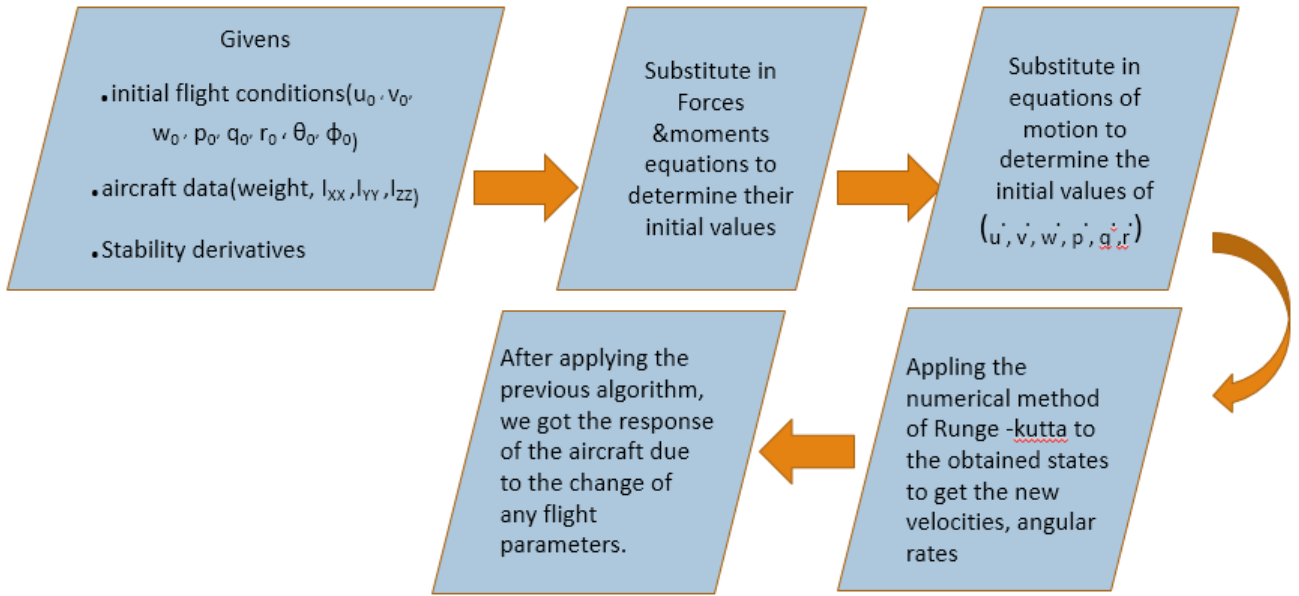


Figure 5: Solution Flow chart

5 Results of nonlinear simulation

It is very important to deal with the airplane as a rigid body has mass and inertia which means that any change in control action will change all its states even for a little time. Therefore we must be aware of the basic motion caused by any control action not only the small disturbance.

5.1 Comparison with the TA's results using his submitted data

5.1.1 Firstly: Aircraft Data

- Initial flight conditions (Sea level flight conditions):

$u_0 =$	67.5 m/s
$v_0 =$	0
$w_0 =$	3.192
$p_0 =$	0
$q_0 =$	0
$r_0 =$	0
$\theta_0 =$	0
$\phi_0 =$	0

- Aircraft data (FOXTROT):

mass =	264000 Kg
$I_{xx} =$	2.6E7
$I_{yy} =$	4.25E7
$I_{zz} =$	6.37E7
$I_{xy} =$	3.4E6

- Stability Derivatives:

Longitudinal motion		Lateral motion	
X_u	-0.02	Y_v	-0.078
X_w	0.1	Y_p	0
X_{δ_e}	0.14	Y_r	0
X_{δ_T}	1.7E-05	Y_{δ_R}	0.0065
Z_u	-0.23	L_β	-0.635
Z_w	-0.634	L_p	-1.09
$Z_{\dot{w}}$	0	L_r	0.613
Z_q	0	L_{δ_A}	0.46
Z_{δ_e}	-2.9	L_v	-0.00941
Z_{δ_T}	-6E-07	L_{δ_R}	0.1
M_u	-2.55E-05	N_β	0.11
M_w	-0.005	N_p	-0.16
$M_{\dot{W}}$	-0.003	N_r	-0.23
M_q	-0.61	N_v	0.00162963
M_{δ_E}	-0.64	N_{δ_a}	0.05
$M_{\delta_{th}}$	1.44E-05	N_{δ_r}	-0.21

5.1.2 Secondly: Results with different inputs

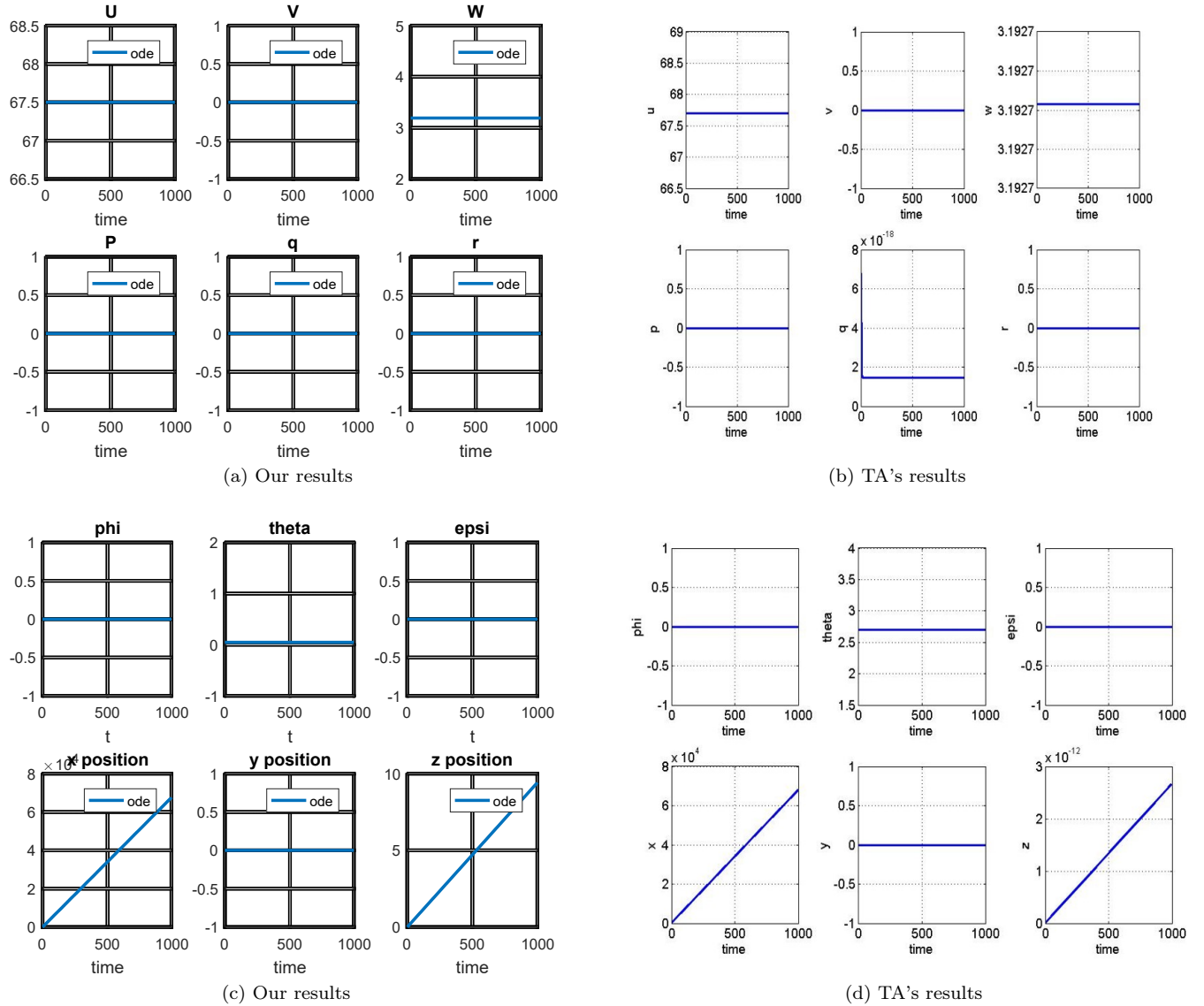
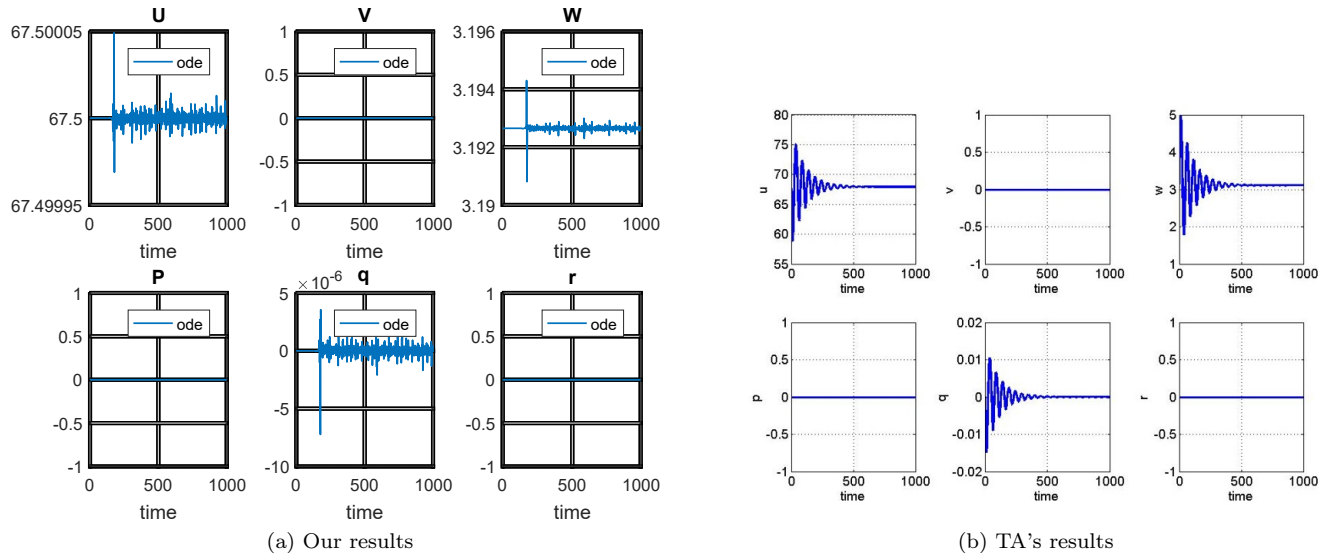
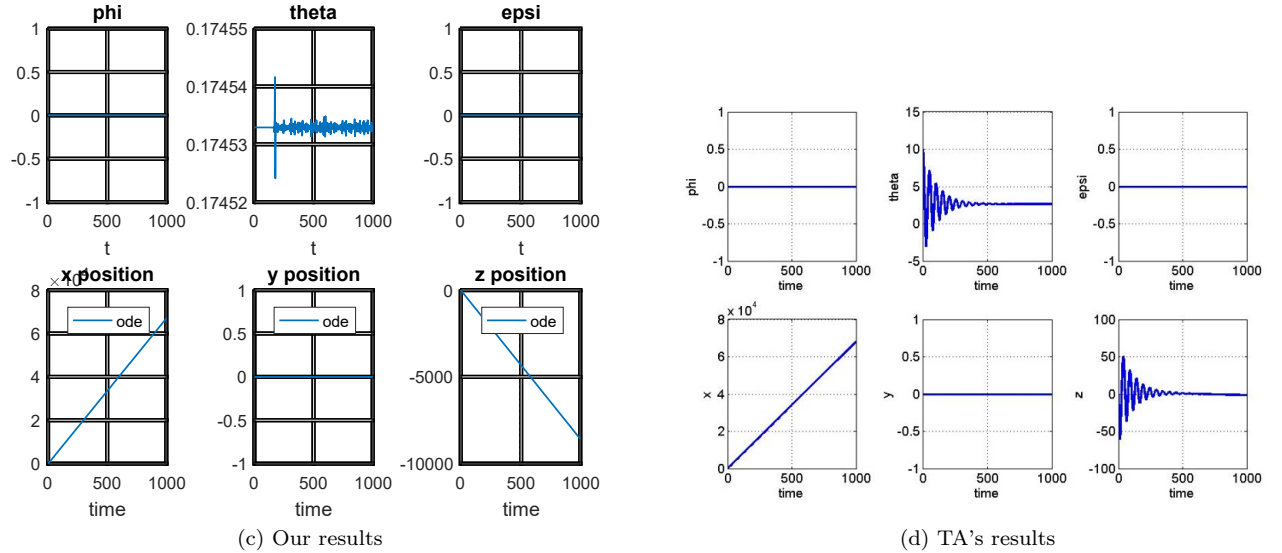


Figure 6: Steady State (No inputs): ($\theta_0 = 2.7^\circ$)



(a) Our results

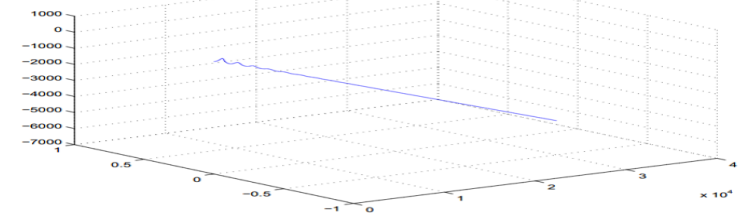
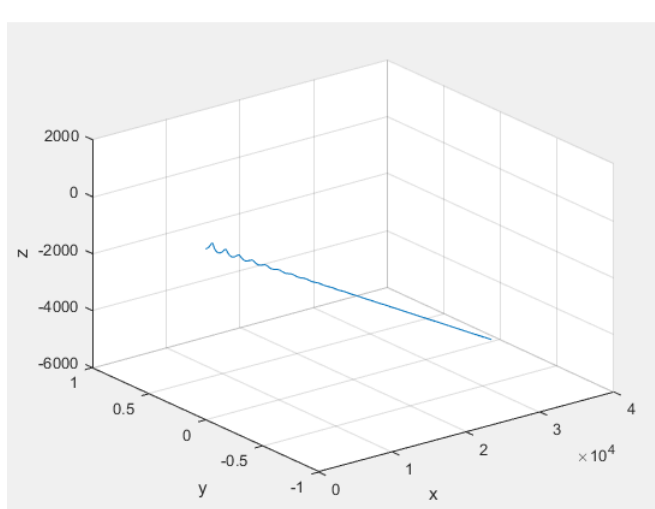
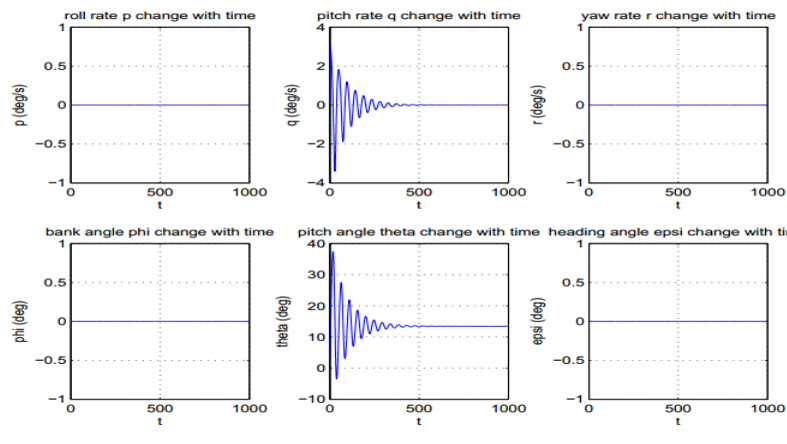
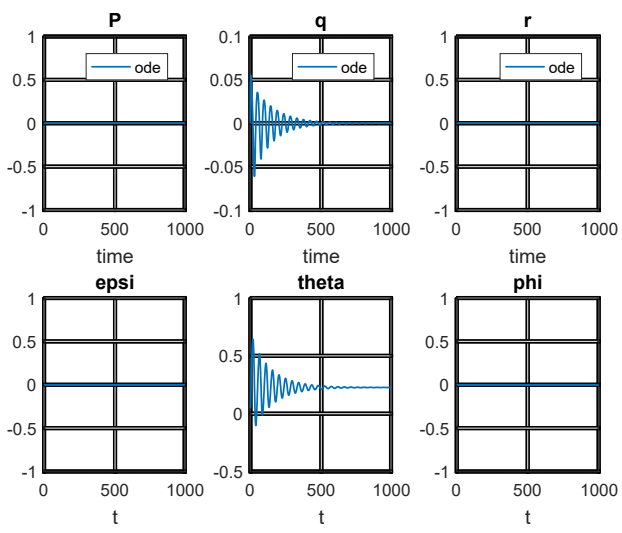
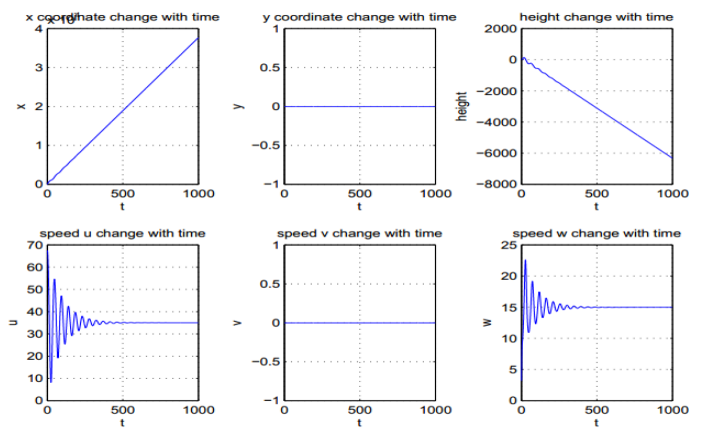
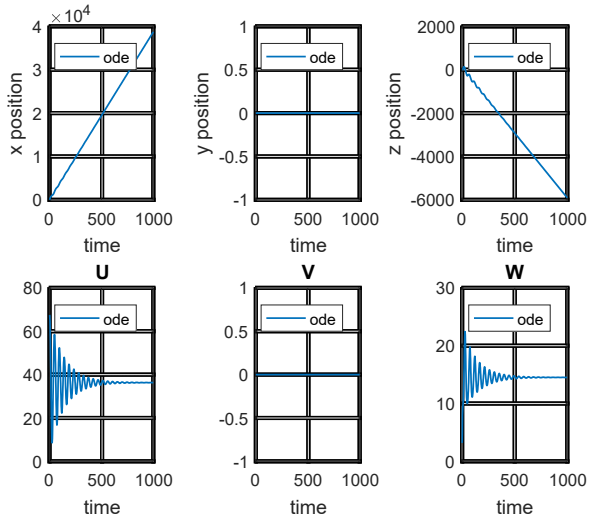
(b) TA's results



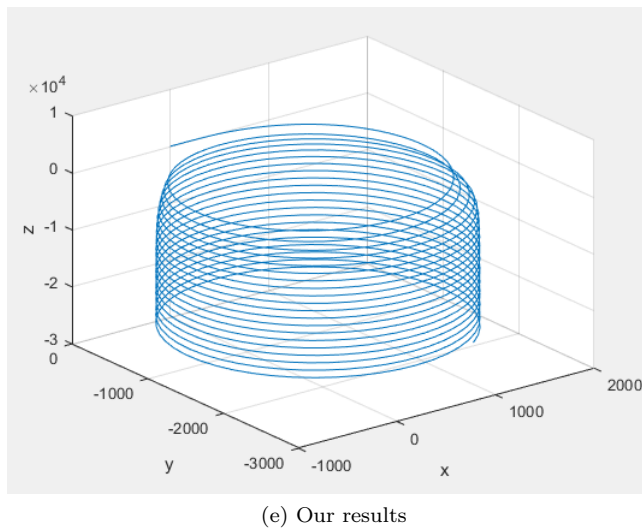
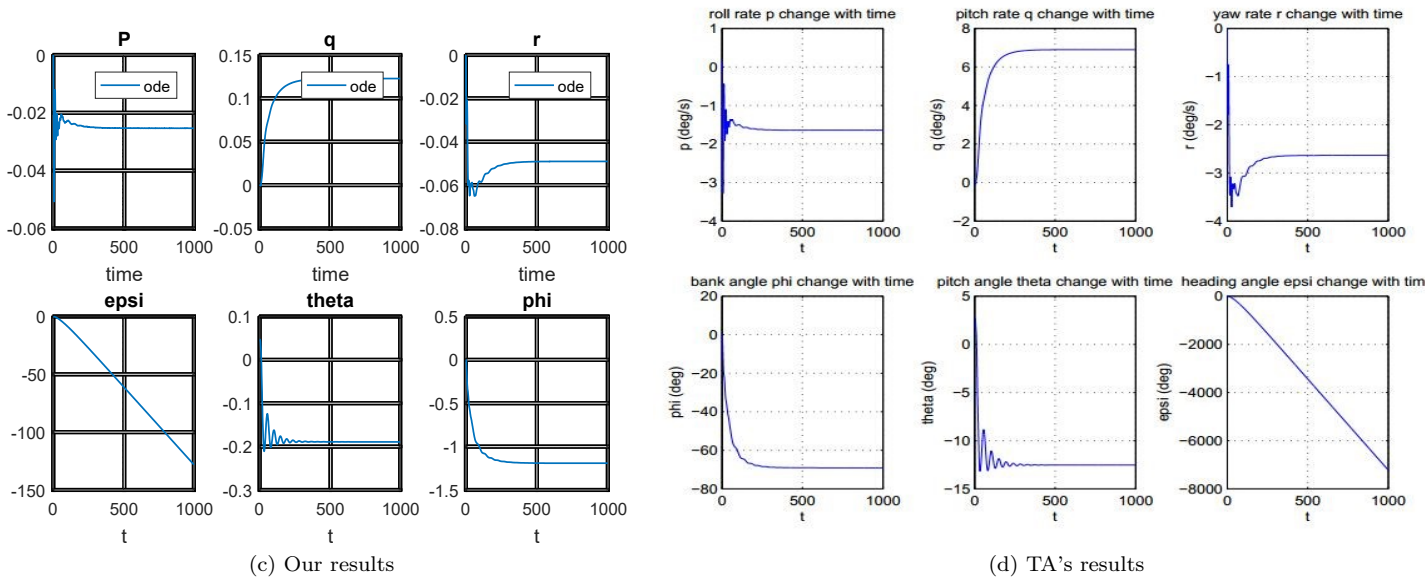
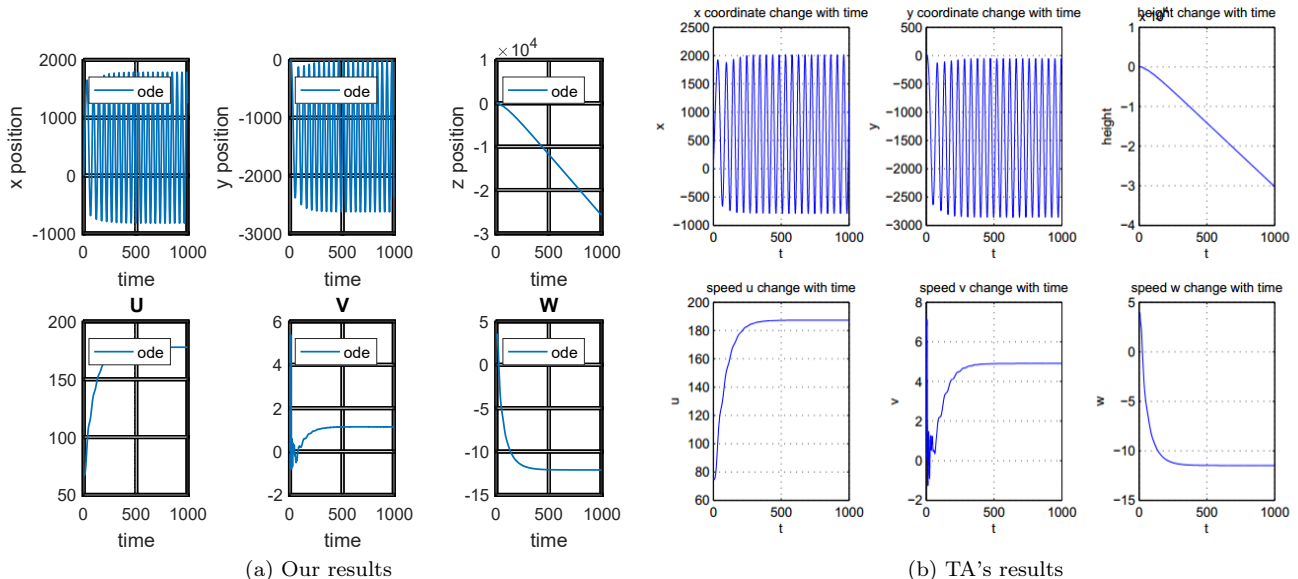
(c) Our results

(d) TA's results

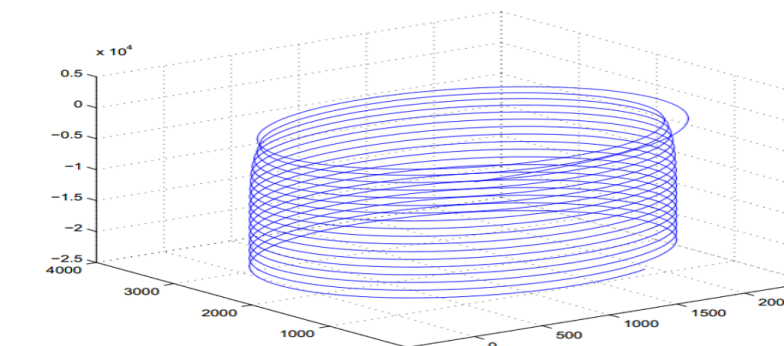
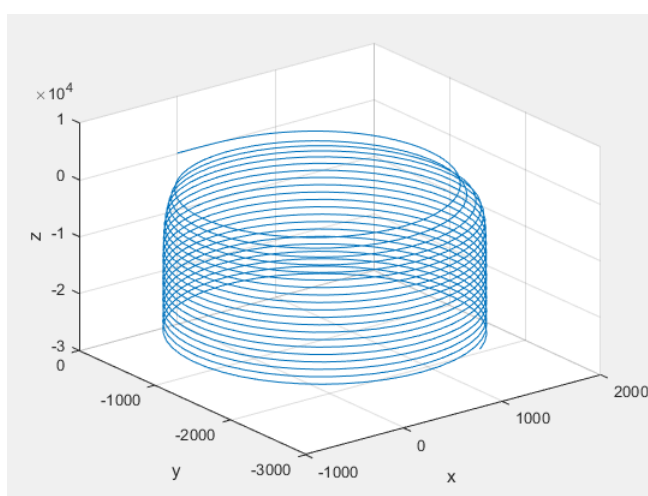
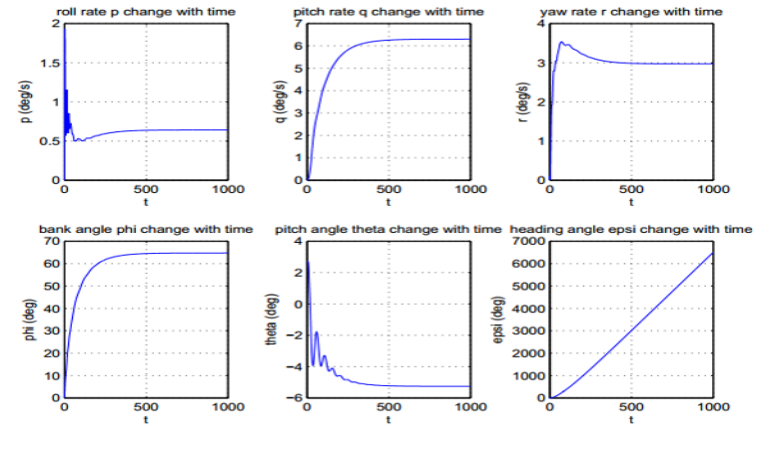
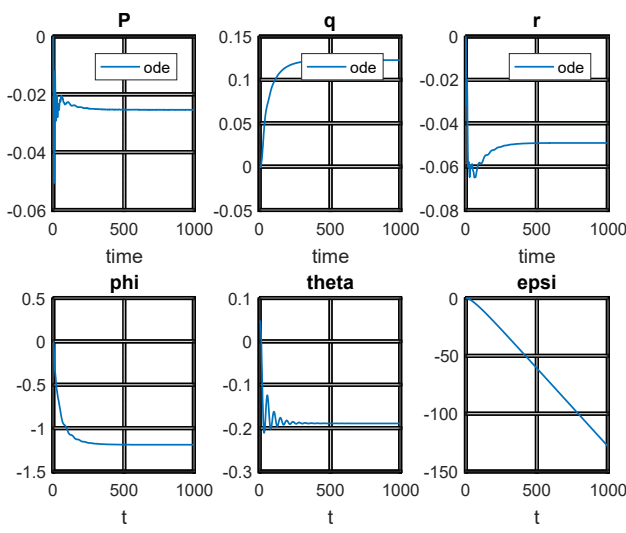
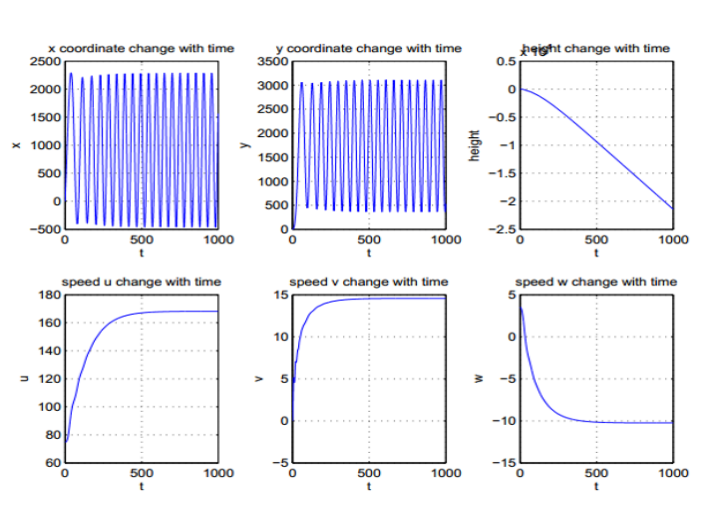
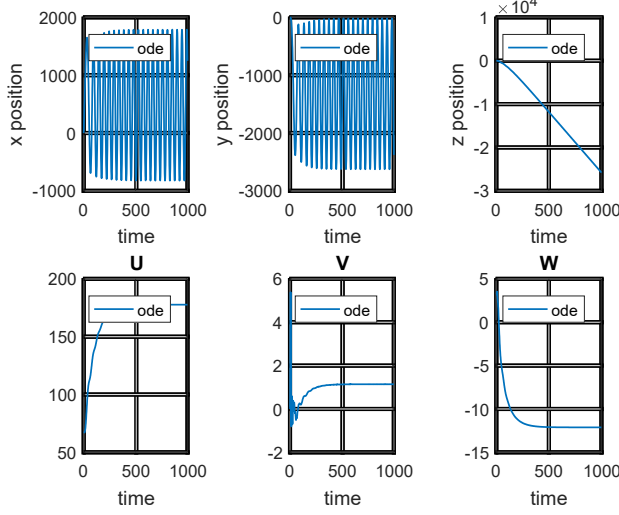
Figure 7: Steady State (No inputs): ($\theta_0 = 10^\circ$)



Since the input control action is a change in elevator angle' ve angle ' ,that cause airplane to pitch up, due to airplane inertia it takes some times to gain its stability again that is obvious in oscillation in q and w . As elevator affects altitude the Z is increasing, and since thrust did not change, the airplane speed has decreased.

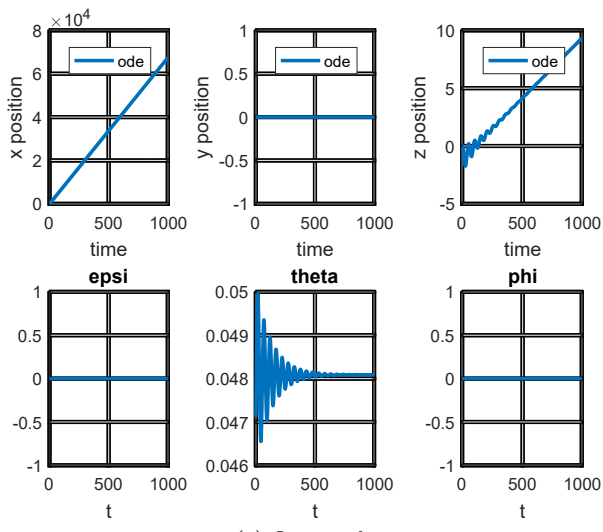


Rudder is responsible for yaw that is shown in the trajectory of the airplane, it rotates in a circle which continue oscillating in x-y plane. Rudder affects Ψ which is the rate of change about Z-axis. As previously seen no increase in thrust to compensate for this motion, consequently altitude and velocity have decreased.

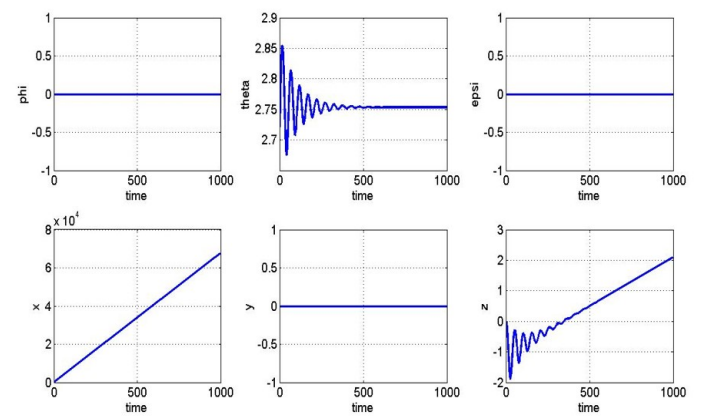


Aileron is responsible for the roll motion, the airplane is somehow stable as there is almost no oscillation in φ .

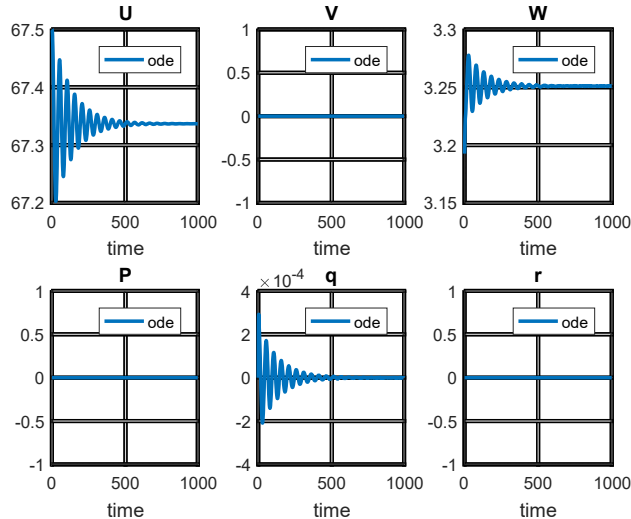
Figure 10: For ($\delta_a = 5^\circ$)



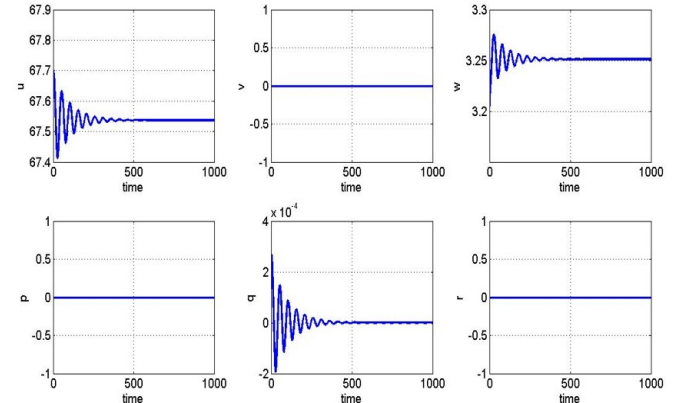
(a) Our results



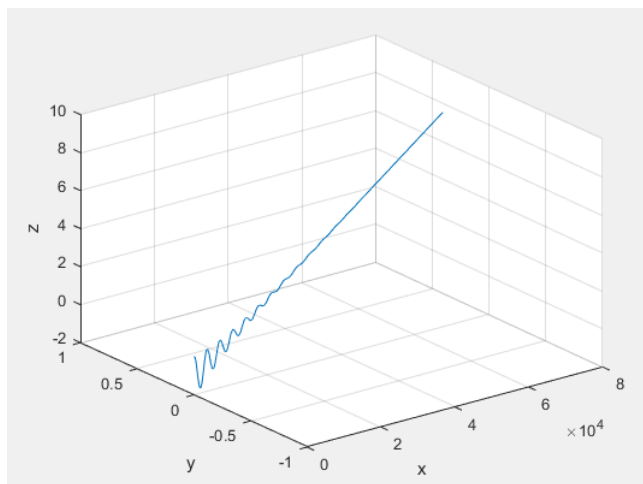
(b) TA's results



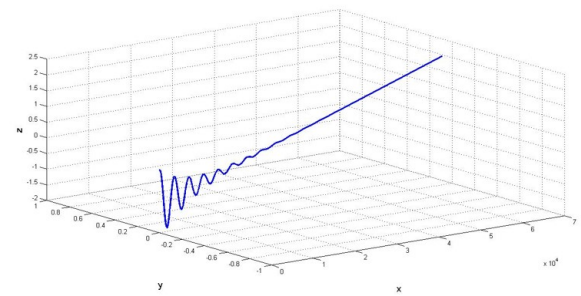
(c) Our results



(d) TA's results



(e) Our results



(f) TA's results

Change in thrust would result in change in altitude or velocity, it is seen from the trajectory that altitude is increasing and the velocity is almost constant.

Figure 11: For ($\delta_t = 20$)

6 Linearized equations of motion solution

The aircraft motion can be divided into two motions the longitudinal and lateral motion.

6.1 Longitudinal motion

We only have three equations (X-Force, Z-force & M-pitching moment)

Their linearized form is written as following:

$$\begin{aligned} \left(\frac{d}{dt} - X_u \right) \Delta u - X_w \Delta w + (g \cos \theta_0) \Delta \theta &= X_{\delta} \delta + X_{\delta T} \Delta \delta_T \\ -Z_u \Delta u + ((1 - Z_{\dot{w}}) \frac{d}{dt} - Z_w) \Delta w - ((u_0 + Z_q) \frac{d}{dt} - g \sin \theta_0) \Delta \theta &= Z_{\delta} \Delta \delta + Z_{\delta T} \Delta \delta_T \\ -M_u \Delta u - (M_{\dot{w}} \frac{d}{dt} + M_w) \Delta w + (\frac{d^2}{dt^2} - M_q \frac{d}{dt}) \Delta \theta &= M_{\delta} \Delta \delta + M_{\delta T} \Delta \delta_T \end{aligned} \quad (15)$$

$$\Delta \dot{\theta} = \Delta q \quad (16)$$

In state space form they can be written in the following form :

$$\dot{X} = A X + B u \quad (17)$$

where

$$A = \begin{bmatrix} X_u & X_w & 0 & -g \cos \theta_0 \\ \frac{Z_u}{1-Z_{\dot{w}}} & \frac{Z_w}{1-Z_{\dot{w}}} & \frac{Z_q+u_0}{1-Z_{\dot{w}}(Z_q+u_0)} & \frac{g \sin \theta_0}{1-Z_{\dot{w}}} \\ M_u + \frac{M_{\dot{w}} Z_u}{1-Z_{\dot{w}}} & M_w + \frac{M_{\dot{w}} Z_w}{1-Z_{\dot{w}}} & M_q + \frac{M_{\dot{w}}(Z_q+u_0)}{1-Z_{\dot{w}}} & -\frac{M_{\dot{w}} m g \sin \theta_0}{1-Z_{\dot{w}}} \\ 0 & 0 & 1 & 0 \end{bmatrix}$$

$$B = \begin{bmatrix} X_{\delta e} & X_{\delta T} \\ Z_{\delta e} & Z_{\delta T} \\ M_{\delta e} + M_{\dot{w}} Z_w & M_{\delta T} + M_{\dot{w}} Z_{\delta T} \\ 0 & 0 \end{bmatrix}$$

So the complete state space model can be written in the following form :

$$\begin{bmatrix} \Delta \dot{u} \\ \Delta \dot{w} \\ \Delta \dot{q} \\ \Delta \dot{\theta} \end{bmatrix} = \begin{bmatrix} X_u & X_w & 0 & -g \cos \theta_0 \\ \frac{Z_u}{1-Z_{\dot{w}}} & \frac{Z_w}{1-Z_{\dot{w}}} & \frac{Z_q+u_0}{1-Z_{\dot{w}}(Z_q+u_0)} & \frac{g \sin \theta_0}{1-Z_{\dot{w}}} \\ M_u + \frac{M_{\dot{w}} Z_u}{1-Z_{\dot{w}}} & M_w + \frac{M_{\dot{w}} Z_w}{1-Z_{\dot{w}}} & M_q + \frac{M_{\dot{w}}(Z_q+u_0)}{1-Z_{\dot{w}}} & -\frac{M_{\dot{w}} m g \sin \theta_0}{1-Z_{\dot{w}}} \\ 0 & 0 & 1 & 0 \end{bmatrix} \begin{bmatrix} \Delta u \\ \Delta w \\ \Delta q \\ \Delta \theta \end{bmatrix} + \begin{bmatrix} X_{\delta e} & X_{\delta T} \\ Z_{\delta e} & Z_{\delta T} \\ M_{\delta e} + M_{\dot{w}} Z_w & M_{\delta T} + M_{\dot{w}} Z_{\delta T} \\ 0 & 0 \end{bmatrix} \begin{bmatrix} \Delta \delta_e \\ \Delta \delta_T \end{bmatrix}$$

And the output can be determine using the following equation :

$$Y = C X + D u \quad (18)$$

Where C is the 4x4 identity matrix and D is a 4x2 zero matrix in our case.

As can be seen, we have 4 states and 2 inputs, so we can get a total of 8 transfer functions which is a transfer function between each state and one input only, and from these transfer functions we can get the bode plot and root locus.

6.2 Longitudinal Approximations

6.2.1 Short Period Approximation

- Assumptions:

1. $\Delta u = 0$
2. Drop $X - force$ equation.

Therefore the longitudinal state space model becomes:

$$\begin{bmatrix} \Delta \dot{w} \\ \Delta \dot{q} \end{bmatrix} = \begin{bmatrix} Z_w & u_0 \\ M_w + M_{\dot{w}}Z_w & M_q + M_{\dot{w}}u_0 \end{bmatrix} \begin{bmatrix} \Delta w \\ \Delta q \end{bmatrix}$$

Or in terms of the angle of attack $\Delta\alpha = \frac{\Delta w}{u_0}$ it can be written in the following form :

$$\begin{bmatrix} \Delta \dot{\alpha} \\ \Delta \dot{q} \end{bmatrix} = \begin{bmatrix} \frac{Z_\alpha}{u_0} & 1 \\ M_\alpha + M_{\dot{\alpha}} \frac{Z_\alpha}{u_0} & M_q + M_{\dot{\alpha}} \end{bmatrix} \begin{bmatrix} \Delta\alpha \\ \Delta q \end{bmatrix}$$

where $Z_\alpha = u_0 Z_w$ and $M_{\dot{\alpha}} = u_0 M_{\dot{w}}$

6.2.2 Long Period Approximation

- Assumptions

1. Neglect pitching moment M .
2. Change in angle of attack is zero $\Delta\alpha = 0 \rightarrow \Delta w = 0$.

Therefore the longitudinal state space model becomes:

$$\begin{bmatrix} \Delta \dot{u} \\ \Delta \dot{\theta} \end{bmatrix} = \begin{bmatrix} X_u & -g \cos\theta_0 \\ \frac{-Z_u}{Z_q+u_0} & \frac{g \sin\theta_0}{Z_q+u_0} \end{bmatrix} \begin{bmatrix} \Delta u \\ \Delta\theta \end{bmatrix} + \begin{bmatrix} X_{\delta e} & X_{\delta T} \\ \frac{-Z_{\delta e}}{Z_q+u_0} & \frac{-Z_{\delta T}}{Z_q+u_0} \end{bmatrix} \begin{bmatrix} \Delta\delta_e \\ \Delta\delta_T \end{bmatrix}$$

6.2.3 Results (Using TA's airplane)

- Steady State (No inputs): ($\theta_0 = 2.7^\circ$)

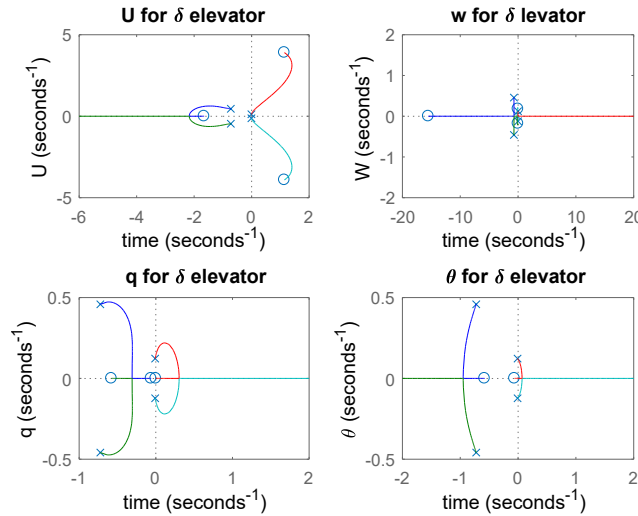


Figure 12

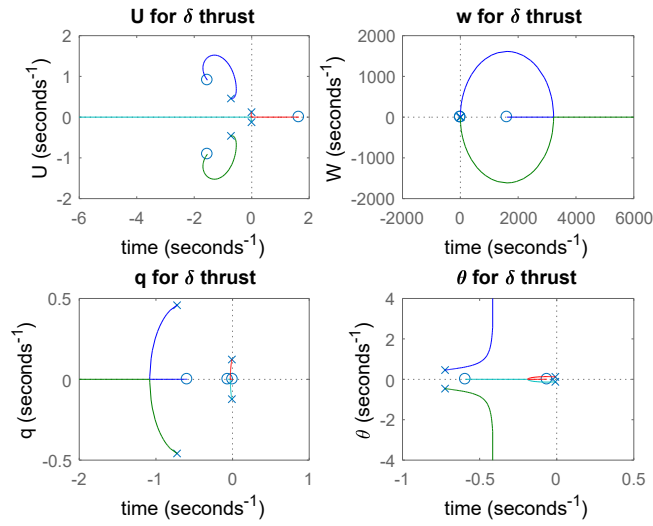


Figure 13

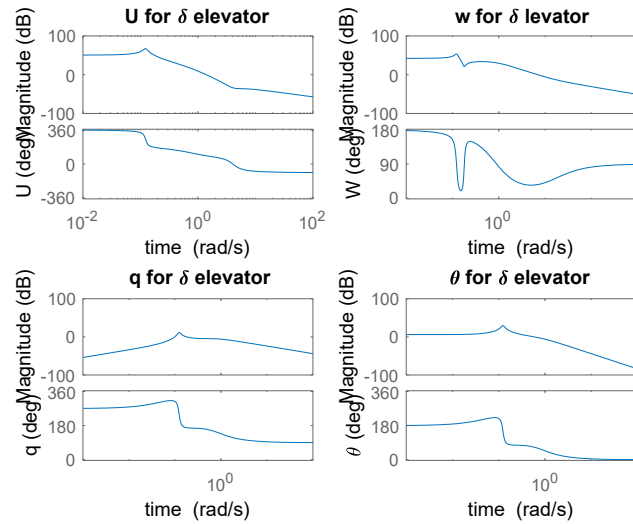


Figure 14

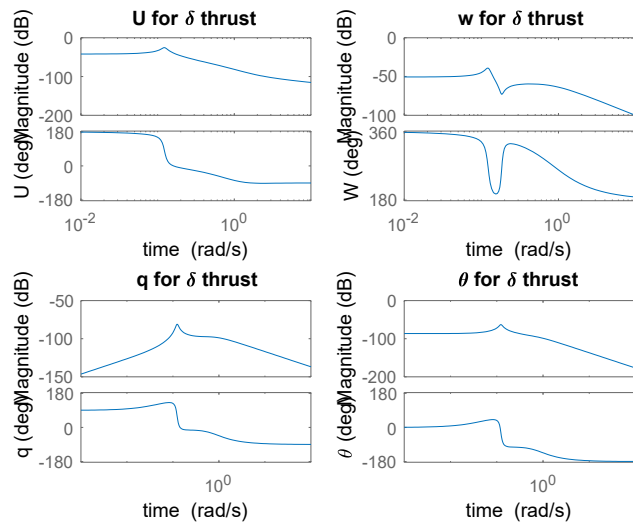


Figure 15

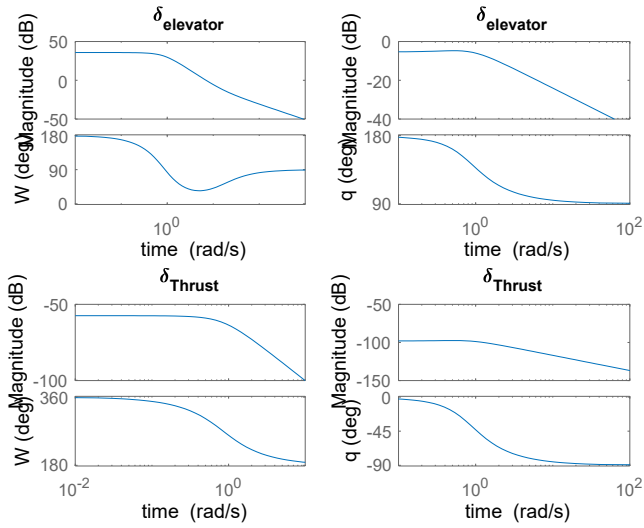


Figure 16

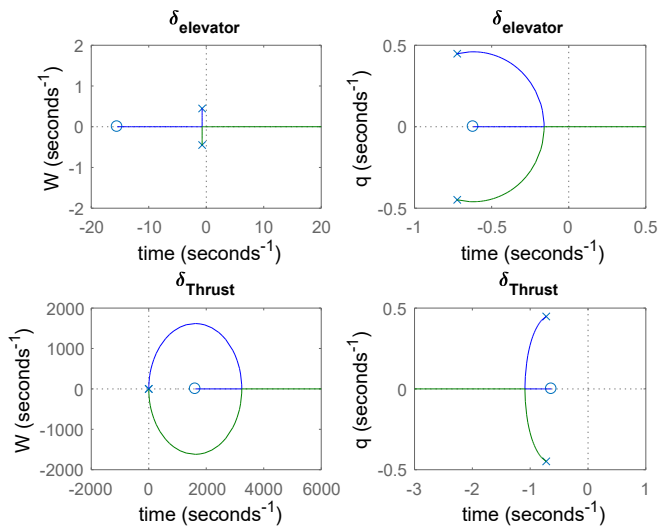


Figure 17

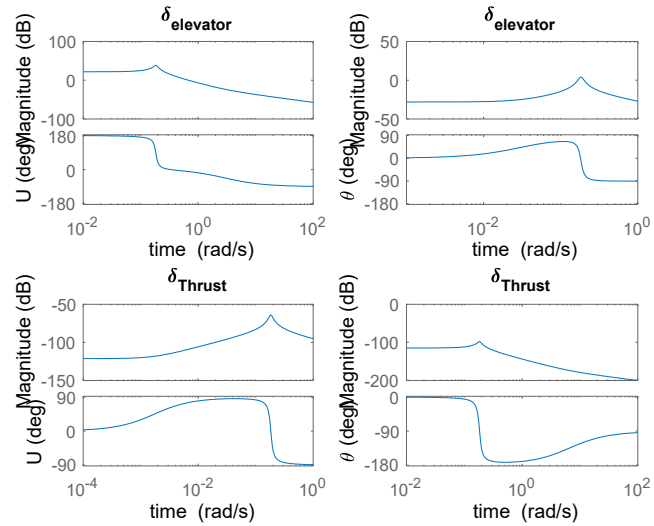


Figure 18

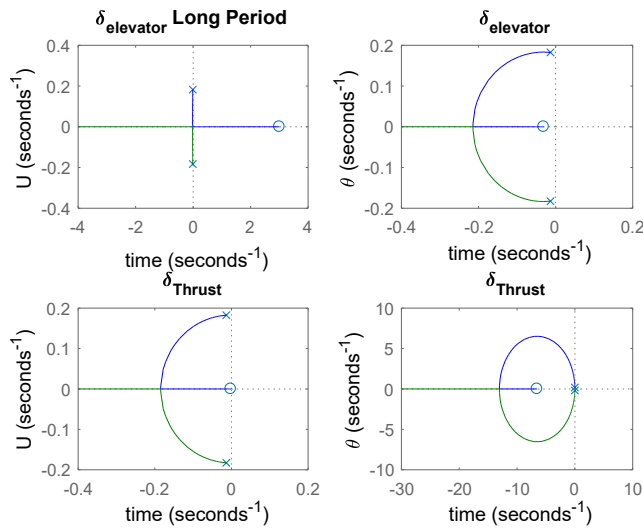


Figure 19

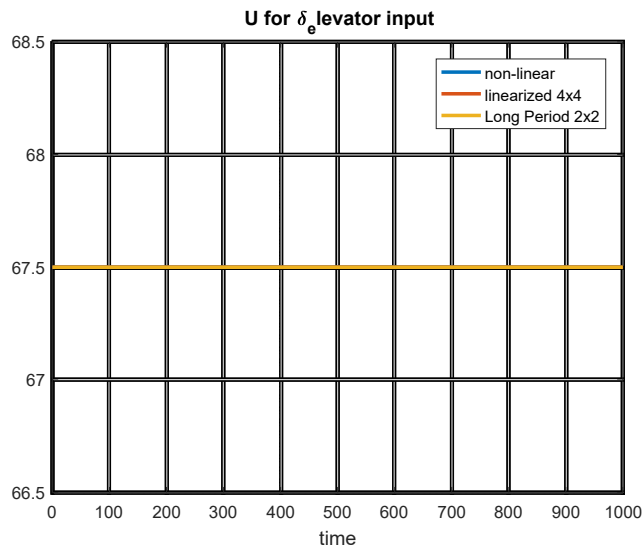


Figure 20

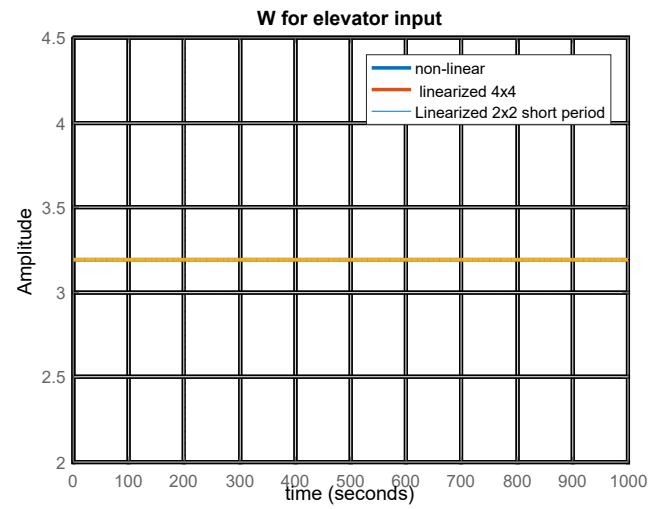


Figure 21

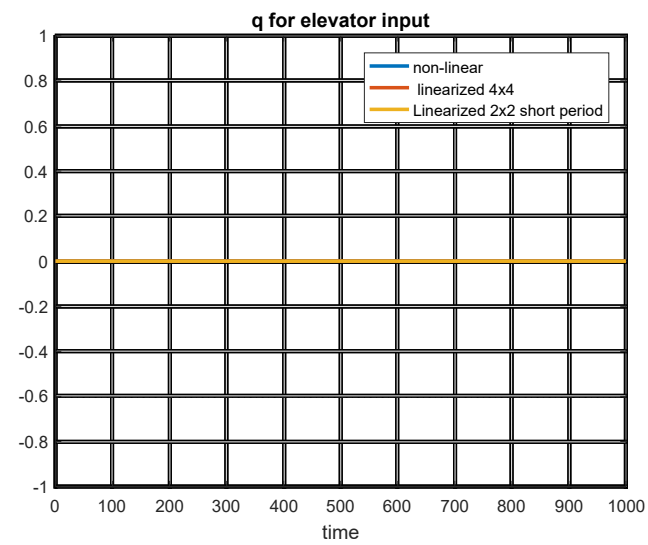


Figure 22

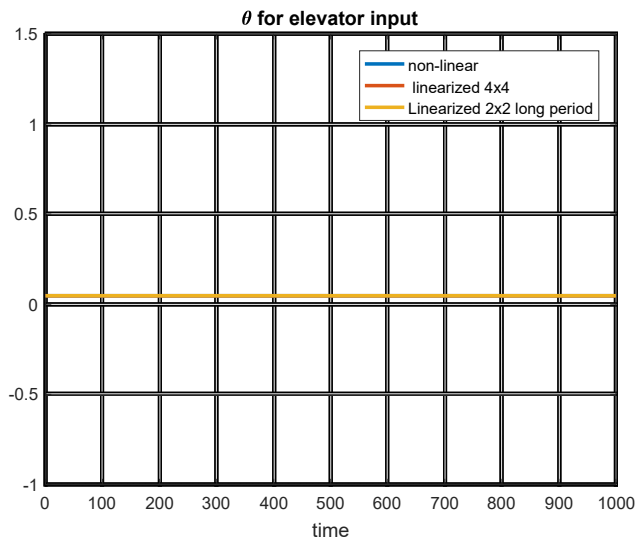


Figure 23

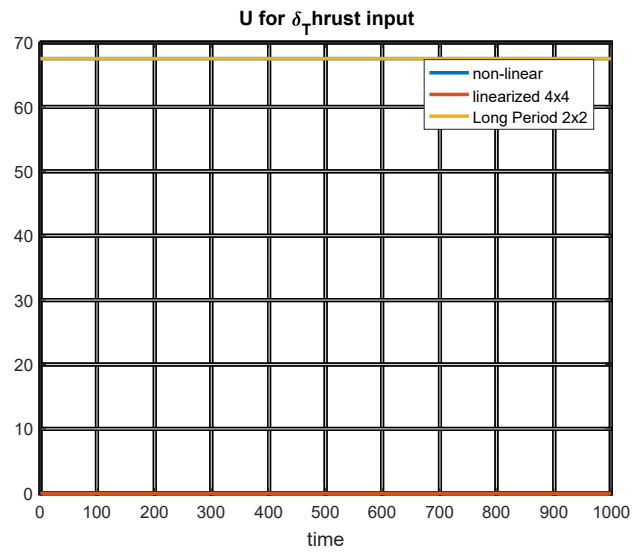


Figure 24

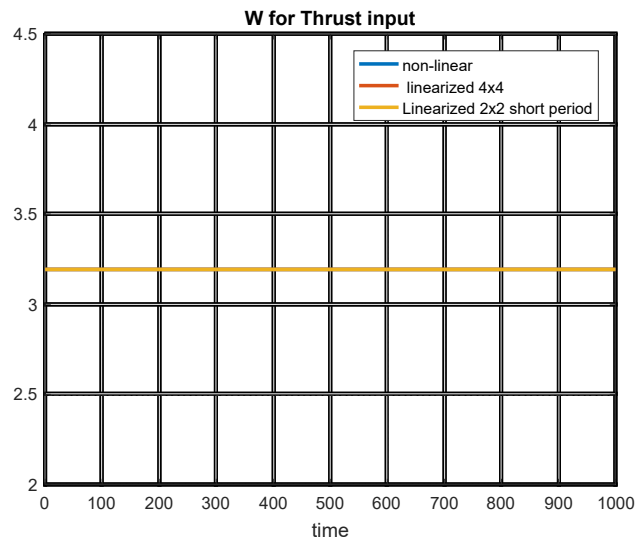


Figure 25

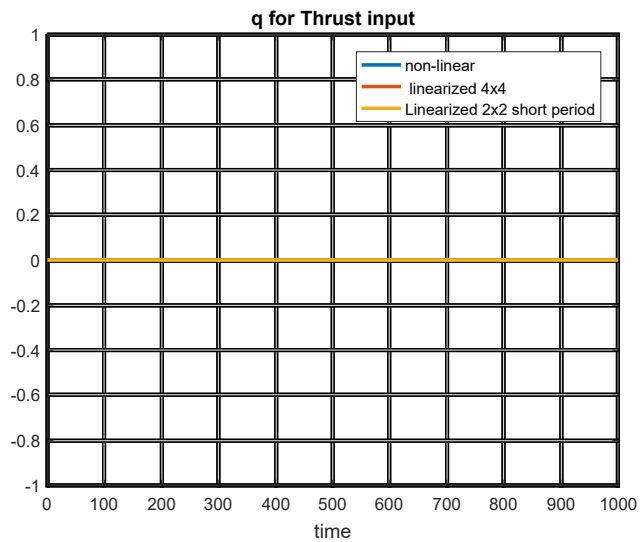


Figure 26

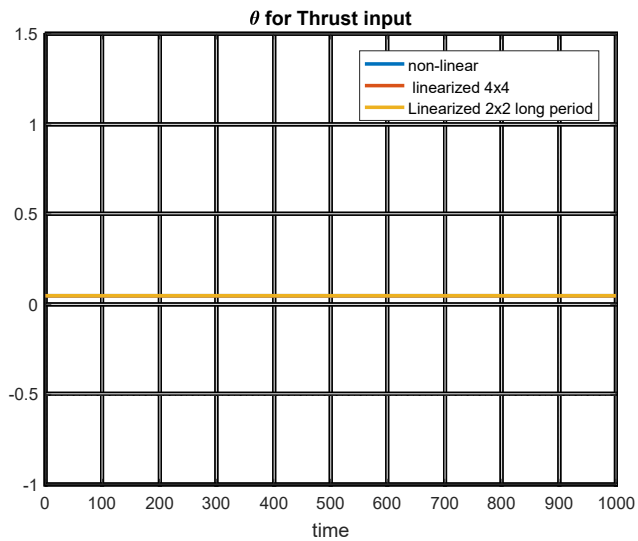


Figure 27

- For ($\delta_r = 5^\circ$)

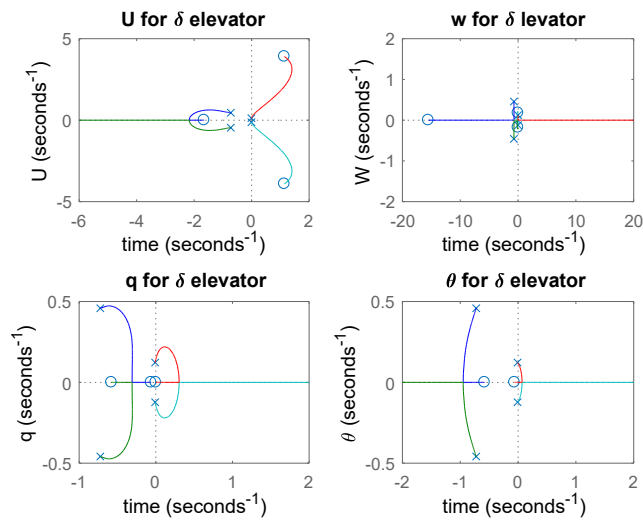


Figure 28

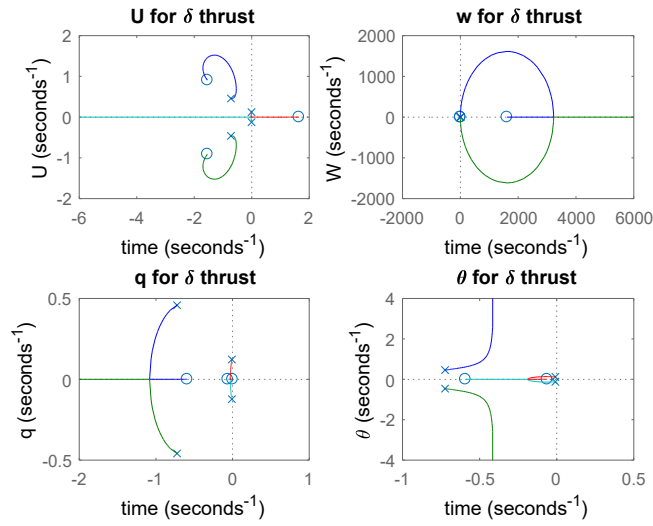


Figure 29

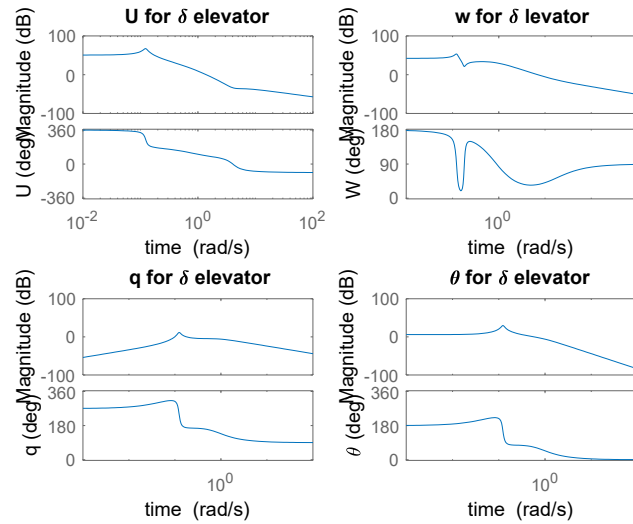


Figure 30

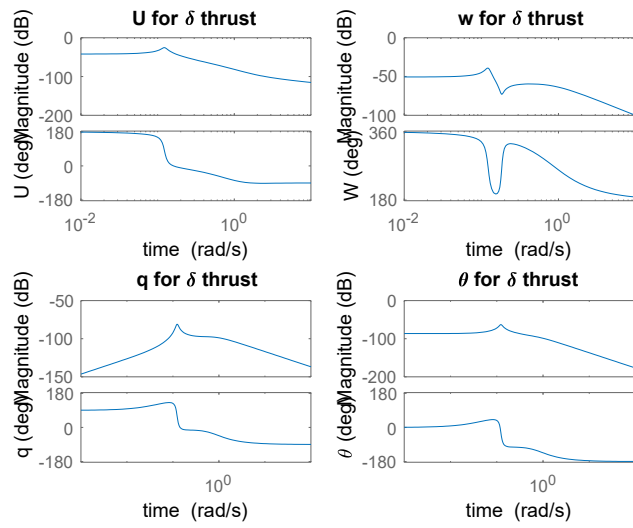


Figure 31

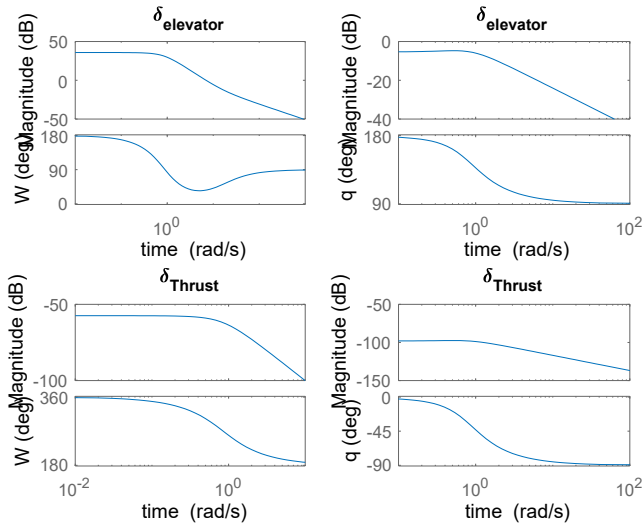


Figure 32

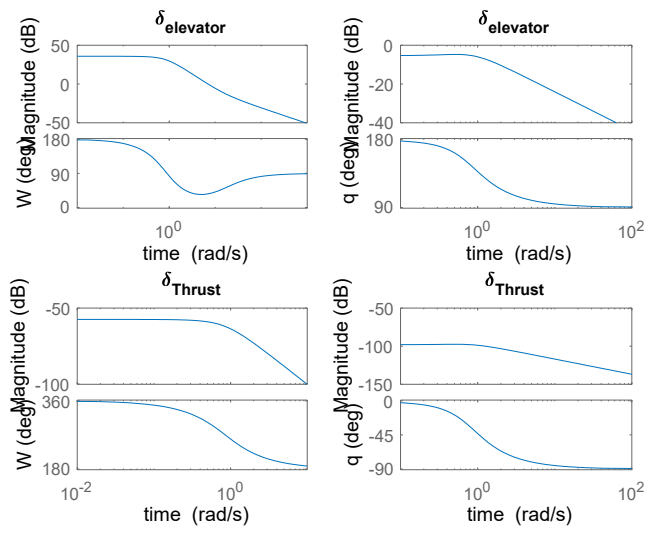


Figure 33

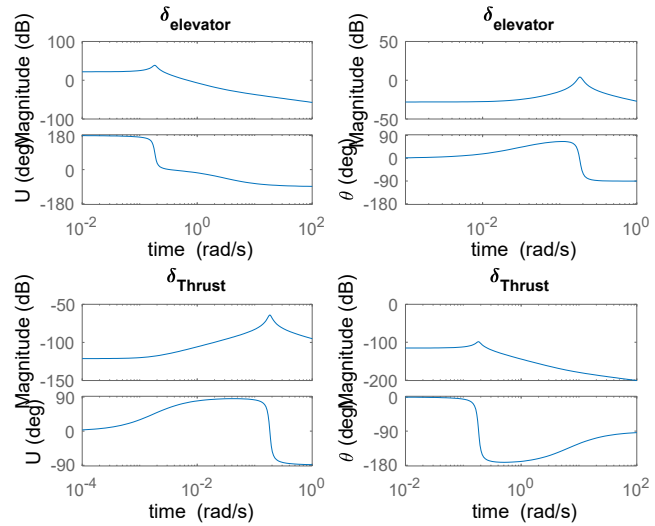


Figure 34

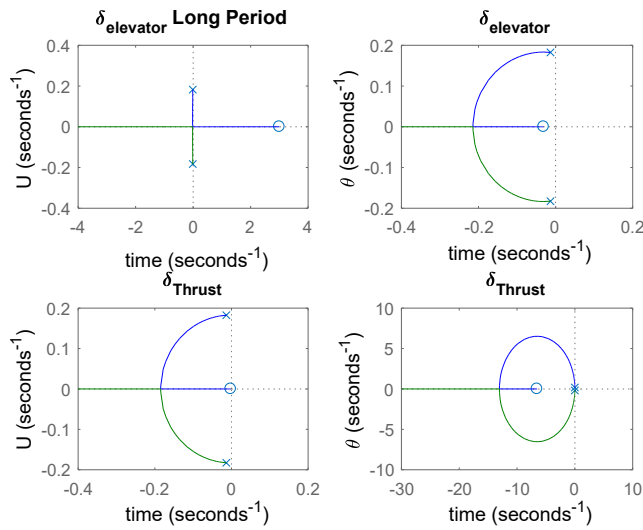


Figure 35

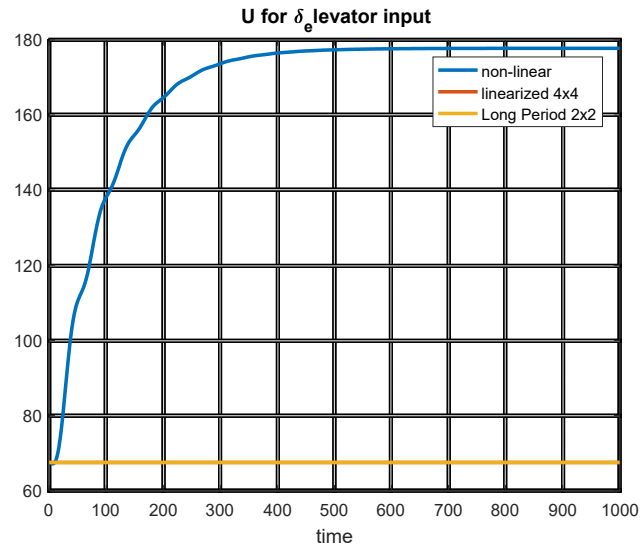


Figure 36

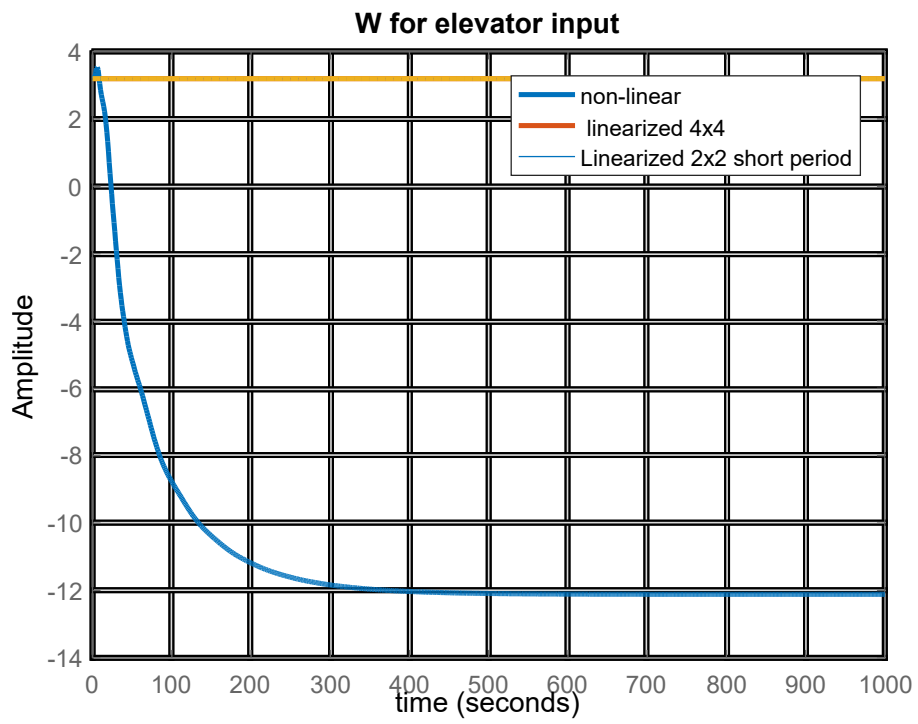


Figure 37

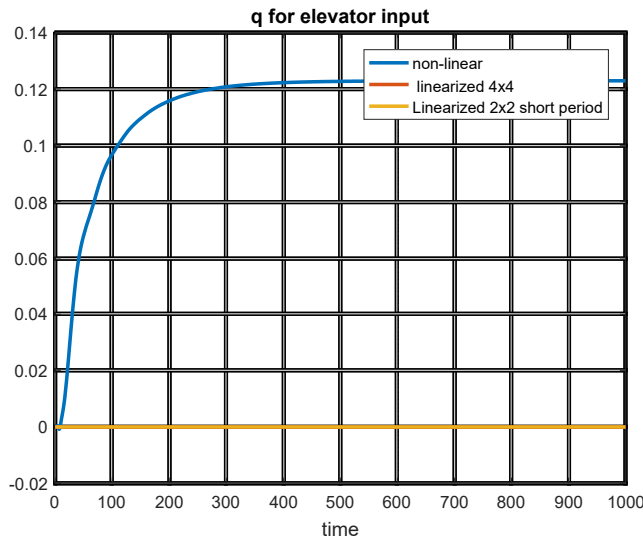


Figure 38

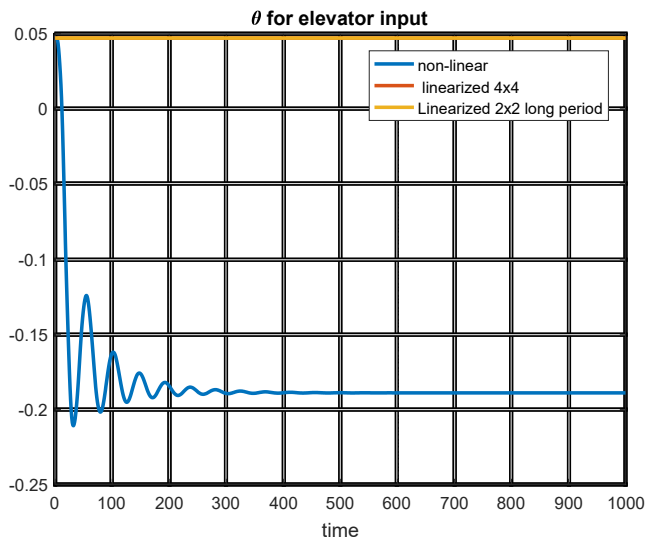


Figure 39

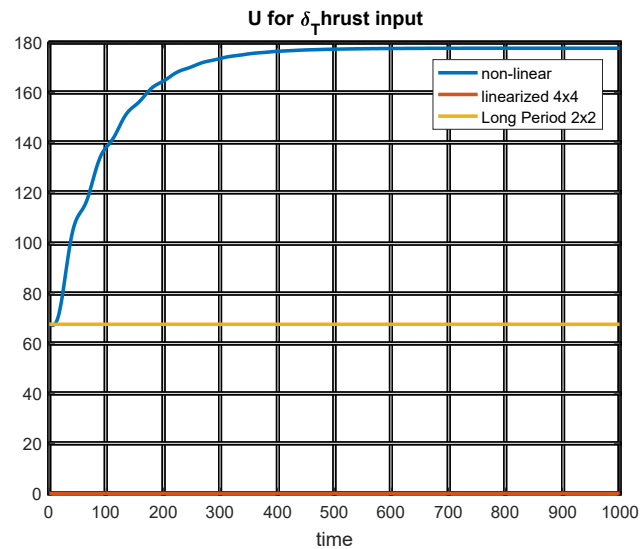


Figure 40

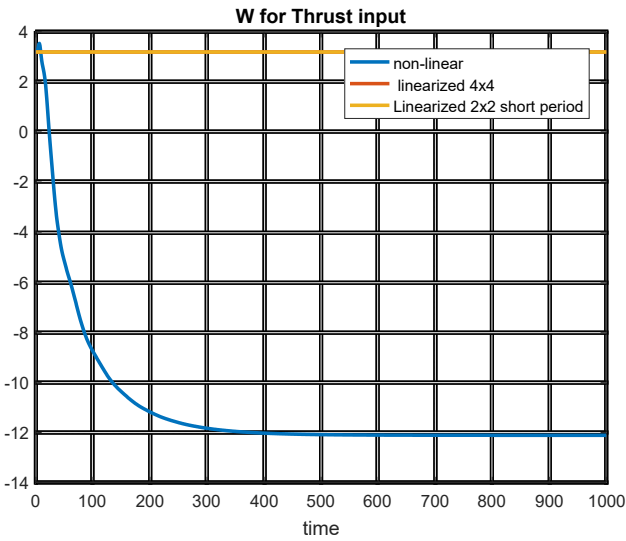


Figure 41

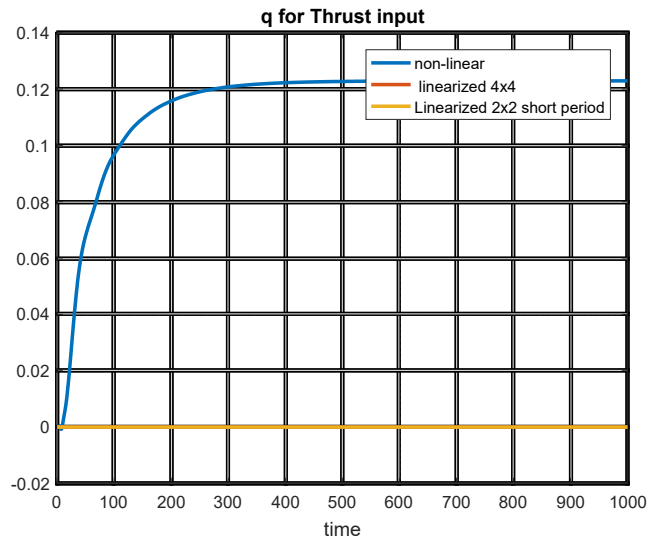


Figure 42

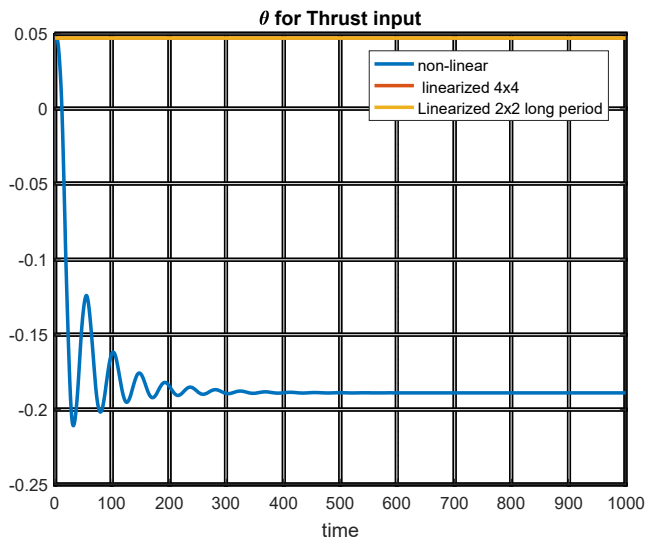


Figure 43

- For ($\delta_e = -5^\circ$)

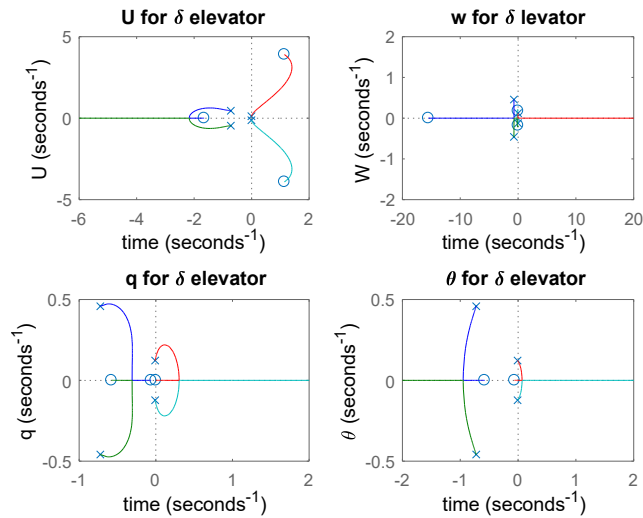


Figure 44

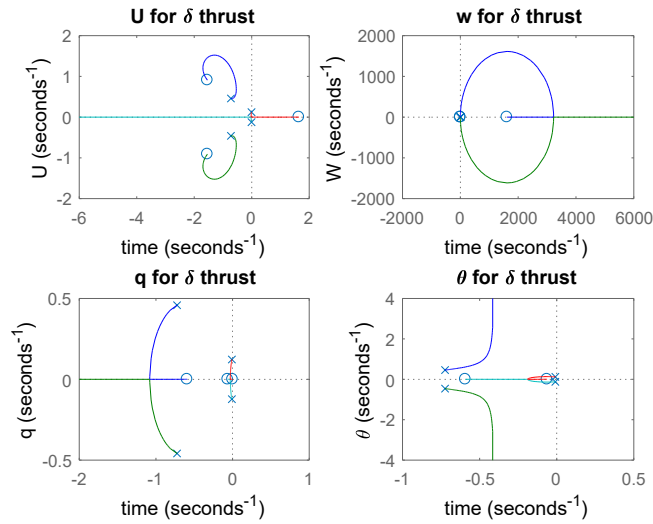


Figure 45

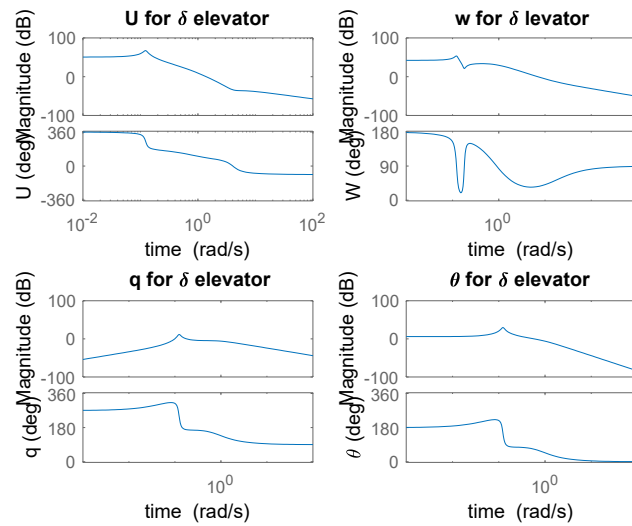


Figure 46

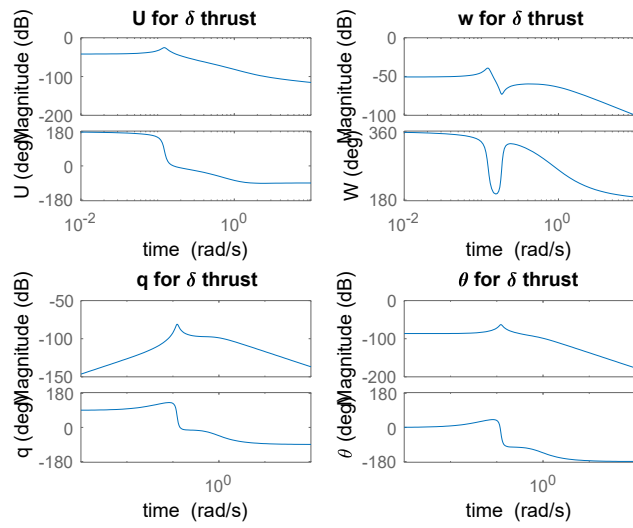


Figure 47

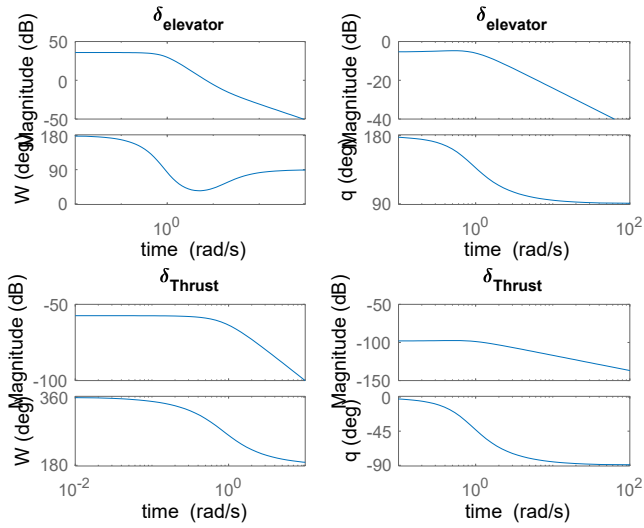


Figure 48

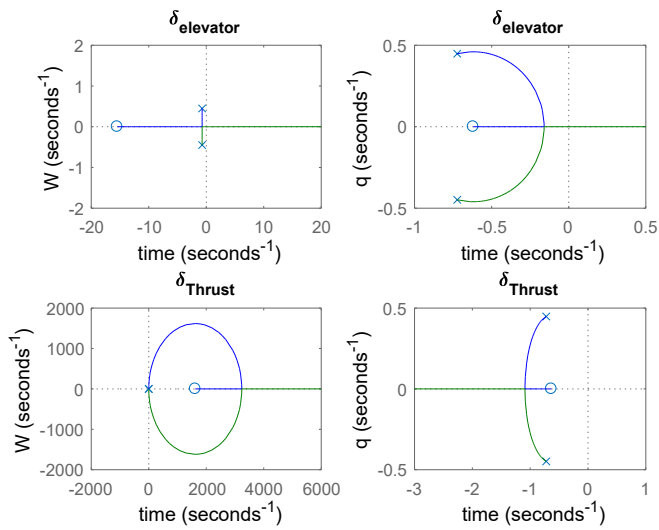


Figure 49

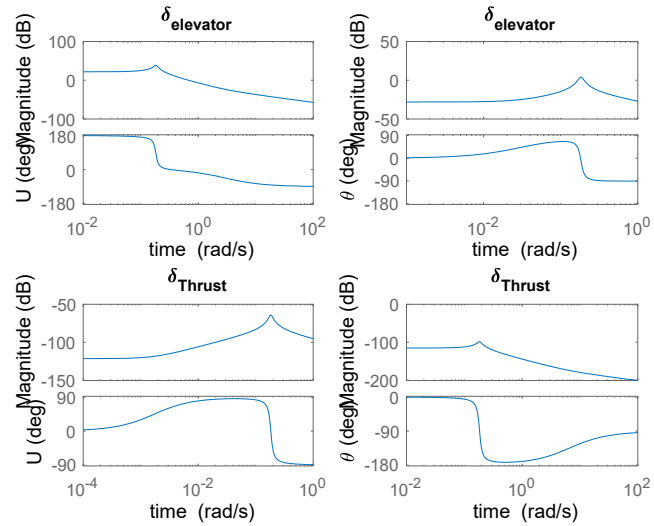


Figure 50

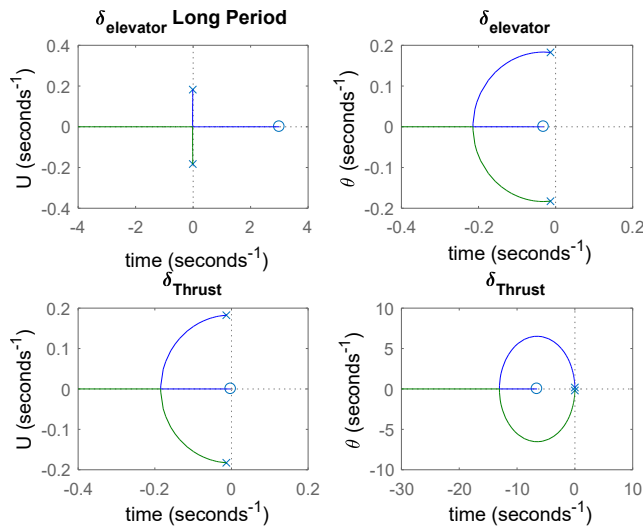


Figure 51

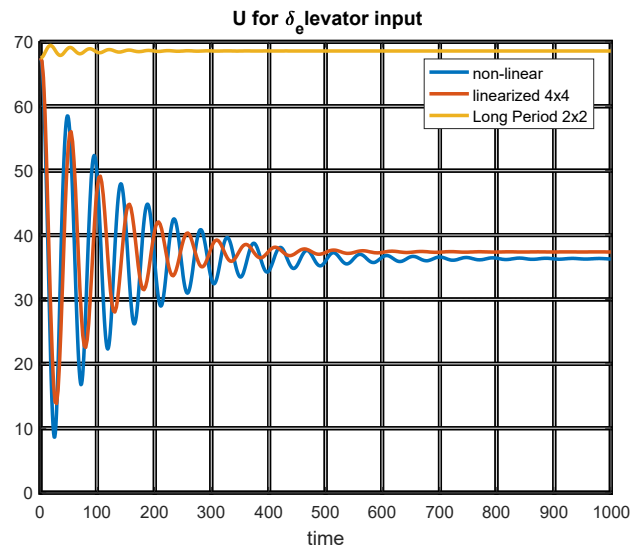


Figure 52

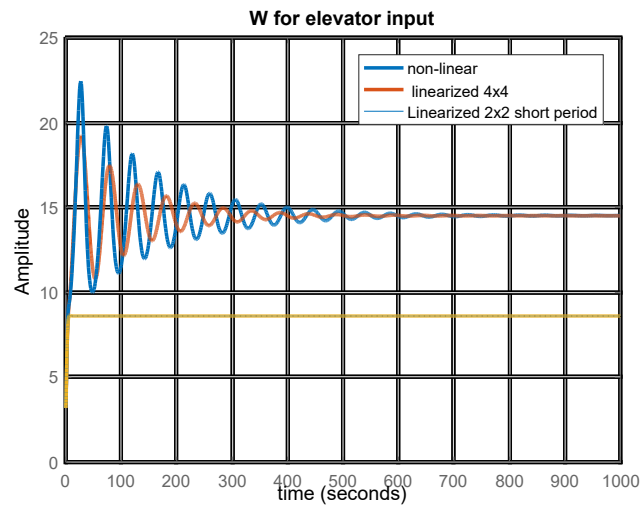


Figure 53

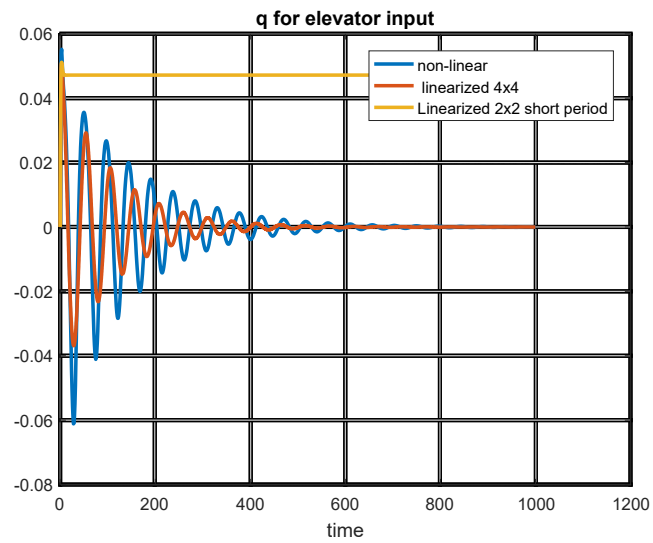


Figure 54

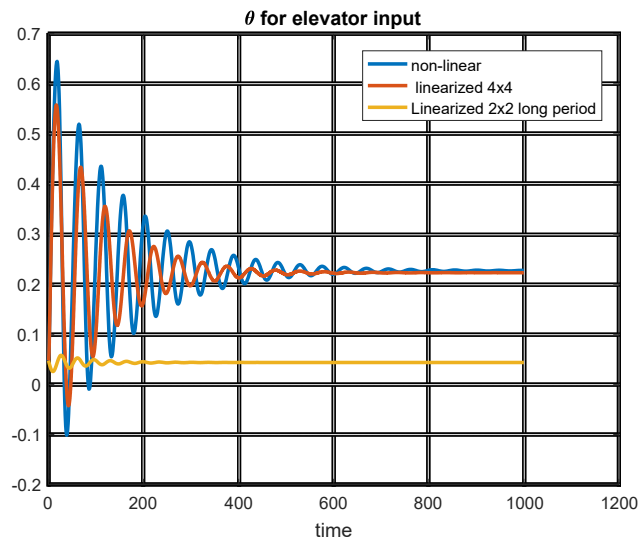


Figure 55

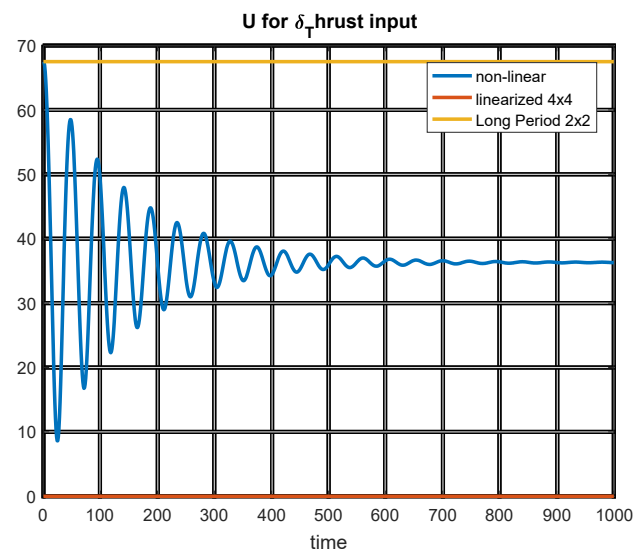


Figure 56

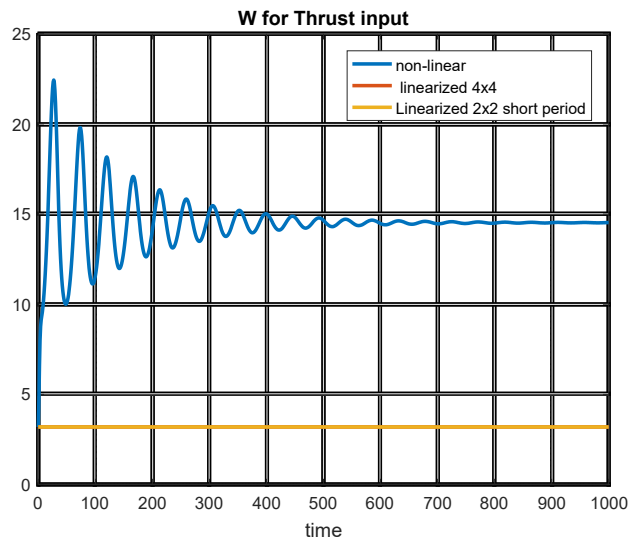


Figure 57

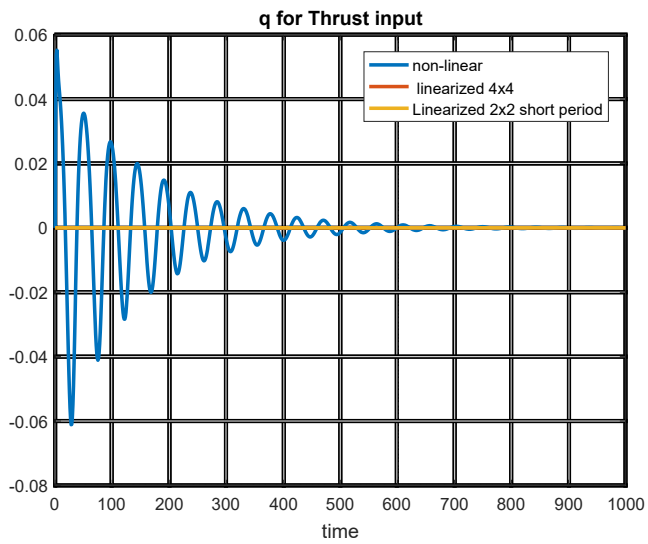


Figure 58

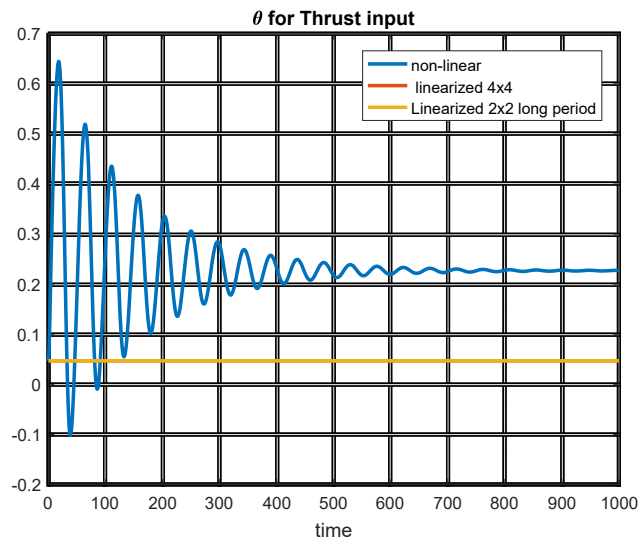


Figure 59

- For ($\delta_a = 5^\circ$)

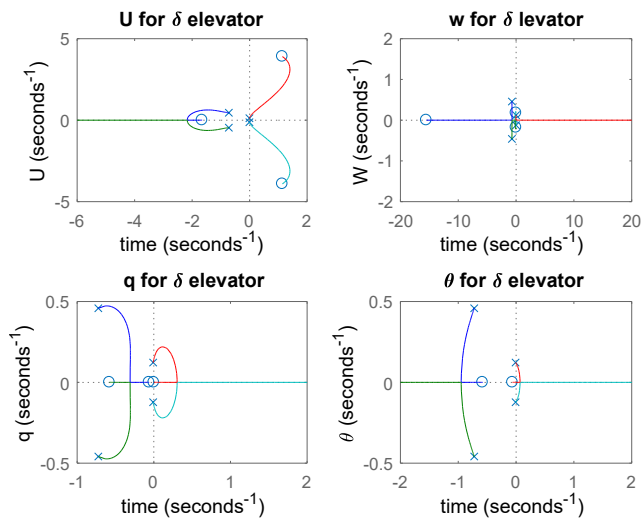


Figure 60

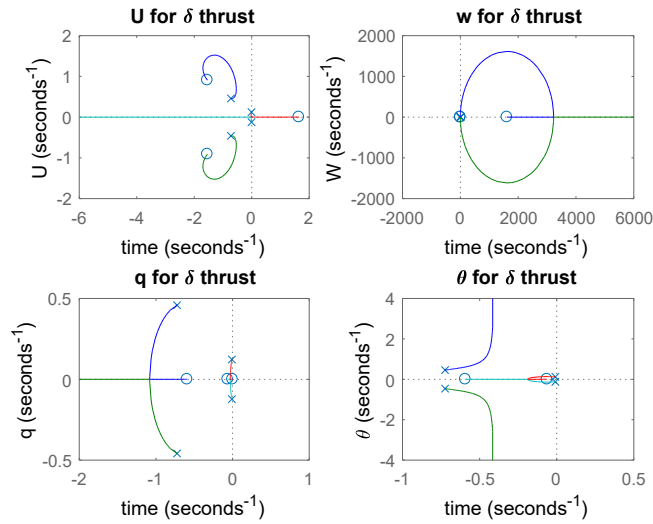


Figure 61

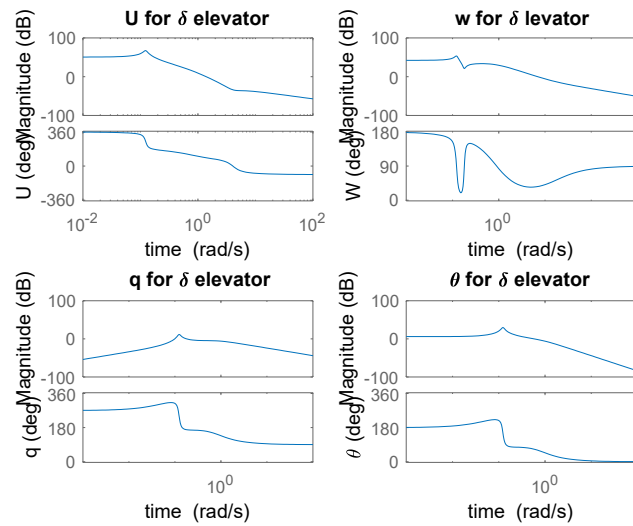


Figure 62

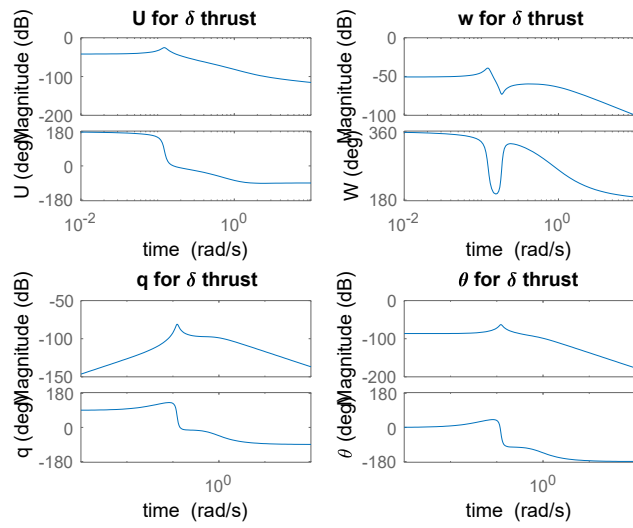


Figure 63

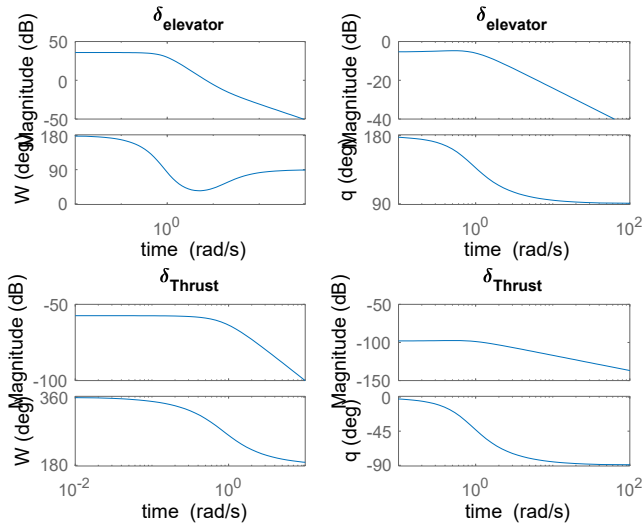


Figure 64

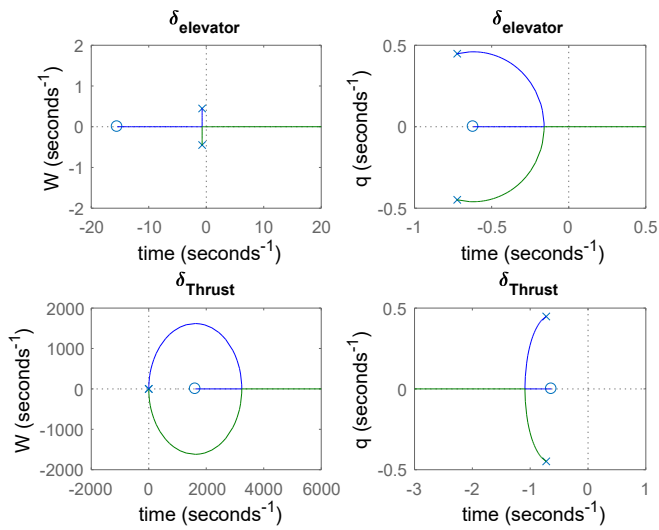


Figure 65

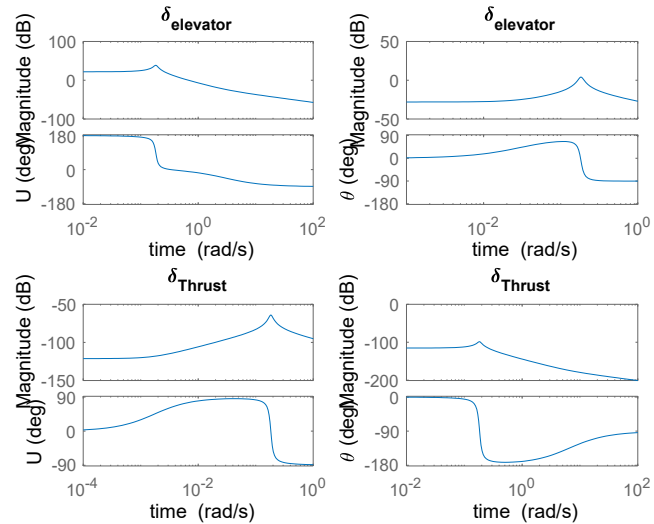


Figure 66

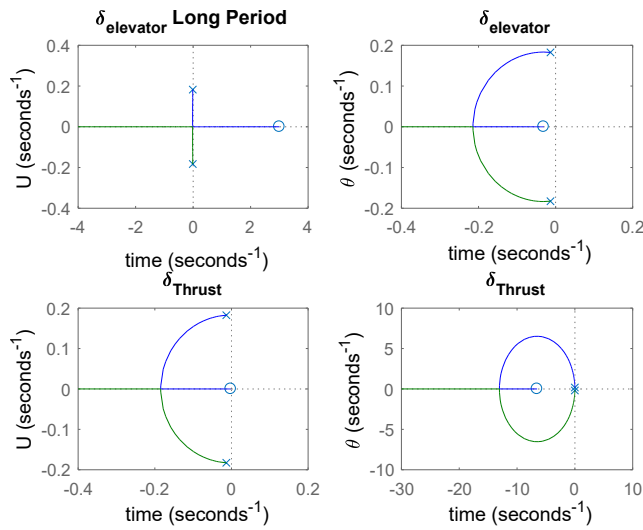


Figure 67

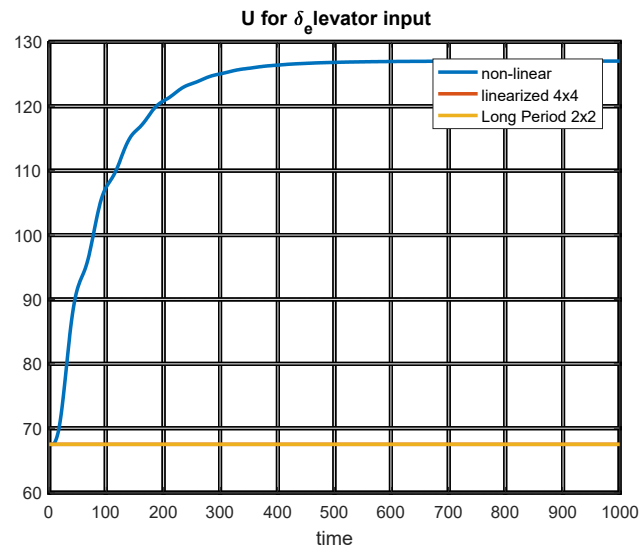


Figure 68

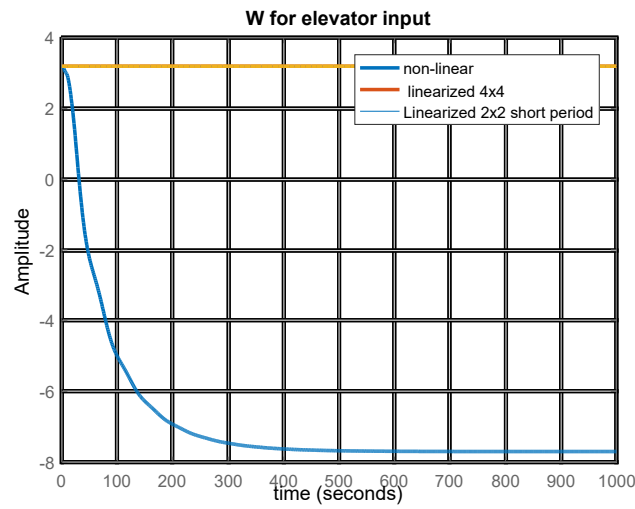


Figure 69

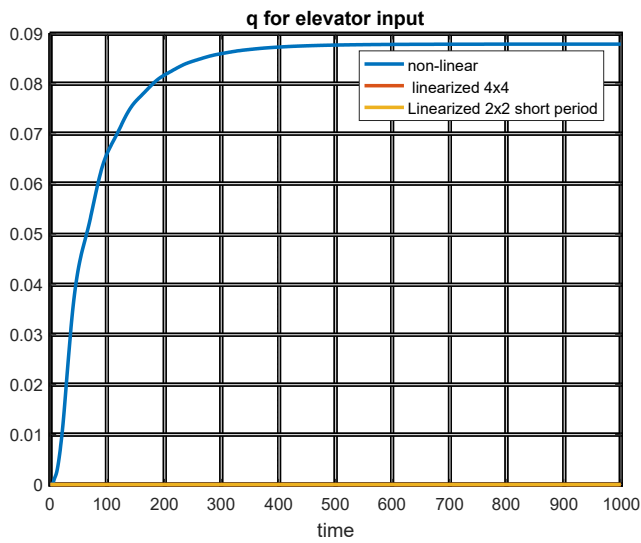


Figure 70

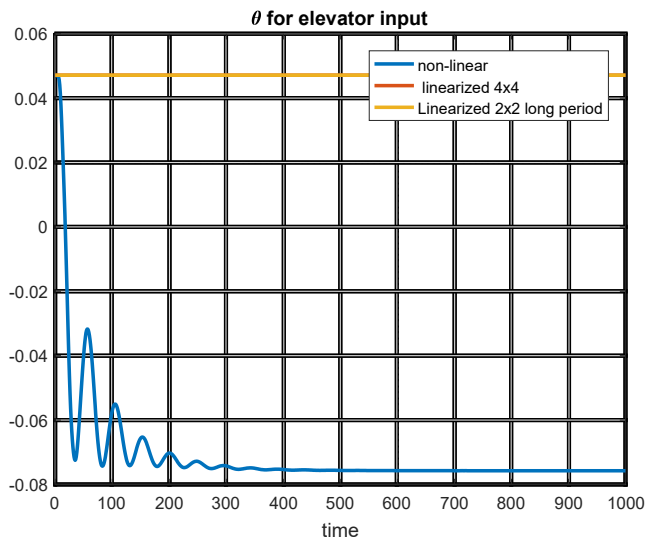


Figure 71

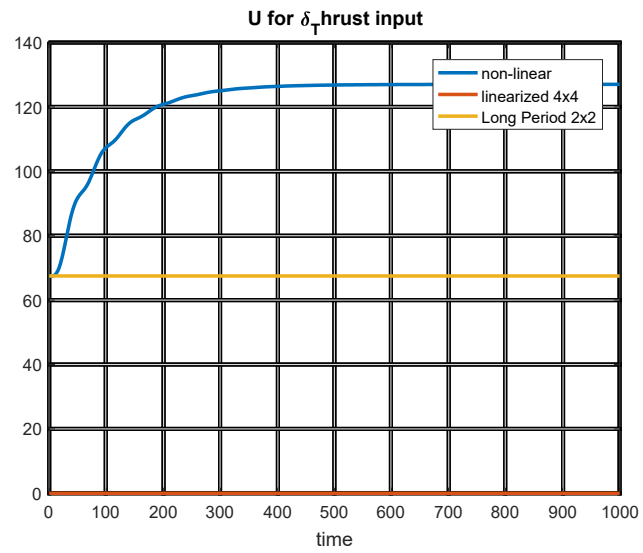


Figure 72

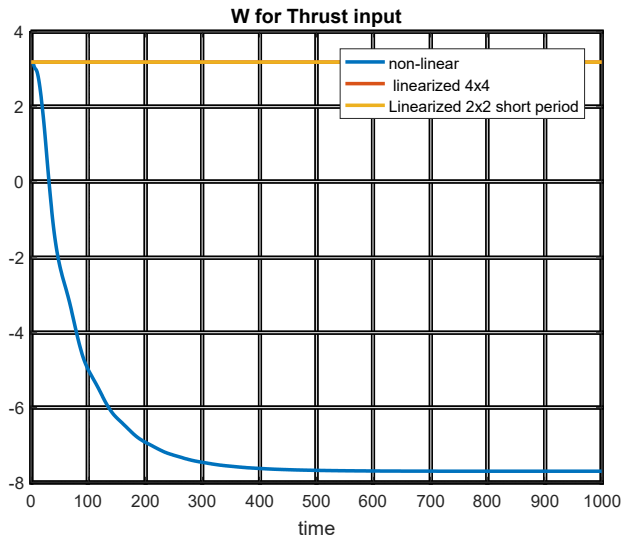


Figure 73

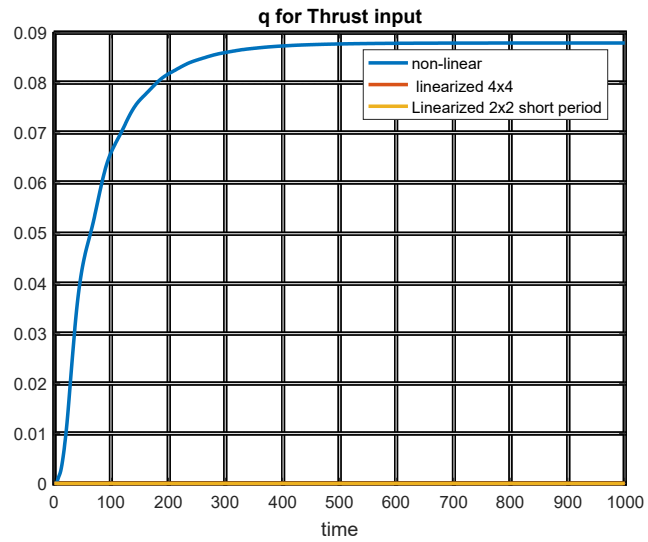


Figure 74

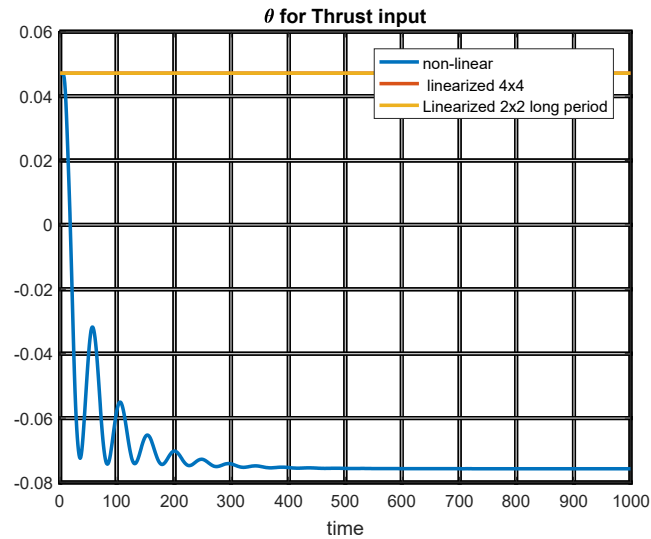


Figure 75

- For ($\delta_{th} = 20$)

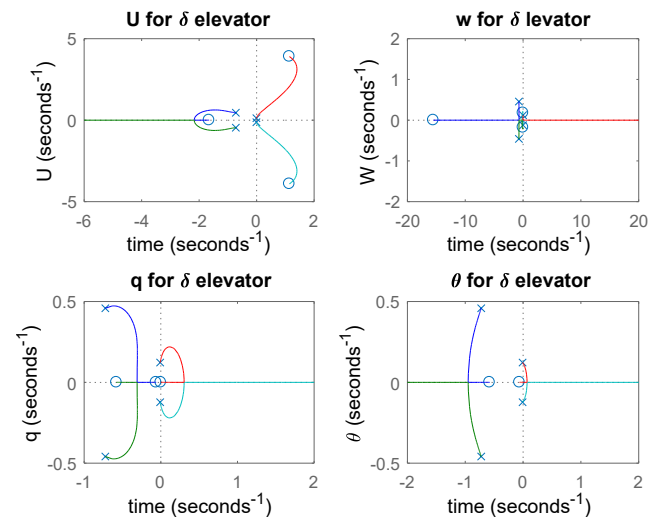


Figure 76

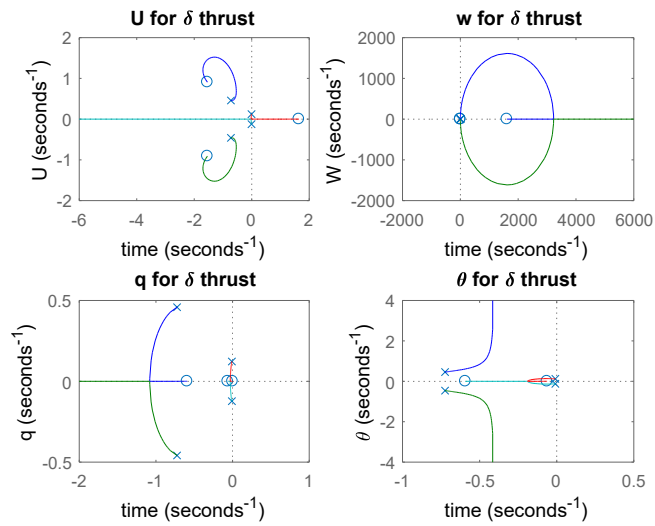


Figure 77

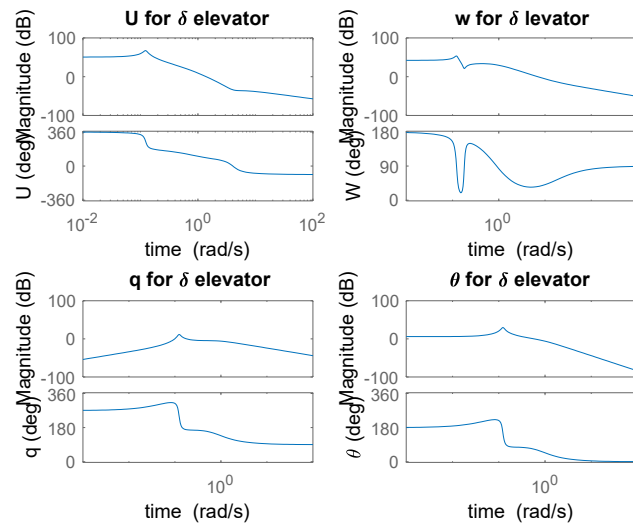


Figure 78

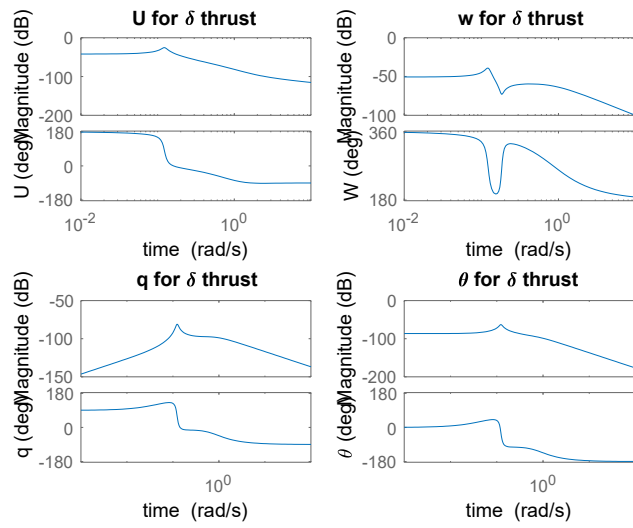


Figure 79

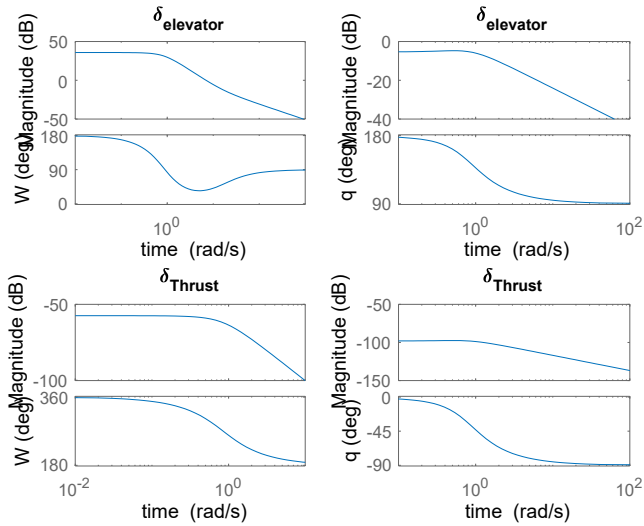


Figure 80

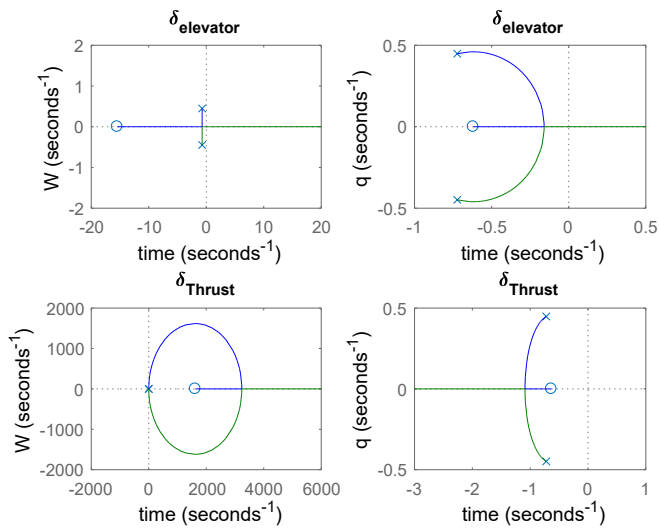


Figure 81

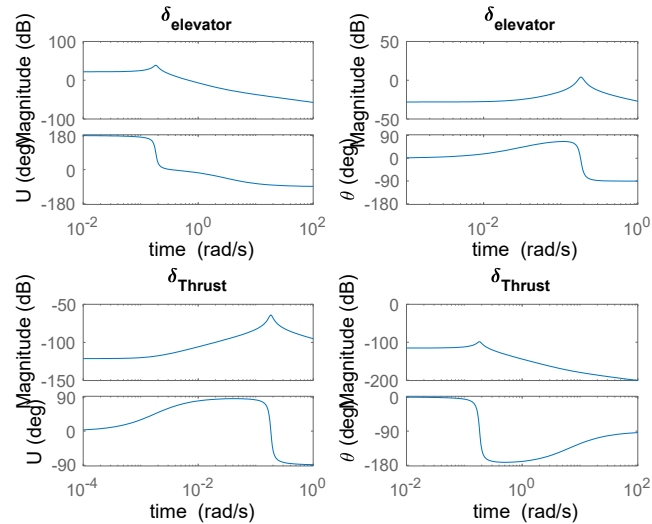


Figure 82

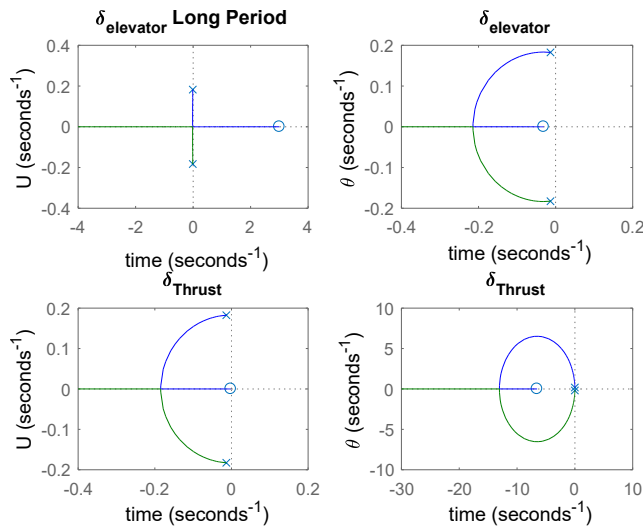


Figure 83

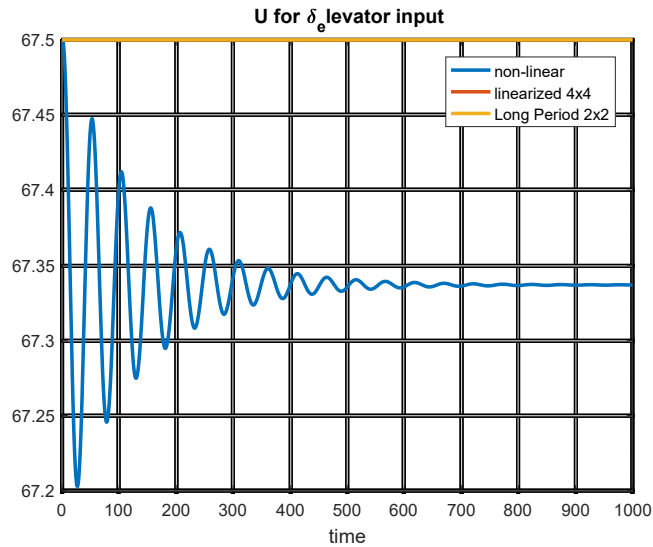


Figure 84

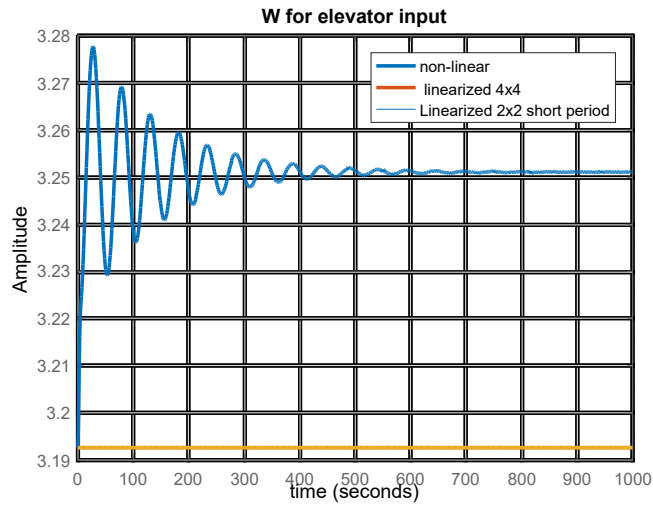


Figure 85

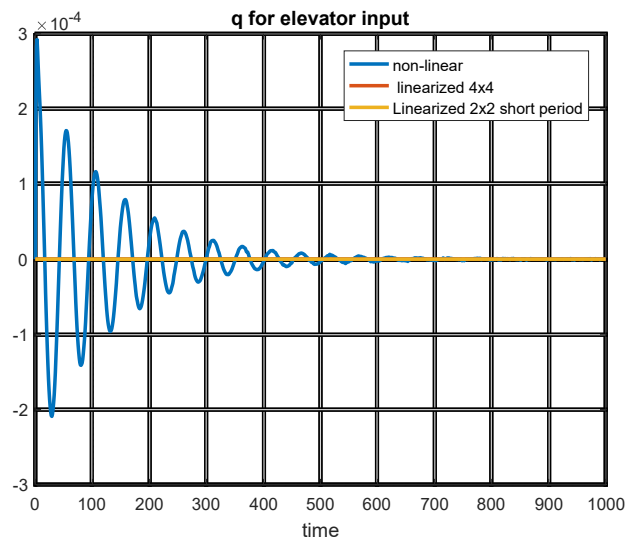


Figure 86

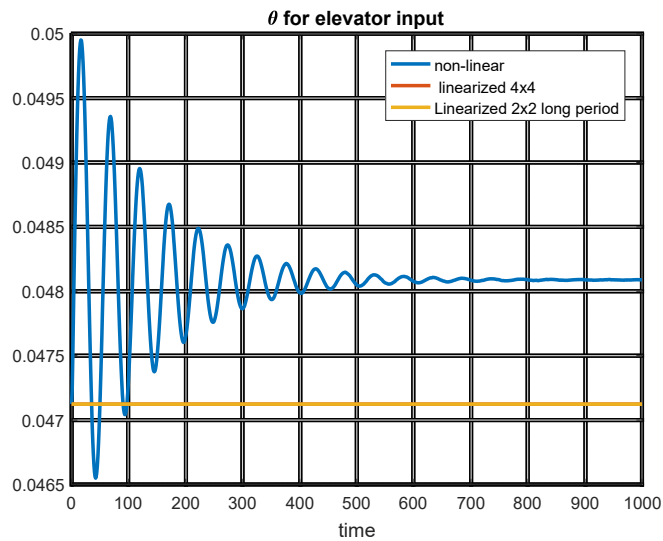


Figure 87

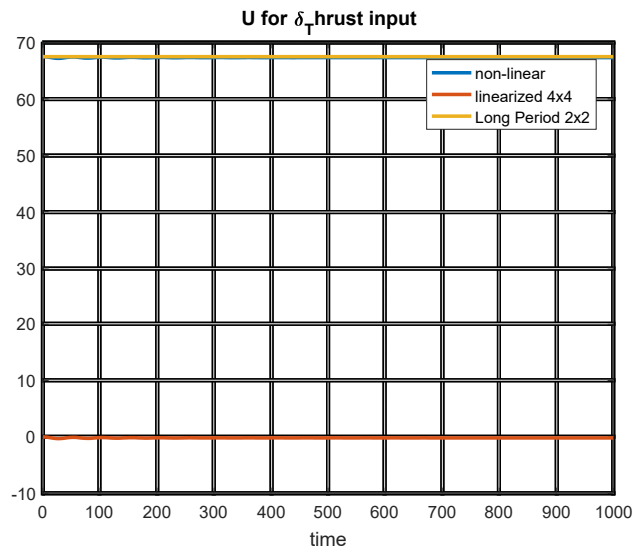


Figure 88

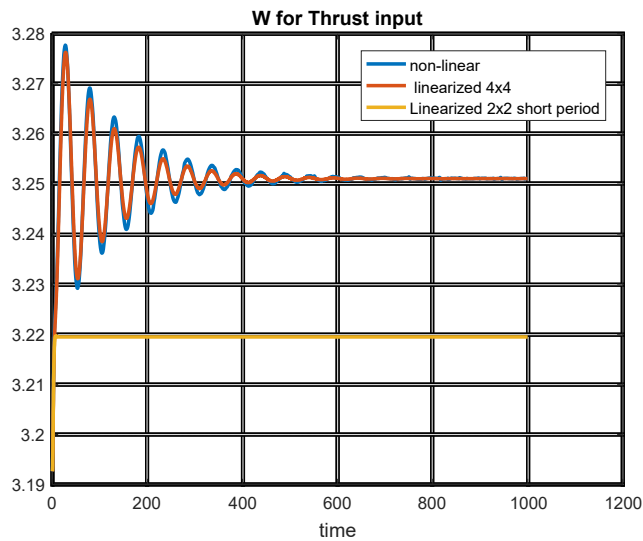


Figure 89

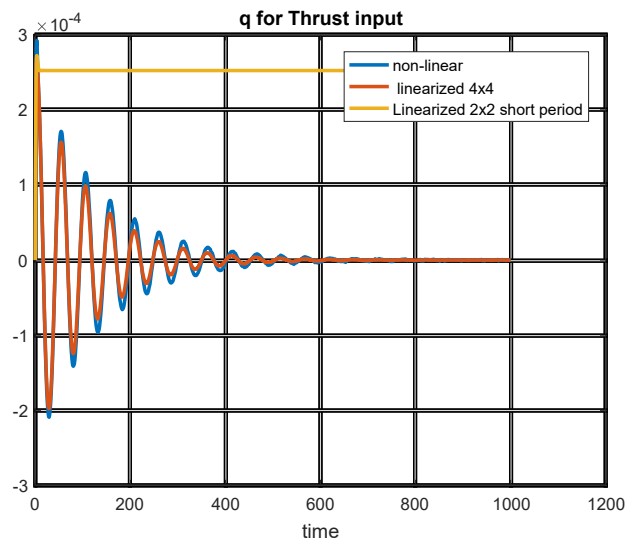


Figure 90

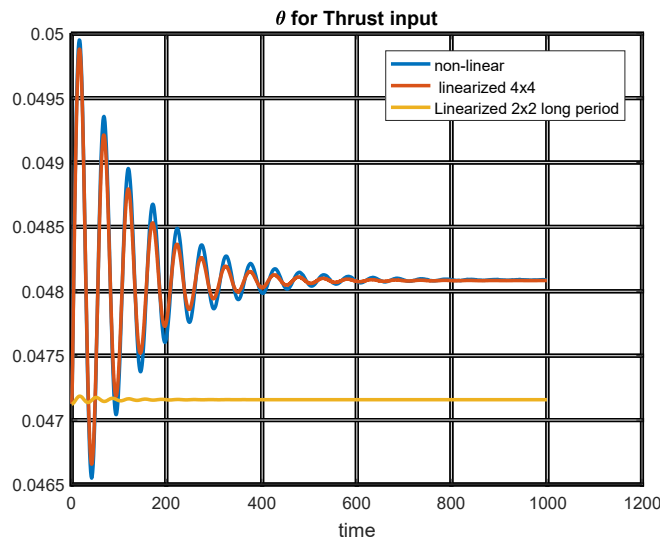


Figure 91

6.3 Lateral motion

6.3.1 Introduction (Lateral Modes)

Roll Damping – well damped

- As the plane rolls, the wing going down has an increased α (wind is effectively “coming up” more at the wing)
- Opposite effect for other wing.
- There is a difference in the lift generated by both wings \rightarrow more on side going down
- The differential lift creates a moment that tends to restore the equilibrium. Recall that $L_p < 0$
- After a disturbance, the roll rate builds up exponentially until the restoring moment balances the disturbing moment, and a steady roll is established.

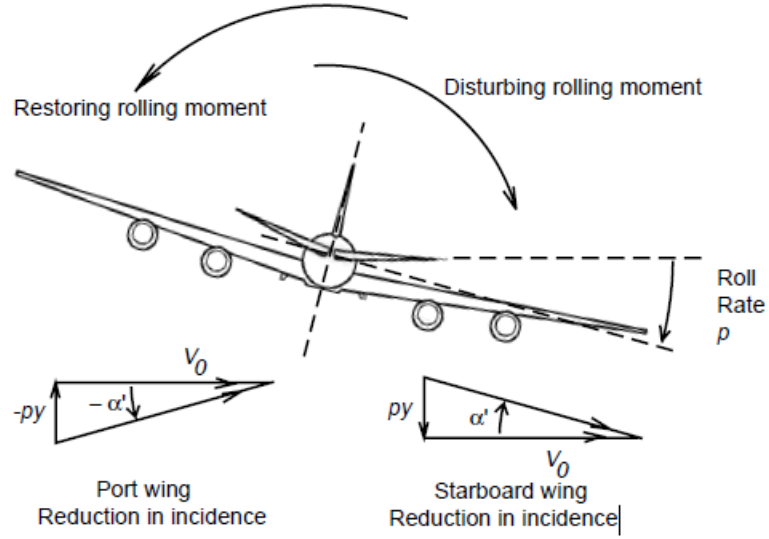


Figure 92: Roll

Spiral Mode – slow, often unstable

- From level flight, consider a disturbance that creates a small roll angle $\phi > 0 \rightarrow$ This results in a small sideslip v (vehicle slides downhill)
- Now the tail fin hits on the oncoming air at an incidence angle $\beta \rightarrow$ extra tail lift \rightarrow positive yawing moment
- Moment creates positive yaw rate that creates positive roll moment ($L_r > 0$) that increases the roll angle and tends to increase the sideslip \rightarrow makes things worse.
- If unstable and left unchecked, the aircraft would fly a slowly diverging path in roll, yaw, and altitude \Rightarrow it would tend to spiral into the ground!!

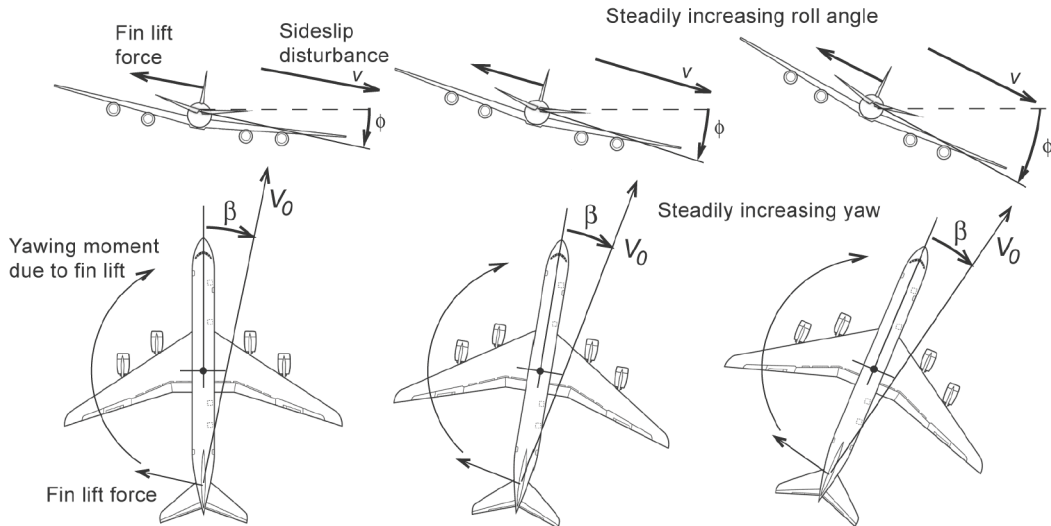


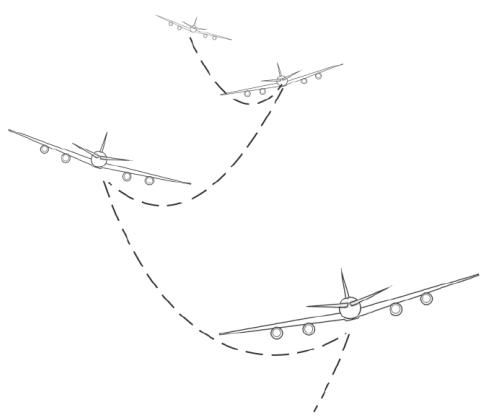
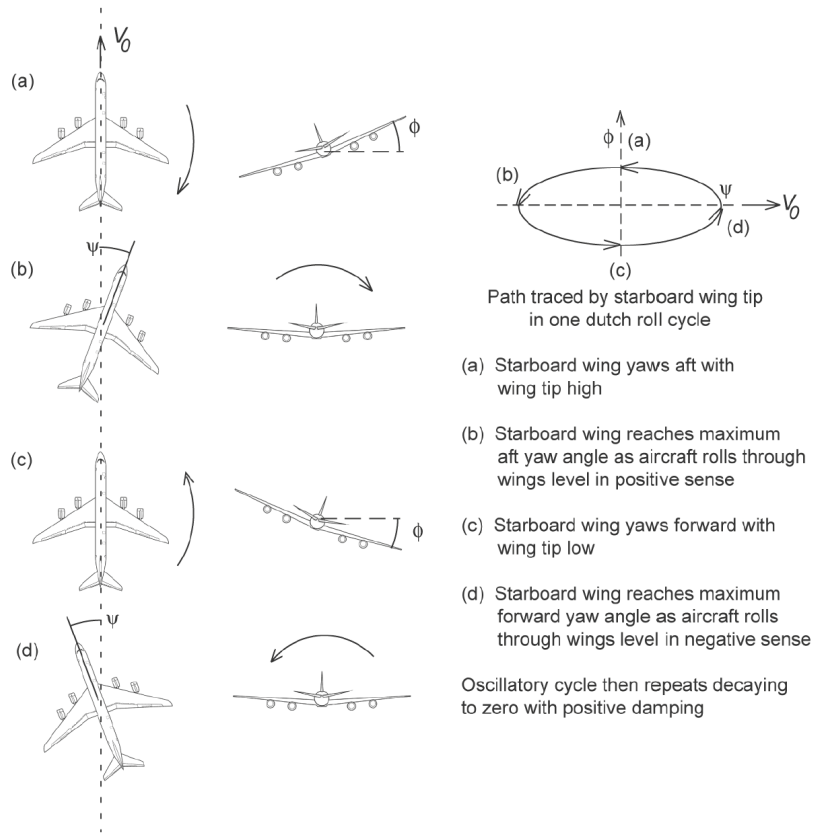
Figure 93: Spiral

- *Can get a restoring torque from the wing dihedral*
- *Want a small tail to reduce the impact of the spiral mode.*

Dutch Roll damped oscillation in yaw, that couples into roll.

• Frequency similar to longitudinal short period mode, not as well damped (fin less effective than horizontal tail).

- Consider a disturbance from straightlevel flight
→ Oscillation in yaw ψ (fin provides the aerodynamic stiffness)
→ Wings moving back and forth due to yaw motion result in oscillatory differential lift/drag (wing moving forward generates more lift) $L_r > 0$
→ Oscillation in roll φ that lags ψ by approximately 90°
⇒ Forward going wing is low Oscillating roll
⇒ sideslip in direction of low wing.



6.3.2 Our new Airplane Data (Boeing 747)

- Initial flight conditions (flight conditions 6):

$u_0 =$	205.435m/s
$v_0 =$	0
$w_0 =$	8.9609 m/s
$p_0 =$	0
$q_0 =$	0
$r_0 =$	0
$\theta_0 =$	0
$\phi_0 =$	0

- Aircraft data (FOXTROT):

mass =	288773.232 Kg
$I_{xx} =$	2.47E07
$I_{yy} =$	4.49E07
$I_{zz} =$	6.74E07
$I_{xz} =$	1.32E06

- Stability Derivatives:

Longitudinal motion		Lateral motion	
X_u	-0.0028	Y_v	-0.104
X_w	0.0482	Y_p	0
X_{δ_e}	1.15	Y_r	0
X_{δ_T}	5.5E-05	Y_β	-70.4
Z_u	-0.0832	Y_{δ_R}	0.0142
Z_w	-0.539	L_β	-2.96
$Z_{\dot{w}}$	0.0156	L_p	-0.804
Z_q	-8.09	L_r	0.317
Z_{δ_e}	-26.4	L_{δ_A}	0.21
Z_{δ_T}	-2.20E-06	L_v	-0.00941
M_u	8.85E-05	L_{δ_R}	0.211
M_w	-0.0019	N_β	0.923
$M_{\dot{W}}$	-0.000155	N_p	-0.0531
M_q	-0.535	N_r	-0.193
M_{δ_E}	-1.69	N_v	0.004492905
$M_{\delta_{th}}$	3.02E-07	N_{δ_a}	0.0199
		N_{δ_r}	-0.616

The stick fixed lateral motion of an airplane distributed from its equilibrium state is a complicated combination of rolling, yawing, and sideslipping motions. Three potential lateral dynamic instabilities are of interest to the airplane designer: directional divergence, spiral divergence, and the Dutch roll oscillation.

The lateral equations of motion can be written in the state space form as follows:

$$\left(\frac{d}{dt} - Y_v \right) \Delta v - Y_p \Delta p + (u_0 - Y_r) \Delta r - g \cos \theta_0 \Delta \phi = Y_{\delta_r} \Delta \delta_r \quad (19)$$

$$-L_v \Delta v + \left(\frac{d}{dt} - L_p \right) \Delta p - \left(\frac{I_{xz}}{I_x} \frac{d}{dt} + L_r \right) \Delta r = L_{\delta_a} \Delta \delta_a + L_{\delta_r} \Delta \delta_r \quad (20)$$

$$-N_v \Delta v - \left(\frac{I_{xz}}{I_z} \frac{d}{dt} + N_p \right) \Delta p + \left(\frac{d}{dt} - N_r \right) \Delta r = N_{\delta_a} \Delta \delta_a + N_{\delta_r} \Delta \delta_r \quad (21)$$

Rearranging and collecting terms, this equation can be written in the state variable form:

$$\dot{X} = A X + B u \quad (22)$$

where $A = \begin{bmatrix} Y_v & Y_p & -(u_0 - Y_r) & g \cos\theta_0 \\ L_{v^*} + \frac{I_{xz}}{I_x} N_{v^*} & L_{p^*} + \frac{I_{xz}}{I_x} N_{p^*} & L_{r^*} + \frac{I_{xz}}{I_x} N_{r^*} & 0 \\ N_{v^*} + \frac{I_{xz}}{I_z} L_{v^*} & N_{p^*} + \frac{I_{xz}}{I_z} L_{p^*} & N_{r^*} + \frac{I_{xz}}{I_z} L_{r^*} & 0 \\ 0 & 1 & 0 & 0 \end{bmatrix}$

$$B = \begin{bmatrix} 0 & Y_{\delta_r} \\ L_{\delta_a^*} + \frac{I_{xz}}{I_x} N_{\delta_a^*} & L_{\delta_r^*} + \frac{I_{xz}}{I_x} N_{\delta_r^*} \\ N_{\delta_a^*} + \frac{I_{xz}}{I_z} L_{\delta_a^*} & N_{\delta_r^*} + \frac{I_{xz}}{I_z} L_{\delta_r^*} \\ 0 & 0 \end{bmatrix}$$

So the complete state space model can be written in the following form :

$$\begin{bmatrix} \Delta \dot{v} \\ \Delta \dot{p} \\ \Delta \dot{r} \\ \Delta \dot{\phi} \end{bmatrix} = \begin{bmatrix} Y_v & Y_p & -(u_0 - Y_r) & g \cos\theta_0 \\ L_{v^*} + \frac{I_{xz}}{I_x} N_{v^*} & L_{p^*} + \frac{I_{xz}}{I_x} N_{p^*} & L_{r^*} + \frac{I_{xz}}{I_x} N_{r^*} & 0 \\ N_{v^*} + \frac{I_{xz}}{I_z} L_{v^*} & N_{p^*} + \frac{I_{xz}}{I_z} L_{p^*} & N_{r^*} + \frac{I_{xz}}{I_z} L_{r^*} & 0 \\ 0 & 1 & 0 & 0 \end{bmatrix} \begin{bmatrix} \Delta v \\ \Delta p \\ \Delta r \\ \Delta \phi \end{bmatrix} + \begin{bmatrix} 0 & Y_{\delta_r} \\ L_{\delta_a^*} + \frac{I_{xz}}{I_x} N_{\delta_a^*} & L_{\delta_r^*} + \frac{I_{xz}}{I_x} N_{\delta_r^*} \\ N_{\delta_a^*} + \frac{I_{xz}}{I_z} L_{\delta_a^*} & N_{\delta_r^*} + \frac{I_{xz}}{I_z} L_{\delta_r^*} \\ 0 & 0 \end{bmatrix} \begin{bmatrix} \Delta \delta_a \\ \Delta \delta_r \end{bmatrix}$$

The starred derivatives are defined as follows:

$$L_{v^*} = \frac{L_v}{\left[1 - \left(\frac{I_{xz}^2}{I_x I_z}\right)\right]}, \quad N_{v^*} = \frac{N_v}{\left[1 - \left(\frac{I_{xz}^2}{I_x I_z}\right)\right]} \text{ and so on}$$

For our airplane the ratio $\left(\frac{I_{xz}^2}{I_x I_z}\right)$ is very small in comparison to 1, so we neglected it with respect to 1. In other words, in our case $L_{v^*} = L_v$, $N_{v^*} = N_v$ and so on.

.For $I_{xz} = 0$, the equations of motion reduce to the following form:

$$\begin{bmatrix} \Delta \dot{v} \\ \Delta \dot{p} \\ \Delta \dot{r} \\ \Delta \dot{\phi} \end{bmatrix} = \begin{bmatrix} Y_v & Y_p & -(u_0 - Y_r) & g \cos\theta_0 \\ L_v & L_p & L_r & 0 \\ N_v & N_p & N_r & 0 \\ 0 & 1 & 0 & 0 \end{bmatrix} \begin{bmatrix} \Delta v \\ \Delta p \\ \Delta r \\ \Delta \phi \end{bmatrix} + \begin{bmatrix} 0 & Y_{\delta_r} \\ L_{\delta_a} & L_{\delta_r} \\ N_{\delta_a} & N_{\delta_r} \\ 0 & 0 \end{bmatrix} \begin{bmatrix} \Delta \delta_a \\ \Delta \delta_r \end{bmatrix}$$

It is sometimes convenient to use the sideslip angle $\Delta\beta$ instead of the side velocity Δv . These two quantities are related to each other in the following way:

$$\Delta\beta \approx \tan^{-1} \left(\frac{\Delta v}{u_0} \right) \approx \frac{\Delta v}{u_0} \quad (23)$$

Using eqn (25)

$$\begin{bmatrix} \Delta \dot{\beta} \\ \Delta \dot{p} \\ \Delta \dot{r} \\ \Delta \dot{\phi} \end{bmatrix} = \begin{bmatrix} \frac{Y_\beta}{U_0} & \frac{Y_p}{U_0} & -(1 - \frac{Y_r}{U_0}) & \frac{g}{U_0} \\ L_\beta & L_p & L_r & 0 \\ N_\beta & N_p & N_r & 0 \\ 0 & 1 & 0 & 0 \end{bmatrix} \begin{bmatrix} \Delta \beta \\ \Delta p \\ \Delta r \\ \Delta \phi \end{bmatrix} + \begin{bmatrix} Y_{\delta_a}^* & Y_{\delta_r}^* \\ L_{\delta_a}^* & L_{\delta_r}^* \\ N_{\delta_a}^* & N_{\delta_r}^* \\ 0 & 0 \end{bmatrix} \begin{bmatrix} \Delta \delta_a \\ \Delta \delta_r \end{bmatrix}$$

By adding the ψ d.o.f.

$$\begin{bmatrix} \Delta \dot{\beta} \\ \Delta \dot{p} \\ \Delta \dot{r} \\ \Delta \dot{\phi} \\ \Delta \dot{\psi} \end{bmatrix} = \begin{bmatrix} \frac{Y_\beta}{U_0} & \frac{Y_p}{U_0} & -(1 - \frac{Y_r}{U_0}) & \frac{g \cos(\theta_0)}{U_0} & 0 \\ L_\beta & L_p + \frac{I_{xz}}{I_x} N_p & L_r + \frac{I_{xz}}{I_x} N_r & 0 & 0 \\ N_\beta & N_p + \frac{I_{xz}}{I_z} L_p & N_r + \frac{I_{xz}}{I_z} L_p & N_r + \frac{I_{xz}}{I_z} L_r & 0 \\ 0 & 1 & \tan(\theta_0) & 0 & 0 \\ 0 & 0 & \sec(\theta_0) & 0 & 0 \end{bmatrix} \begin{bmatrix} \Delta \beta \\ \Delta p \\ \Delta r \\ \Delta \phi \\ \Delta \psi \end{bmatrix} + \begin{bmatrix} 0 & \frac{Y_{\delta_r}}{u_0} \\ L_{\delta_a} & L_{\delta_r} \\ N_{\delta_a} & N_{\delta_r} \\ 0 & 0 \\ 0 & 0 \end{bmatrix} \begin{bmatrix} \Delta \delta_a \\ \Delta \delta_r \end{bmatrix}$$

Finally our A matrix in numbers is:

$$A = \begin{bmatrix} -0.3427 & 0 & -1 & 0.0478 \\ -2.9138 & -0.8077 & 0.307 & 0 \\ 0.8661 & -0.0689 & -0.1870 & 0 \\ 0 & 1 & 0 & 0 \end{bmatrix}$$

6.4 Approximations

6.4.1 Three degrees of freedom :

Dutch roll (β, p, r)

$$\begin{bmatrix} \dot{\Delta\beta} \\ \dot{\Delta p} \\ \dot{\Delta r} \end{bmatrix} = \begin{bmatrix} \frac{Y_\beta}{U_0} & \frac{Y_p}{U_0} & -\left(1 - \frac{Y_r}{u_0}\right) \\ \dot{L}_\beta & \dot{L}_p & L_r \\ \dot{N}_\beta & \dot{N}_p & \dot{N}_r \end{bmatrix} \begin{bmatrix} \Delta\beta \\ \Delta p \\ \Delta r \end{bmatrix} + \begin{bmatrix} 0 & \frac{Y_{\delta_r}}{u_0} \\ L_{\delta_a} & L_{\delta_r} \\ N_{\delta_a} & N_{\delta_r} \end{bmatrix} \begin{bmatrix} \Delta\delta_a \\ \Delta\delta_r \end{bmatrix}$$

Spiral (p, r, ϕ)

$$\begin{bmatrix} \dot{\Delta p} \\ \dot{\Delta r} \\ \dot{\Delta\phi} \end{bmatrix} = \begin{bmatrix} \dot{L}_p & \dot{L}_r & 0 \\ \dot{N}_p & \dot{N}_r & 0 \\ 0 & 0 & 0 \end{bmatrix} \begin{bmatrix} \Delta p \\ \Delta r \\ \Delta\phi \end{bmatrix} + \begin{bmatrix} L_{\delta_a} & L_{\delta_r} \\ N_{\delta_a} & N_{\delta_r} \\ 0 & 0 \end{bmatrix} \begin{bmatrix} \Delta\delta_a \\ \Delta\delta_r \end{bmatrix}$$

6.4.2 Two degrees of freedom :

Dutch roll (β, r)

$$\begin{bmatrix} \dot{\Delta\beta} \\ \dot{\Delta r} \end{bmatrix} = \begin{bmatrix} \frac{Y_\beta}{U_0} & -\left(1 - \frac{Y_r}{u_0}\right) \\ \dot{N}_\beta & \dot{N}_r \end{bmatrix} \begin{bmatrix} \Delta\beta \\ \Delta r \end{bmatrix} + \begin{bmatrix} 0 & \frac{Y_{\delta_r}}{u_0} \\ N_{\delta_a} & N_{\delta_r} \end{bmatrix} \begin{bmatrix} \Delta\delta_a \\ \Delta\delta_r \end{bmatrix}$$

Spiral-Roll Approximation(p, ϕ)

$$\begin{bmatrix} \dot{\Delta p} \\ \dot{\Delta\phi} \end{bmatrix} = \begin{bmatrix} \dot{L}_p & 0 \\ 1 & 0 \end{bmatrix} \begin{bmatrix} \Delta p \\ \Delta\phi \end{bmatrix} + \begin{bmatrix} \dot{L}_{\delta_a} \\ 0 \end{bmatrix} [\Delta\delta_a]$$

6.4.3 One degree of freedom

Pure rolling (p)

$$\dot{\Delta p} = \dot{L}_p \Delta p + \dot{L}_{\delta_a} \Delta\delta_a$$

6.4.4 Transfer Functions

Linearized 4x4

$$\frac{\dot{\Delta\beta}}{\delta_a} = \frac{-0.02402s^2 + 0.005235s + 0.0022391}{s^4 + 1.337s^3 + 1.379s^2 + 1.098s + 0.01332}$$

$$\frac{\dot{\Delta p}}{\delta_a} = \frac{0.2113s^3 + 0.1193s^2 + 0.2691s}{s^4 + 1.337s^3 + 1.379s^2 + 1.098s + 0.01332}$$

$$\frac{\dot{\Delta r}}{\delta_a} = \frac{0.02402s^3 + 0.01309s^2 + 0.001663s + 0.01208}{s^4 + 1.337s^3 + 1.379s^2 + 1.098s + 0.01332}$$

$$\frac{\dot{\Delta\phi}}{\delta_a} = \frac{0.2113s^2 + 0.1193s + 0.2691}{s^4 + 1.337s^3 + 1.379s^2 + 1.098s + 0.01332}$$

$$\frac{\dot{\Delta\psi}}{\delta_r} = \frac{6.912e-05s^3 + 0.6126s^2 + 0.5155s - 0.007388}{s^4 + 1.337s^3 + 1.379s^2 + 1.098s + 0.01332}$$

$$\frac{\dot{\Delta p}}{\delta_r} = \frac{0.1784s^3 - 0.09379s^2 - 1.683s}{s^4 + 1.337s^3 + 1.379s^2 + 1.098s + 0.01332}$$

$$\frac{\dot{\Delta r}}{\delta_r} = \frac{-0.6125s^3 - 0.7168s^2 - 0.1737s - 0.07785}{s^4 + 1.337s^3 + 1.379s^2 + 1.098s + 0.01332}$$

$$\frac{\dot{\Delta\phi}}{\delta_r} = \frac{0.1784s^2 - 0.09379s - 1.683}{s^4 + 1.337s^3 + 1.379s^2 + 1.098s + 0.01332}$$

Dutch Roll 3x3 d.o.f

$$\begin{aligned}\frac{\Delta\dot{\beta}}{\delta_a} &= \frac{-0.0199s - 0.0048491}{s^3 + 1.34s^2 + 1.437s + 0.9582} \\ \frac{\Delta\dot{p}}{\delta_a} &= \frac{0.21s^2 + 0.1188s + 0.26882}{s^3 + 1.34s^2 + 1.437s + 0.9582} \\ \frac{\Delta\dot{r}}{\delta_a} &= \frac{0.0199s^2 + 0.01167s + 0.0016623}{s^3 + 1.34s^2 + 1.437s + 0.9582}\end{aligned}$$

$$\begin{aligned}\frac{\Delta\dot{\beta}}{\delta_r} &= \frac{6.912e-05s^2 + 0.6161s + 0.50651}{s^3 + 1.34s^2 + 1.437s + 0.9582} \\ \frac{\Delta\dot{p}}{\delta_r} &= \frac{0.211s^2 - 0.08245s - 1.6822}{s^3 + 1.34s^2 + 1.437s + 0.9582} \\ \frac{\Delta\dot{r}}{\delta_r} &= \frac{-0.616s^2 - 0.7175s - 0.17353}{s^3 + 1.34s^2 + 1.437s + 0.9582}\end{aligned}$$

Dutch Roll 2 d.o.f

$$\begin{aligned}\frac{\Delta\dot{\beta}}{\delta_a} &= \frac{-0.0199}{s^2 + 0.5357s + 0.9891} \\ \frac{\Delta\dot{r}}{\delta_a} &= \frac{0.0199s + 0.006819}{s^2 + 0.5357s + 0.9891}\end{aligned}$$

$$\begin{aligned}\frac{\Delta\dot{\beta}}{\delta_r} &= \frac{6.912e-05s + 0.616}{s^2 + 0.5357s + 0.9891} \\ \frac{\Delta\dot{r}}{\delta_r} &= \frac{-0.616s - 0.211}{s^2 + 0.5357s + 0.9891}\end{aligned}$$

Spiral 3 d.o.f

$$\begin{aligned}\frac{\Delta\dot{p}}{\delta_a} &= \frac{0.21s + 0.04684}{s^2 + 0.997s + 0.172} \\ \frac{\Delta\dot{r}}{\delta_a} &= \frac{0.0199s + 0.004849}{s^2 + 0.997s + 0.172}\end{aligned}$$

$$\begin{aligned}\frac{\Delta\dot{p}}{\delta_r} &= \frac{0.211s - 0.1545}{s^2 + 0.997s + 0.172} \\ \frac{\Delta\dot{r}}{\delta_r} &= \frac{-0.616s - 0.5065}{s^2 + 0.997s + 0.172}\end{aligned}$$

Spiral 2 d.o.f

$$\begin{aligned}\frac{\Delta\dot{p}}{\delta_a} &= \frac{0.21}{s + 0.804} \\ \frac{\Delta\dot{\phi}}{\delta_a} &= \frac{0.21}{s^2 + 0.804s}\end{aligned}$$

6.5 Response

- For $\delta_a = 2^\circ$ (Simulation time = 200 sec.)

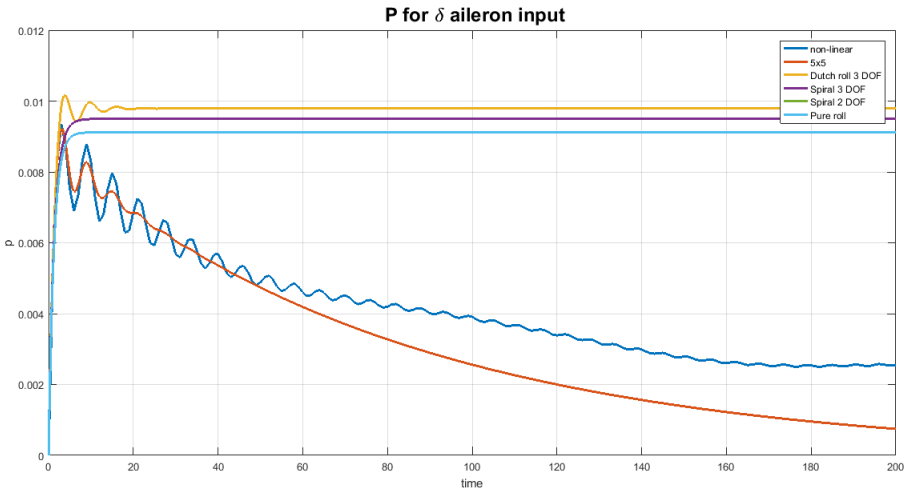


Figure 94: P

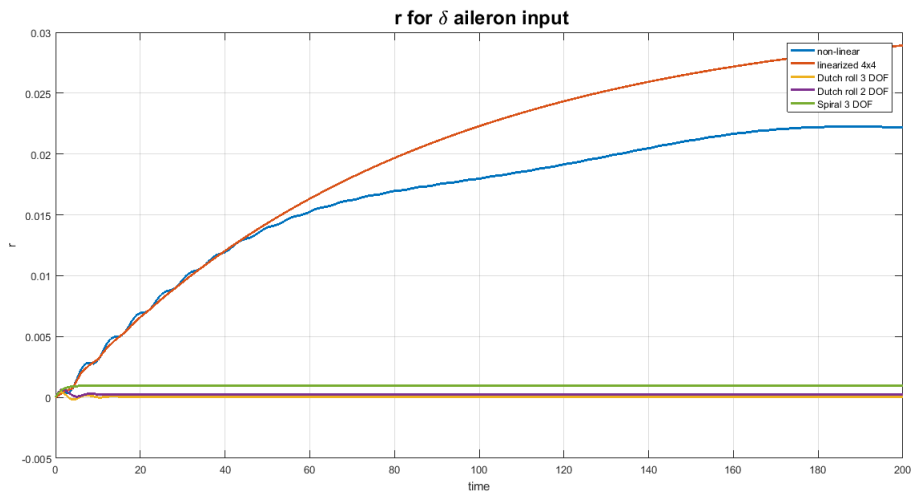


Figure 95: r

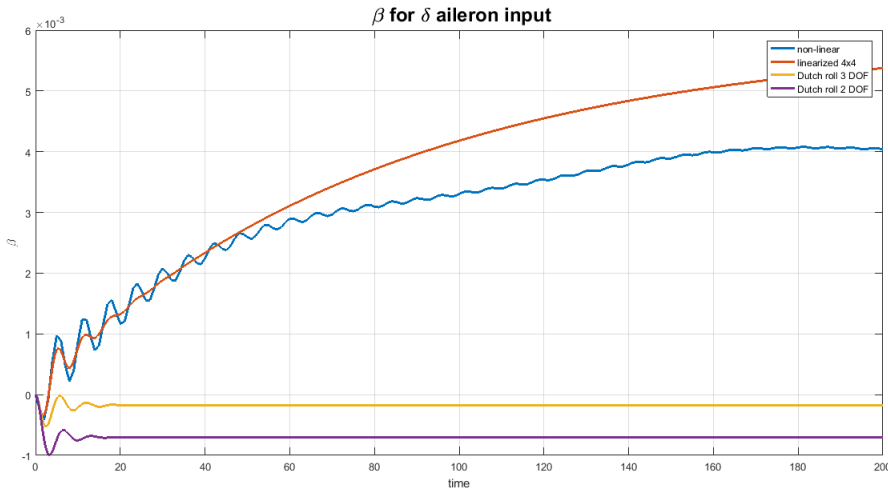


Figure 96: β

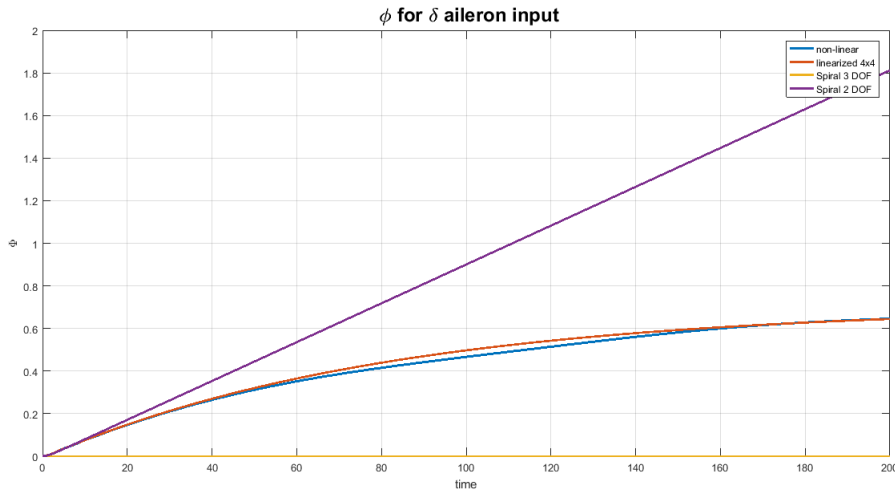


Figure 97: ϕ

- For $\delta_a = 2^0$ (Simulation time = 1000 sec.)

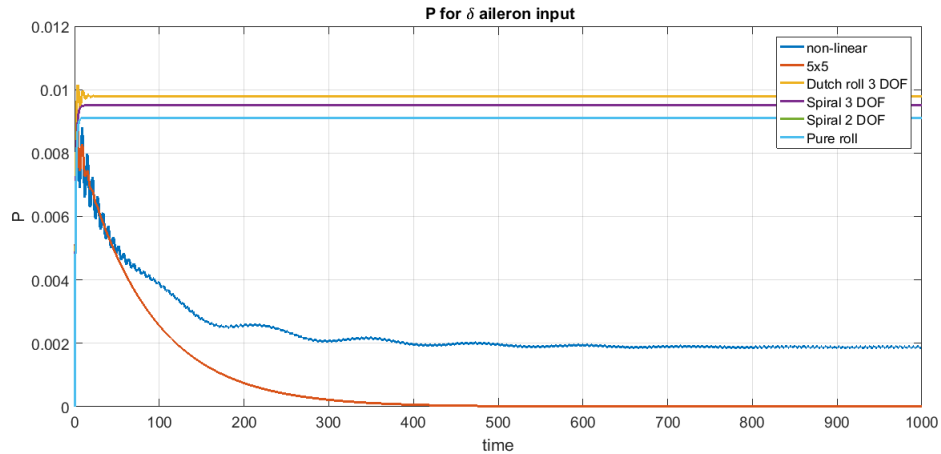


Figure 98: P

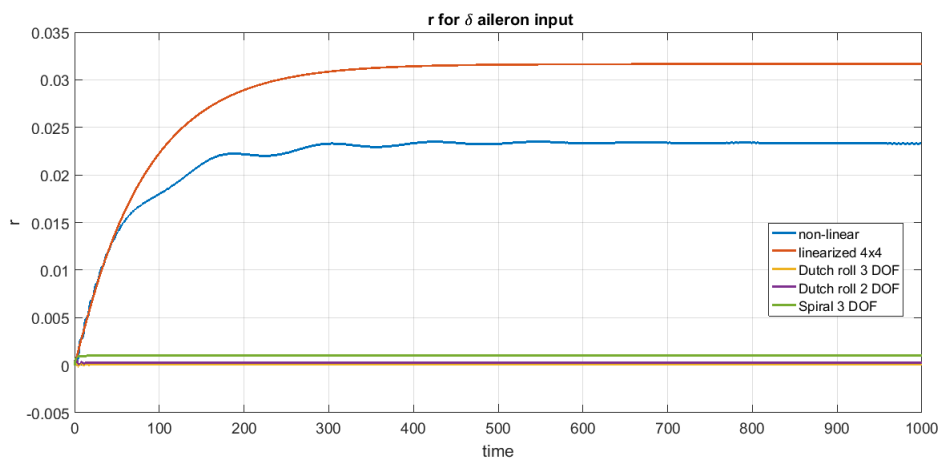


Figure 99: r

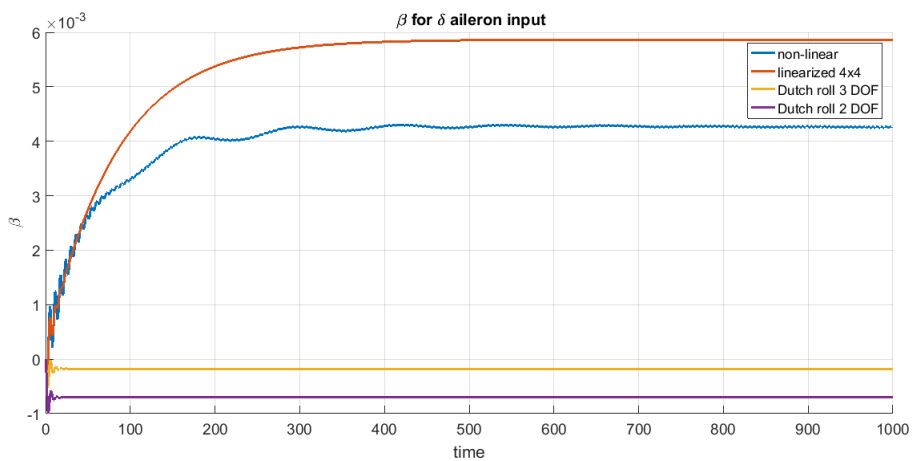


Figure 100: β

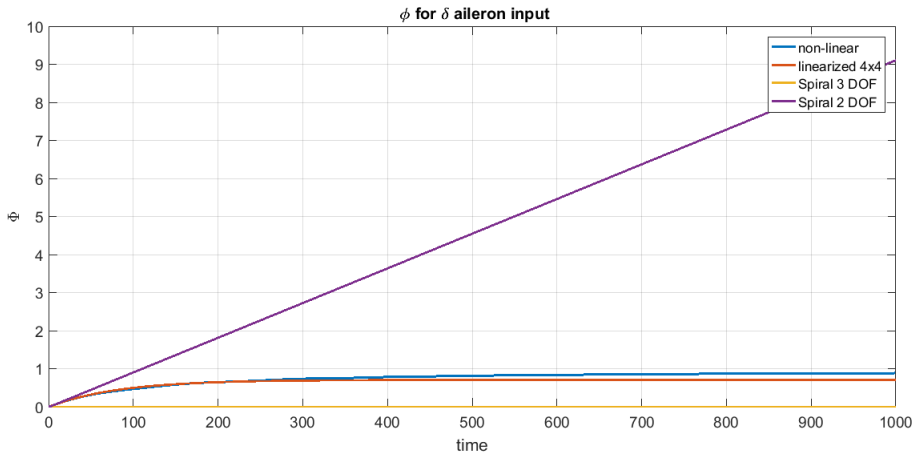


Figure 101: ϕ

- For $\delta_a = 5^0$ (Simulation time = 200 sec.)

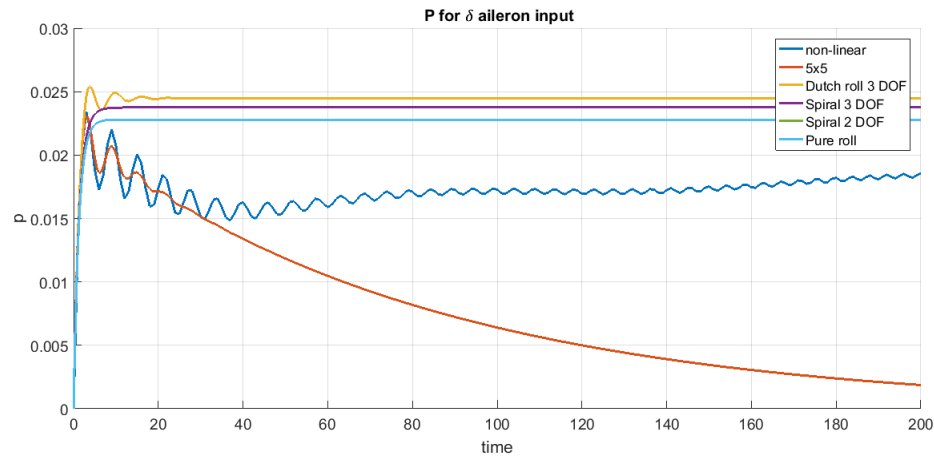


Figure 102: P

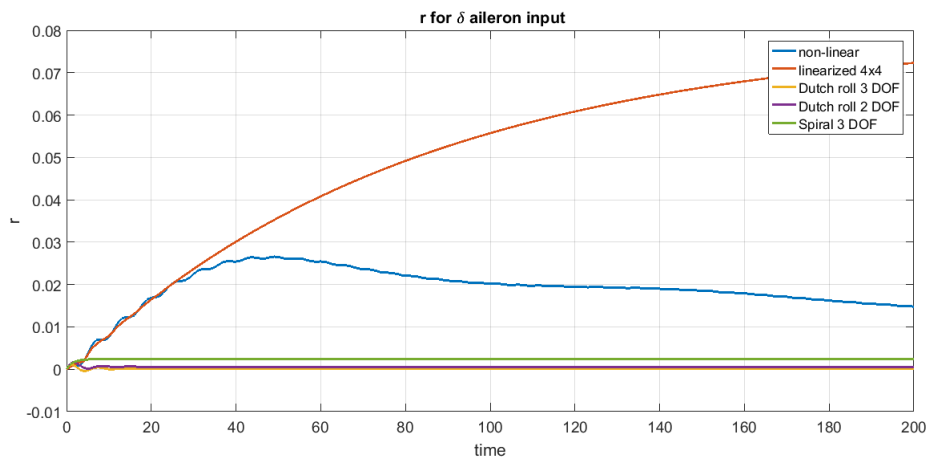


Figure 103: r

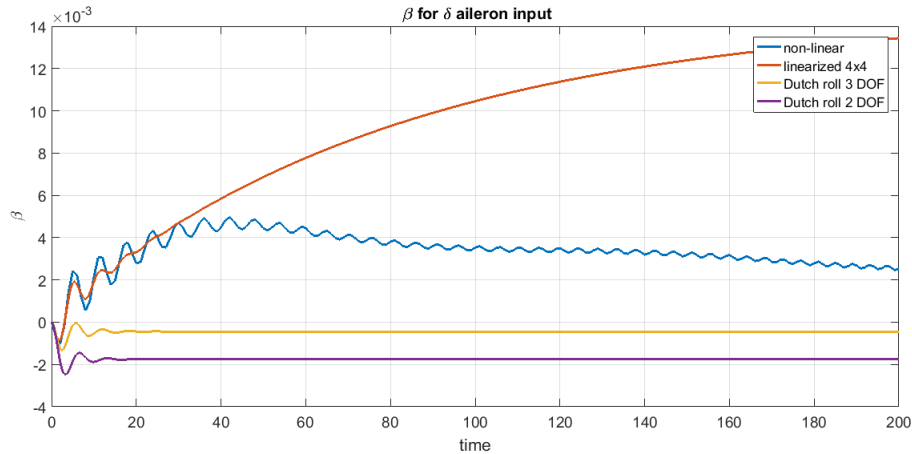


Figure 104: β

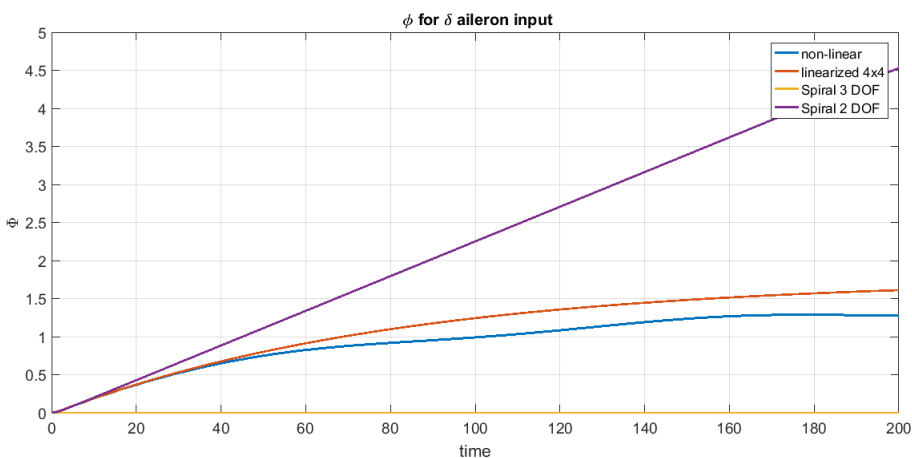


Figure 105: ϕ

- For $\delta_a = 5^0$ (Simulation time = 1000 sec.)

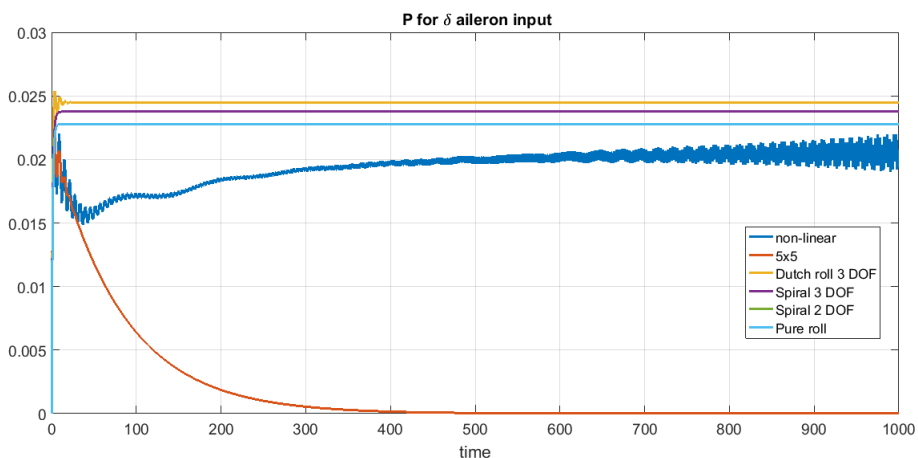


Figure 106: P

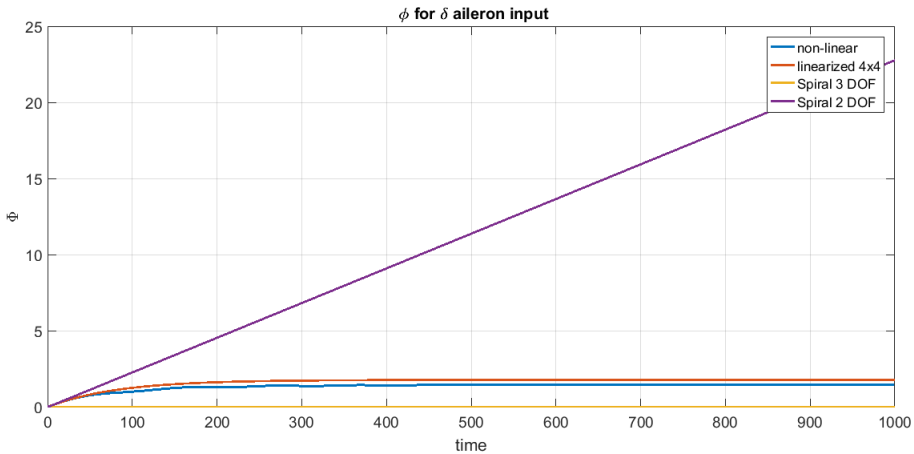


Figure 109: ϕ

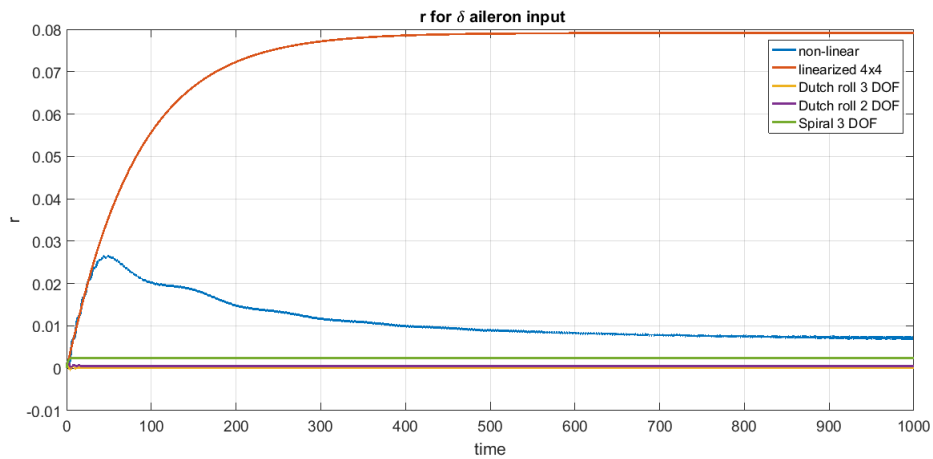


Figure 107: r

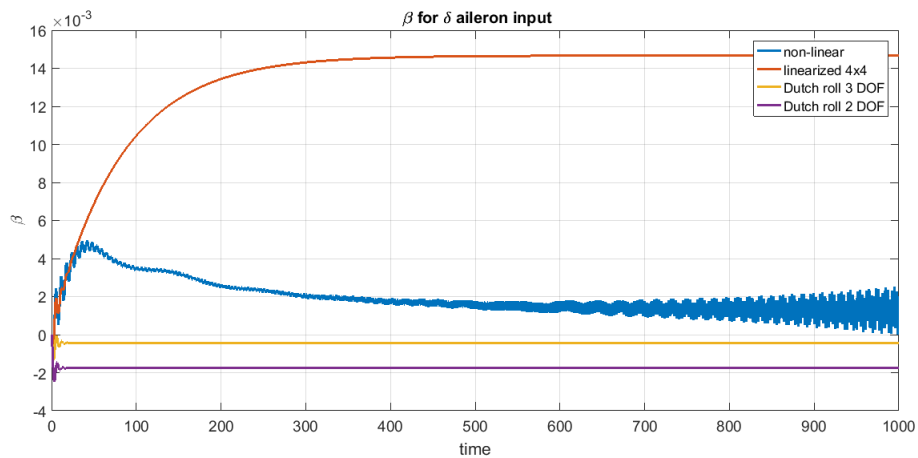


Figure 108: β

- For $\delta_r = 2^0$ (Simulation time = 200 sec.)

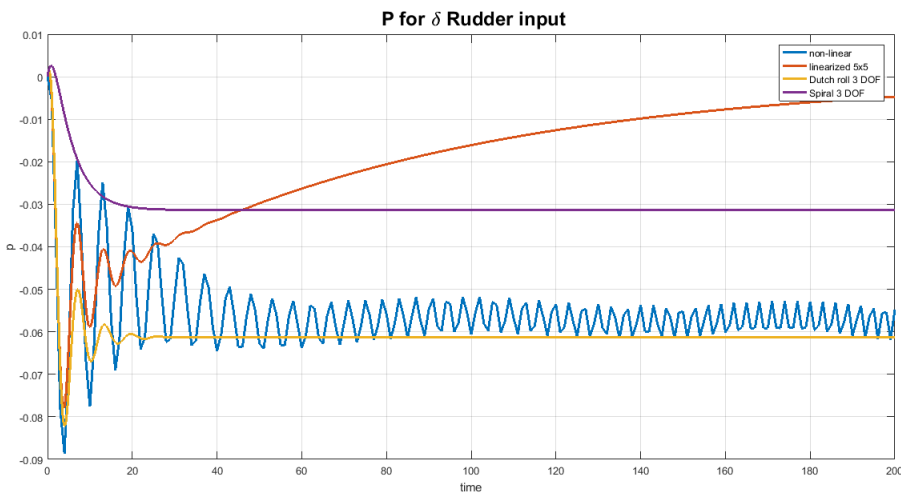


Figure 110: P

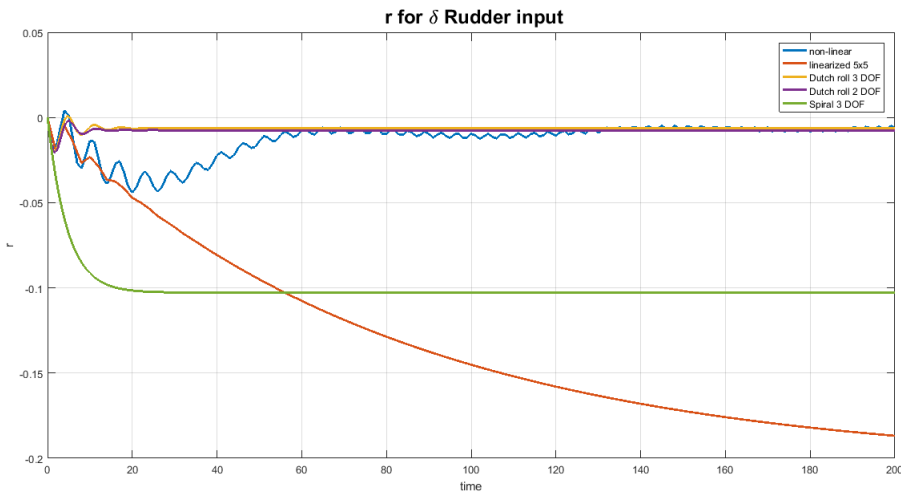


Figure 111: r

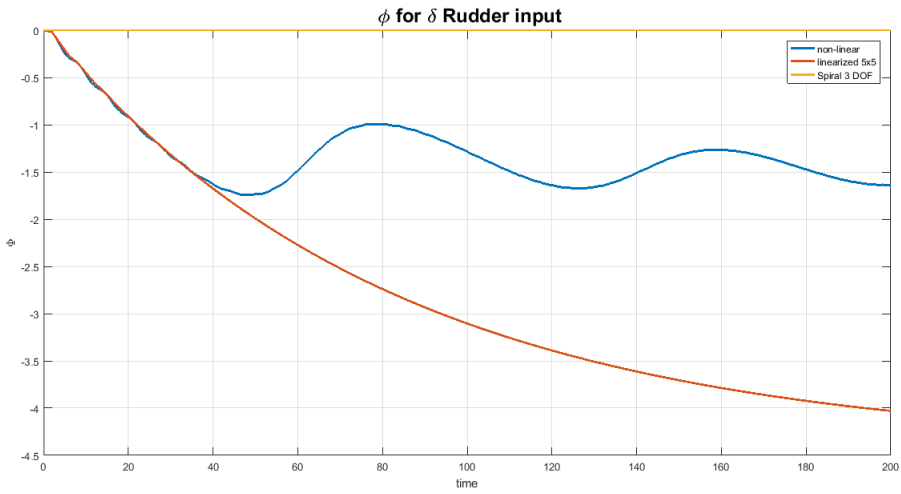


Figure 113: ϕ

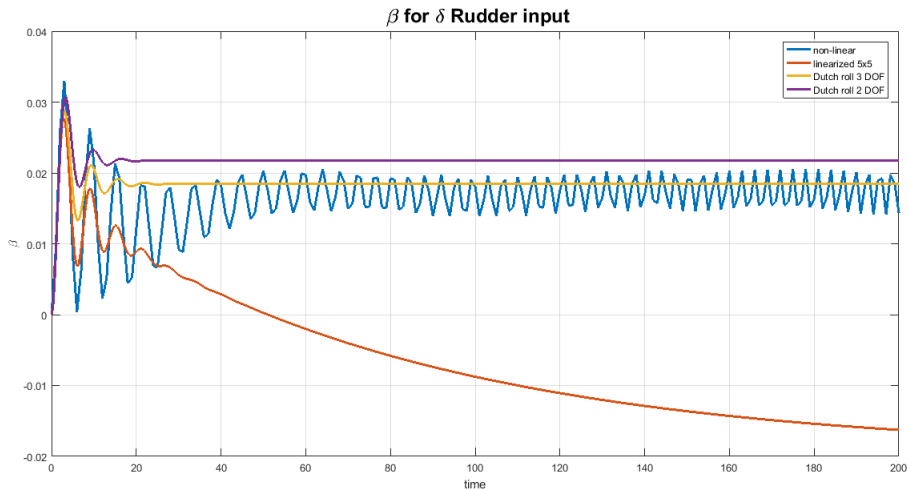


Figure 112: β

- For $\delta_r = 2^0$ (Simulation time = 1000 sec.)

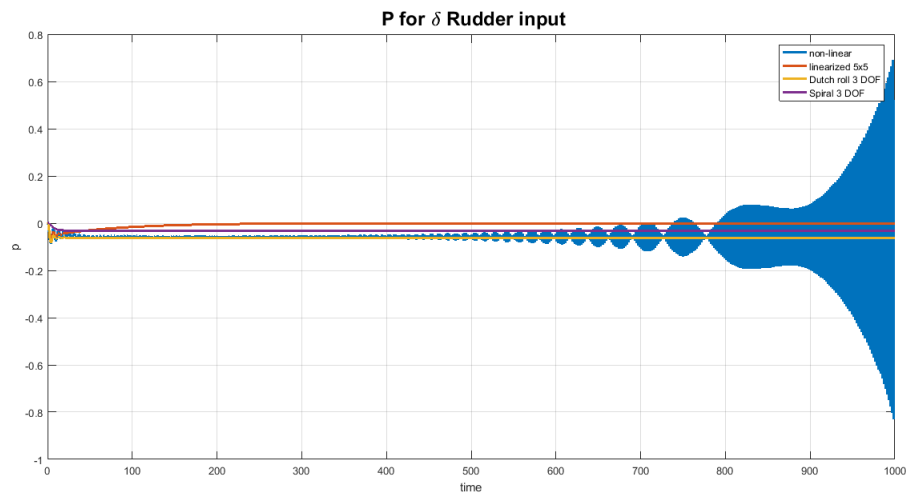


Figure 114: P

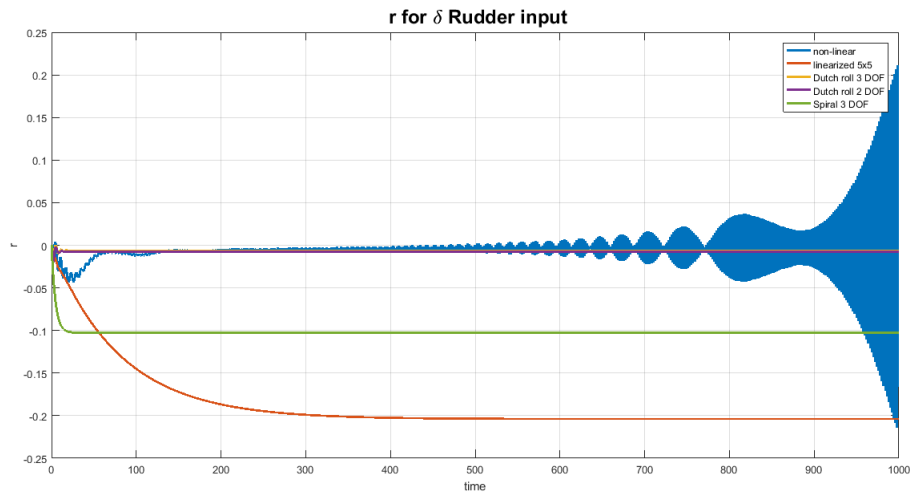


Figure 115: r

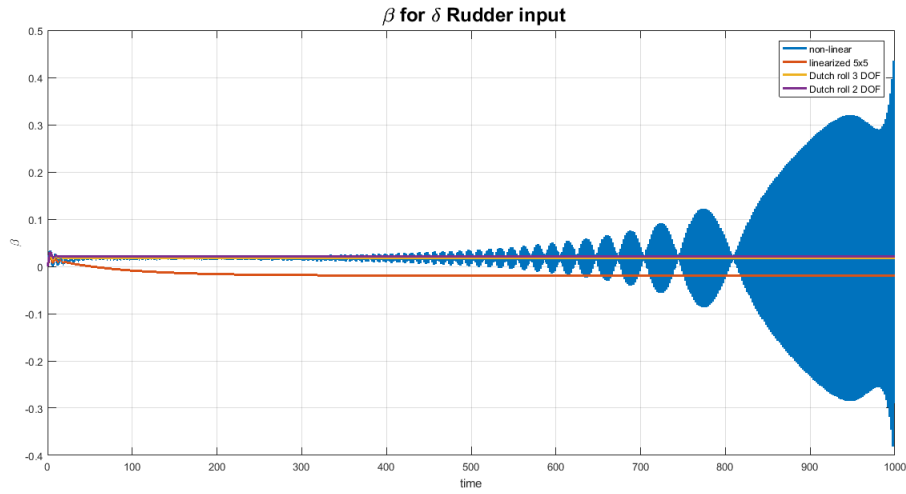


Figure 116: β

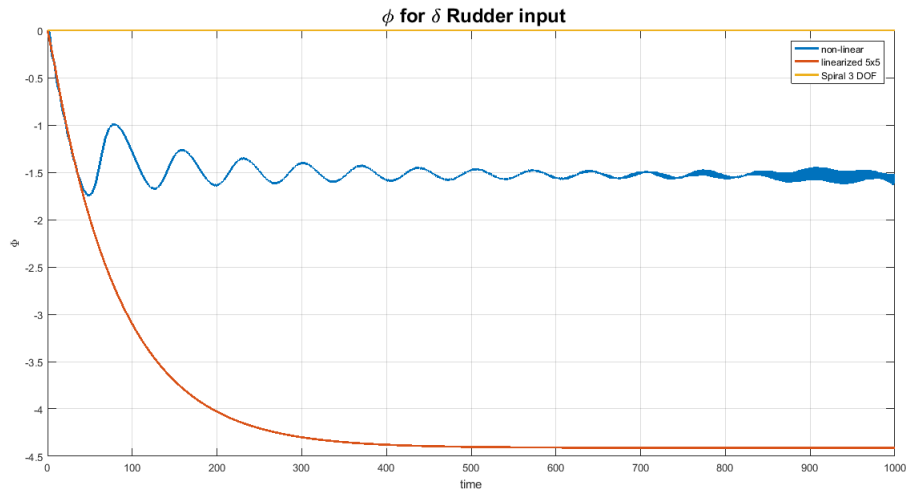


Figure 117: ϕ

- For $\delta_r = 5^0$ (Simulation time = 200 sec.)

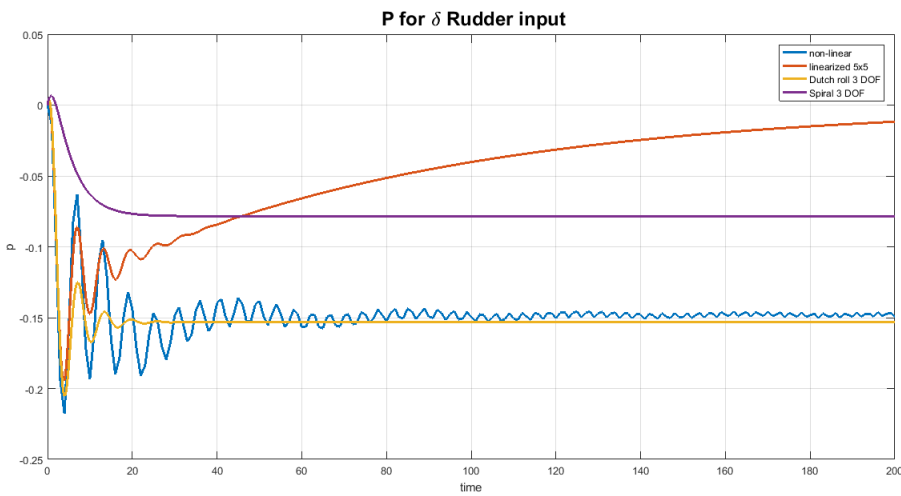


Figure 118: P

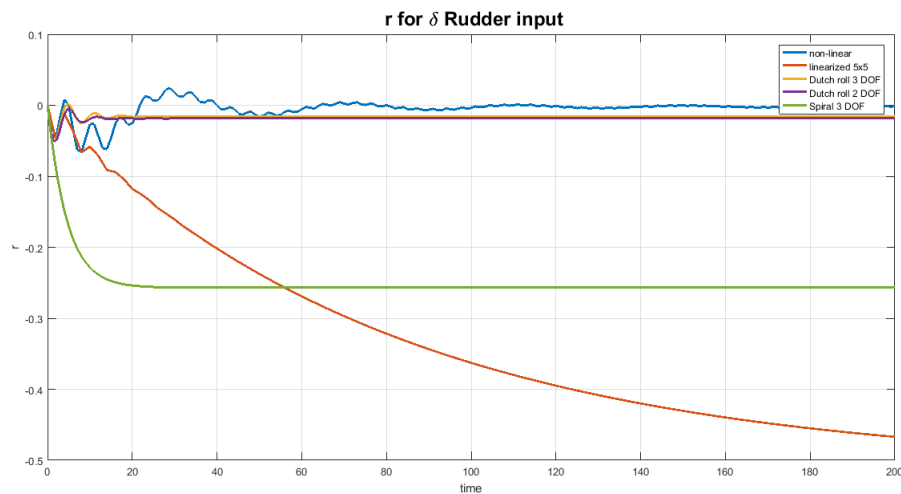


Figure 119: r

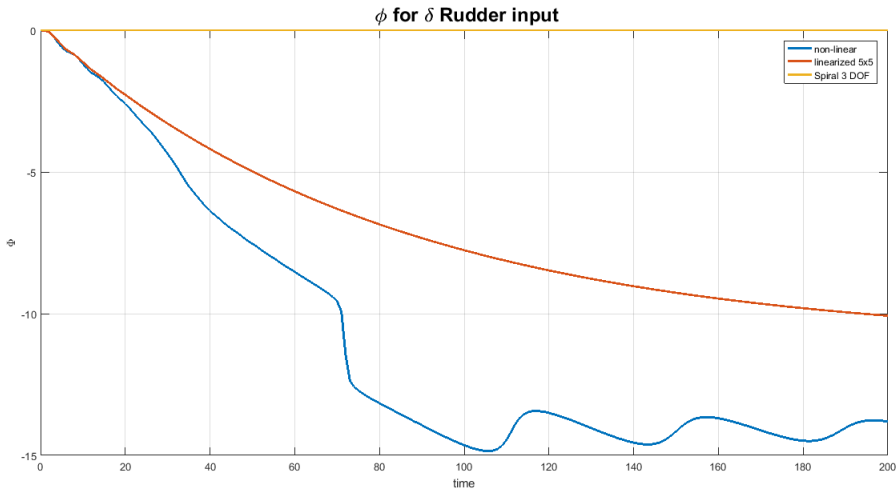


Figure 121: ϕ

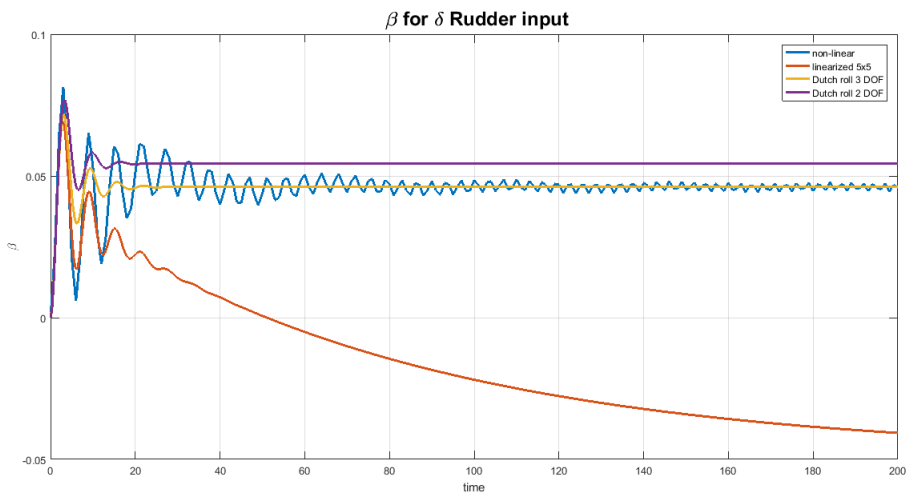


Figure 120: β

- For $\delta_r = 5^0$ (Simulation time = 1000 sec.)

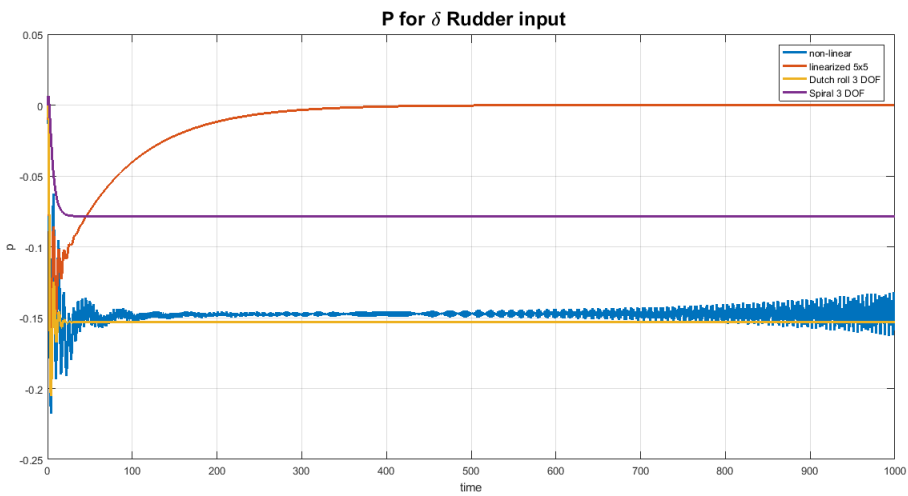


Figure 122: P

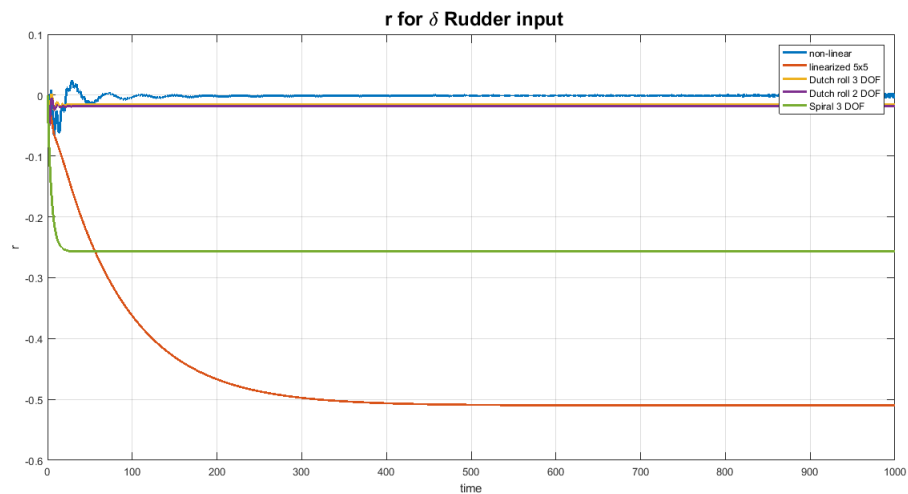


Figure 123: r

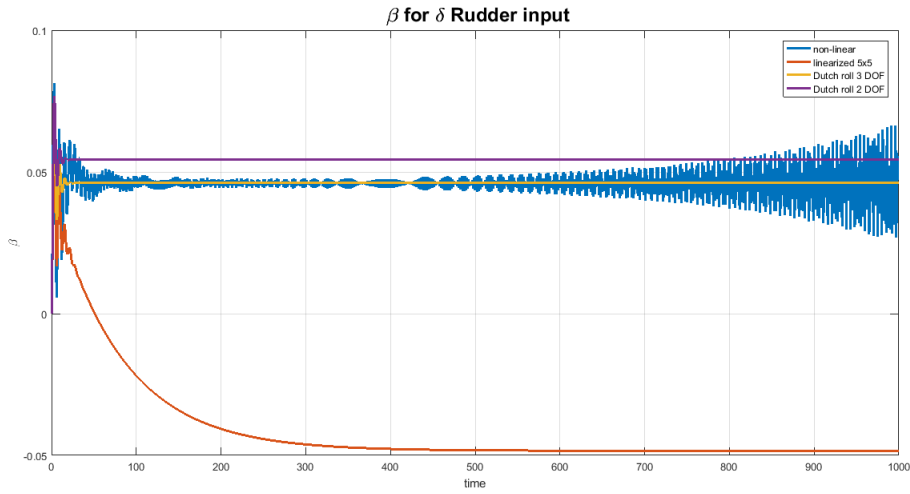


Figure 124: β

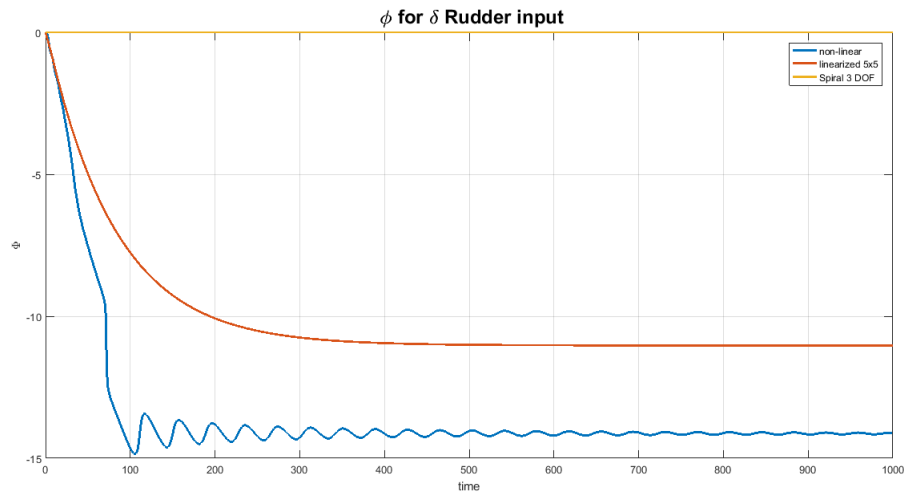


Figure 125: ϕ

6.6 Bode Plot & Root Locus

6.6.1 From Transfer Function of Aileron Input

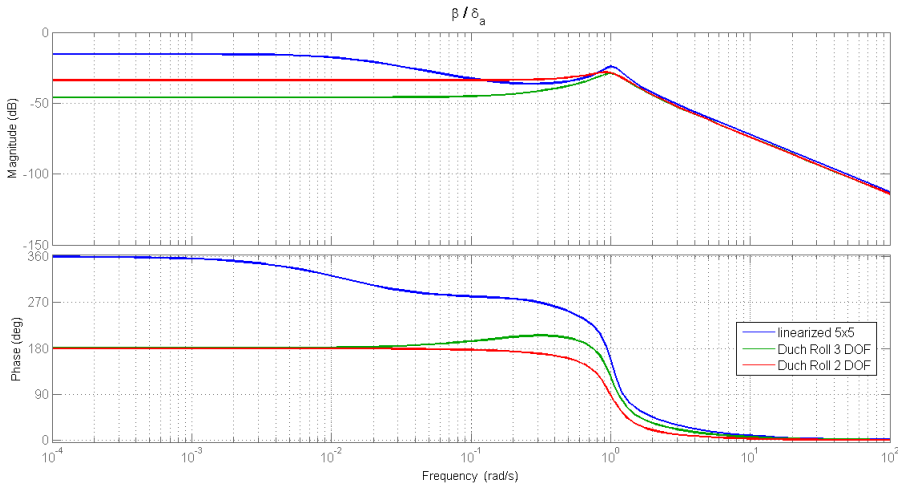


Figure 126: $\frac{\beta}{\delta_a}$

For $\frac{\beta}{\delta_a}$ linearized 4x4
 $GM = 17.8344$

$PM = \infty$

Bandwidth = 0.0123

Dutch Roll 3x3

$GM = 44.33$

$PM = \infty$

Bandwidth = 2.4857

Dutch Roll 2x2

$GM = 49.7055$

$PM = \infty$

Bandwidth = 1.4647

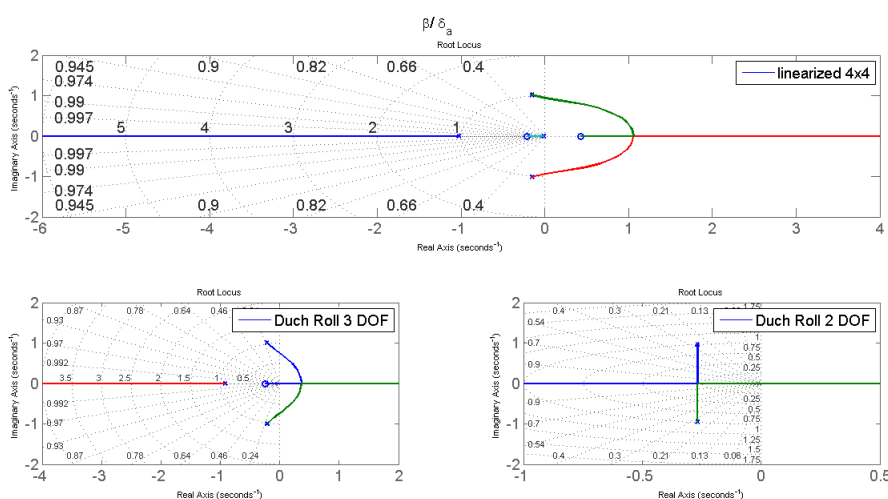


Figure 127: Rott locus for $\frac{\beta}{\delta_a}$

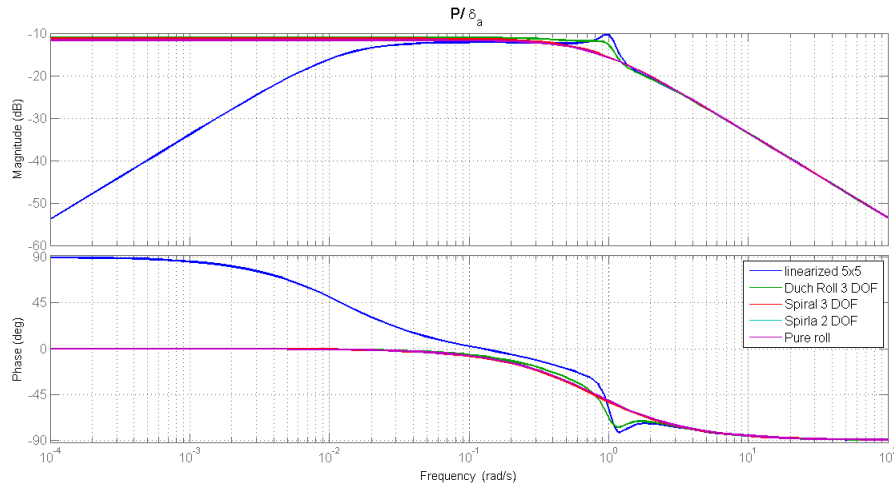


Figure 128: bode polt for $\frac{p}{\delta_a}$

For $\frac{P}{\delta_a}$ Linearized 4x4

$GM = \infty$

$PM = \infty$

$Bandwidth = \infty$

Dutch Roll 3x3

$GM = \infty$

$PM = \infty$

$Bandwidth = 1.0703$

Spiral 3x3

$GM = \infty$

$PM = \infty$

$Bandwidth = .766$

Spiral 2x2

$GM = \infty$

$PM = \infty$

$Bandwidth = .8021$

Pure roll

$GM = \infty$

$PM = \infty$

$Bandwidth = .8021$

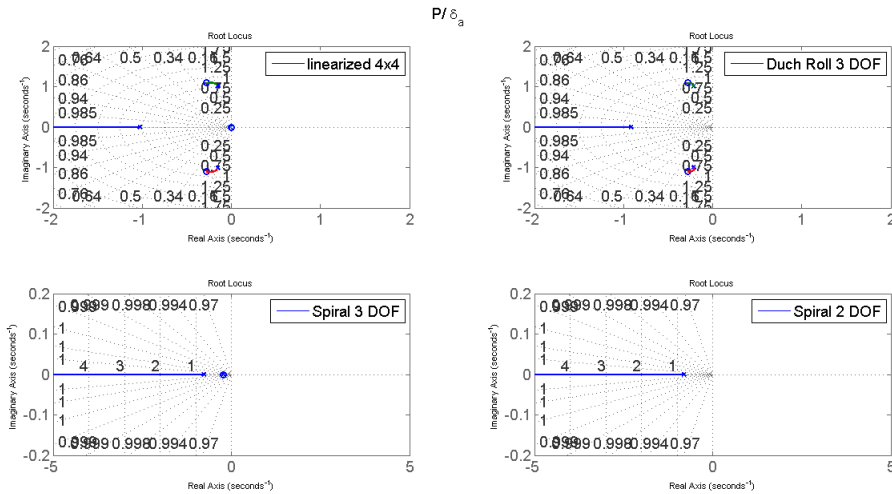


Figure 129: Root locus For $\frac{P}{\delta_a}$

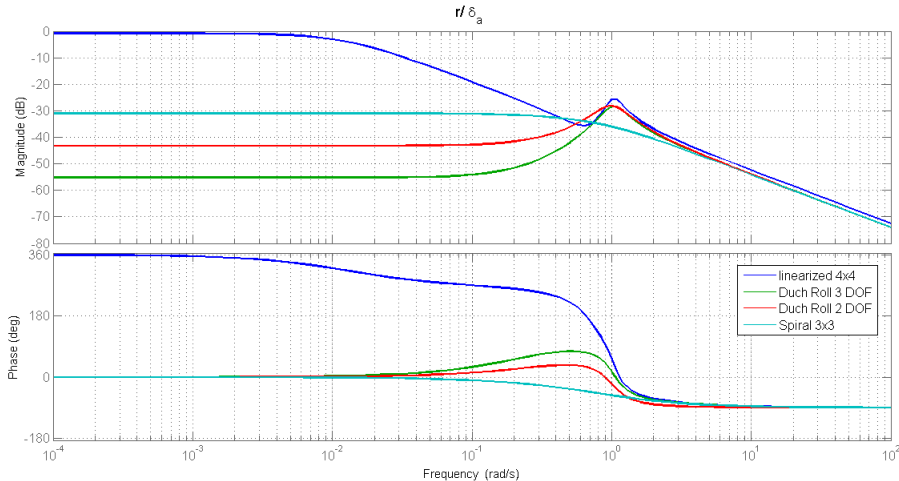


Figure 130: bode plot for $\frac{r}{\delta_a}$

For $\frac{r}{\delta_a}$ Linearized 4x4
 $GM = 60.8689$

$PM = \infty$

Bandwidth = .0123

Dutch Roll 3x3

$GM = \infty$

$PM = \infty$

Bandwidth = 16.2493

Dutch Roll 2x2

$GM = \infty$

$PM = \infty$

Bandwidth = 4.2858

Spiral 3x3

$GM = \infty$

$PM = \infty$

Bandwidth = .6444

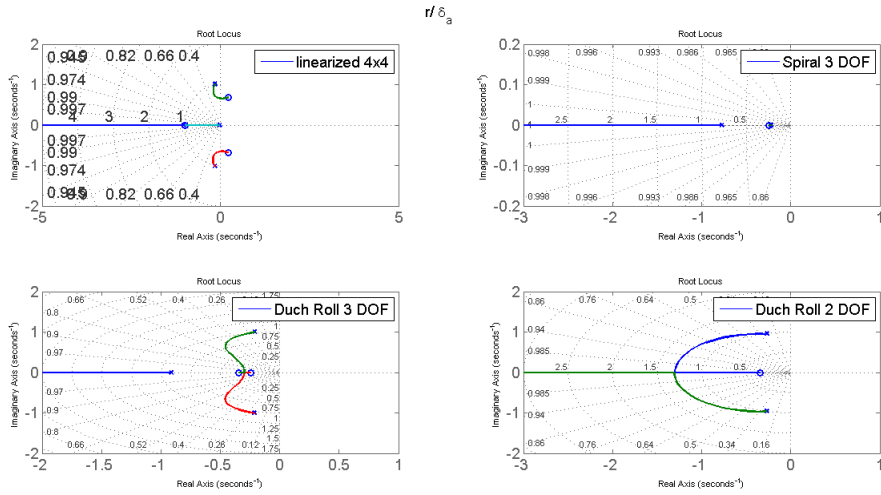


Figure 131: Root locus For $\frac{r}{\delta_a}$

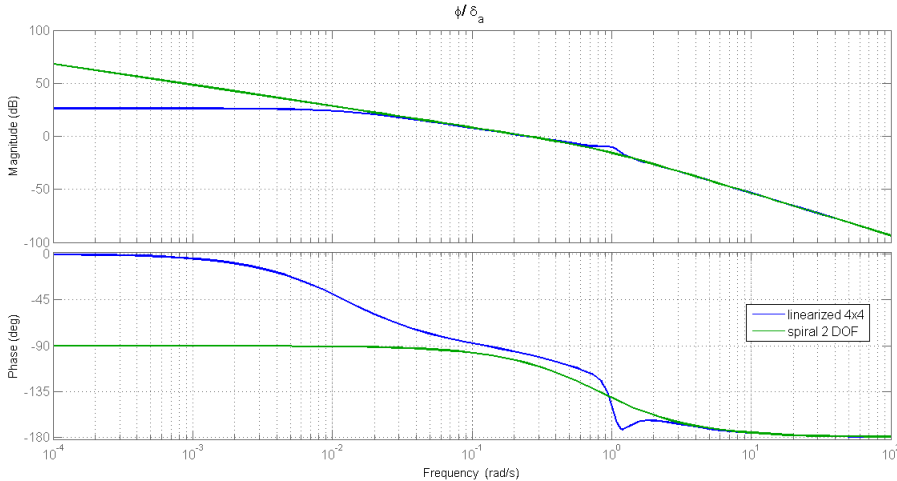


Figure 132: bode plot for $\frac{\phi}{\delta_a}$

For $\frac{\phi}{\delta_a}$ Linearized 4x4

$$GM = 60.8689$$

$$PM = \infty$$

$$Bandwidth = .0123$$

Spiral 2x2

$$GM = \infty$$

$$PM = 72.7621$$

$$Bandwidth = \infty$$

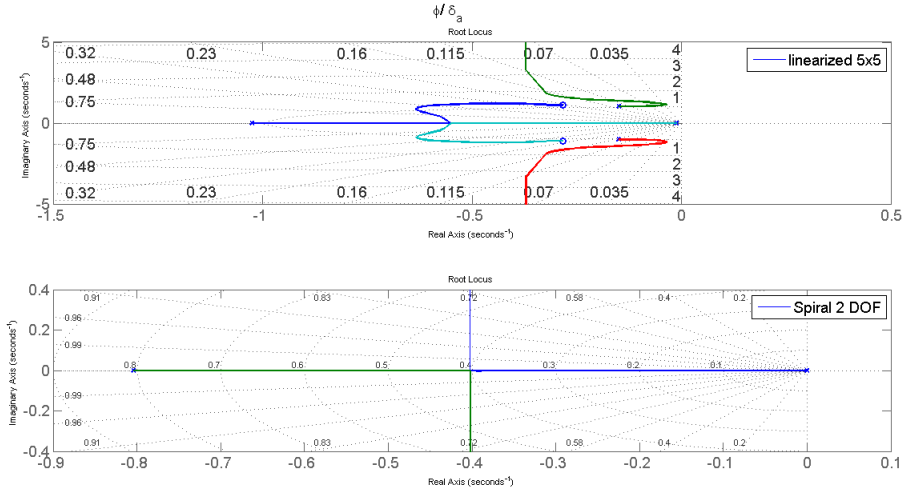


Figure 133: Root locus for $\frac{\phi}{\delta_a}$

6.6.2 From Transfer Function of Rudder Input

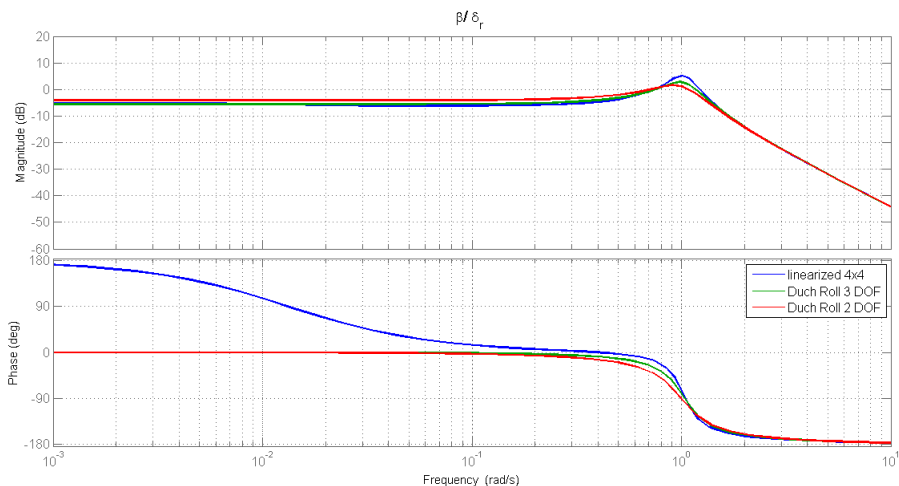


Figure 134: $\frac{\beta}{\delta_a}$

For $\frac{\beta}{\delta_r}$ linearized 4x4
 $GM = 1.8032$

$PM = 46.0582$

Bandwidth = 1.5705

Dutch Roll 3x3

$GM = \infty$

$PM = 59.96$

Bandwidth = 1.5831

Dutch Roll 2x2

$GM = \infty$

$PM = 71.3291$

Bandwidth = 1.4647

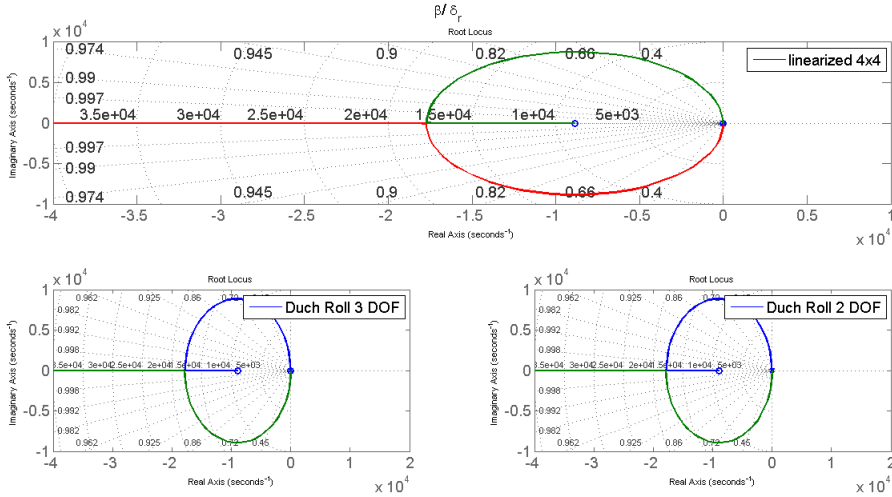


Figure 135: Rott locus for $\frac{\beta}{\delta_r}$

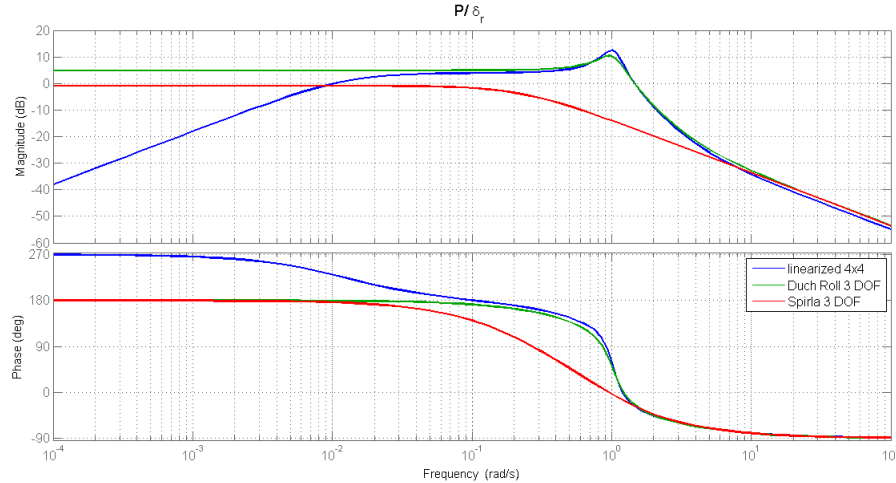


Figure 136: bode plot for $\frac{P}{\delta_r}$

For $\frac{P}{\delta_r}$ Linearized 4x4

$$GM = .6437$$

$$PM = 46.0582$$

$$Bandwidth = \infty$$

Dutch Roll 3x3

$$GM = .5698$$

$$PM = 155.3157$$

$$Bandwidth = 1.3713$$

Spiral 3x3

$$GM = 1.1129$$

$$PM = \infty$$

$$Bandwidth = .2234$$

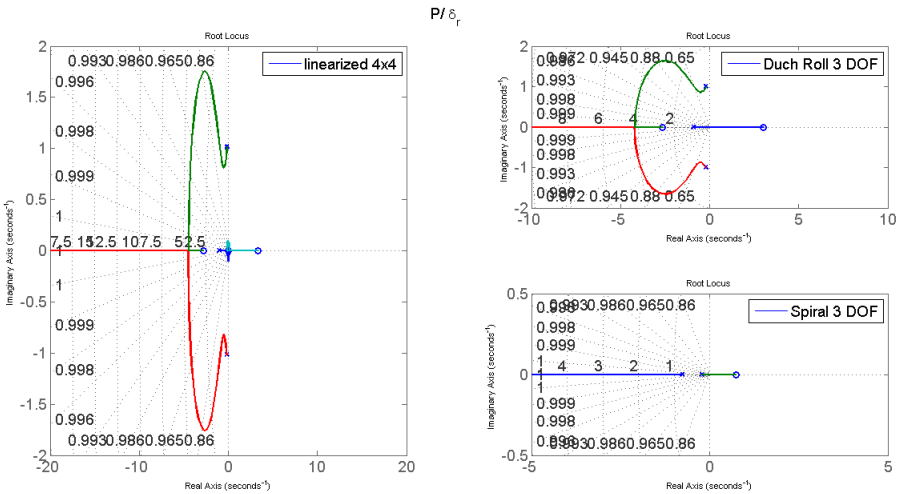


Figure 137: Root locus For $\frac{P}{\delta_r}$

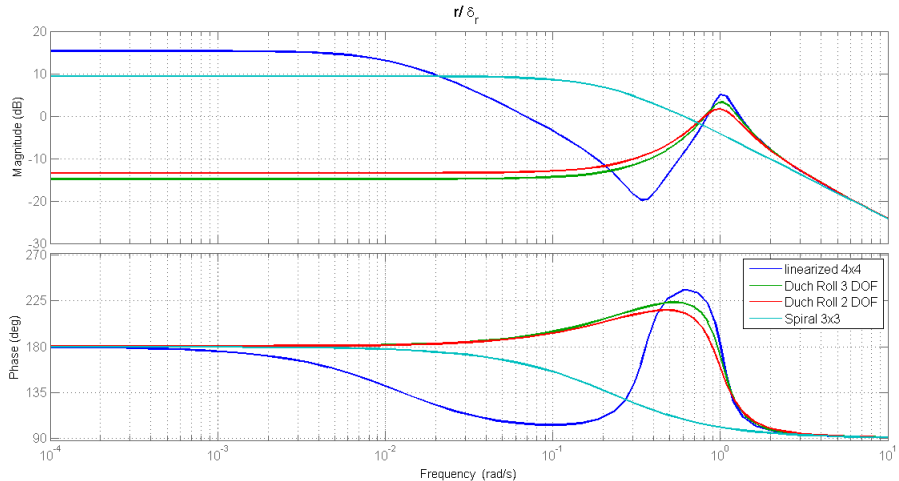


Figure 138: bode plot for $\frac{r}{\delta_r}$

For $\frac{r}{\delta_r}$ Linearized 4x4

$$GM = 1.8032$$

$$PM = 46.0582$$

$$Bandwidth = .0123$$

Dutch Roll 3x3

$$GM = .7116$$

$$PM = 27.9494$$

$$Bandwidth = 4.9929$$

Dutch Roll 2x2

$$GM = .8696$$

$$PM = 13.9051$$

$$Bandwidth = 4.2858$$

Spiral 3x3

$$GM = 1.1129$$

$$PM = \infty$$

Bandwidth = .2234

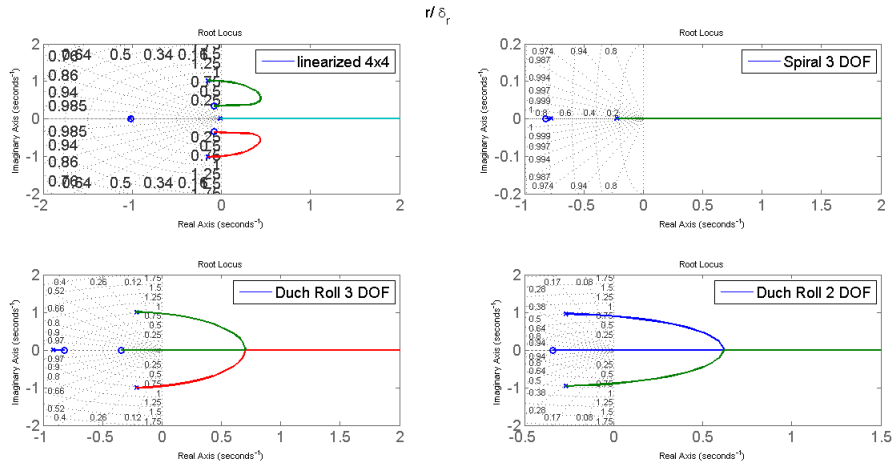


Figure 139: Root locus For $\frac{r}{\delta_a}$

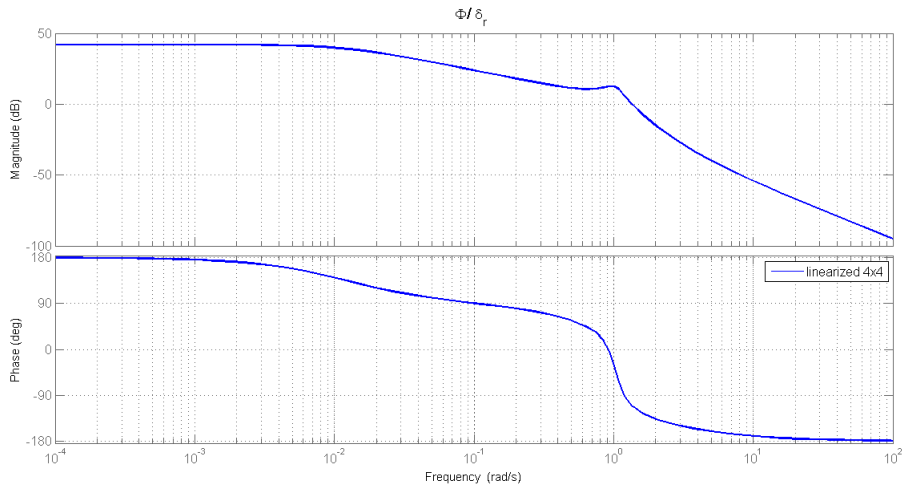


Figure 140: Bode plot for $\frac{\phi}{\delta_r}$

For $\frac{\phi}{\delta_r}$ Linearized 4x4
 $GM = .0079$

$PM = 68.8786$

Bandwidth = .0123

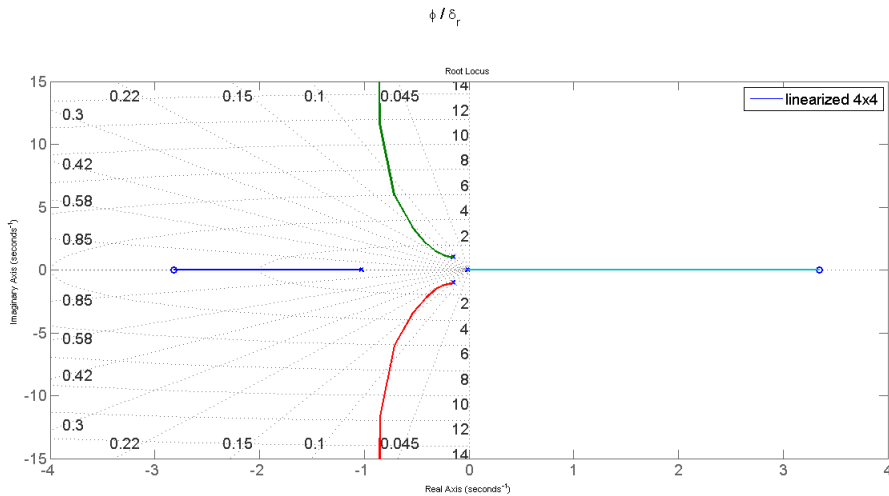


Figure 141: Root locus for $\frac{\phi}{\delta_r}$

7 Autopilot

7.1 Autopilot longitudinal control

This task is to implement a controller for the longitudinal motion, and ensuring the flight qualities are satisfied, which is our main concern to achieve it. By the use of this controller, the system performance is improved. The performance requirements such as the peak overshoot to be less than 15% and short rise and settling times has been achieved by the use of each controller. Traditional control techniques such as PID controller is designed for each of these autopilot modes. Root-locus design technique is applied for tuning the parameters of each controller.

7.1.1 Level Flight

The feedback loops that are enabled while your MicroPilot Autopilot is holding altitude are shown in bold in the Figure below. This example assumes that your MicroPilot Autopilot is configured to use the elevator to control altitude and the throttle to control airspeed. If your MicroPilot Autopilot were configured to use the elevator to control airspeed, then the pitch from airspeed feedback loop would be enabled instead of the pitch from altitude and throttle from altitude would be enabled instead of throttle from airspeed.

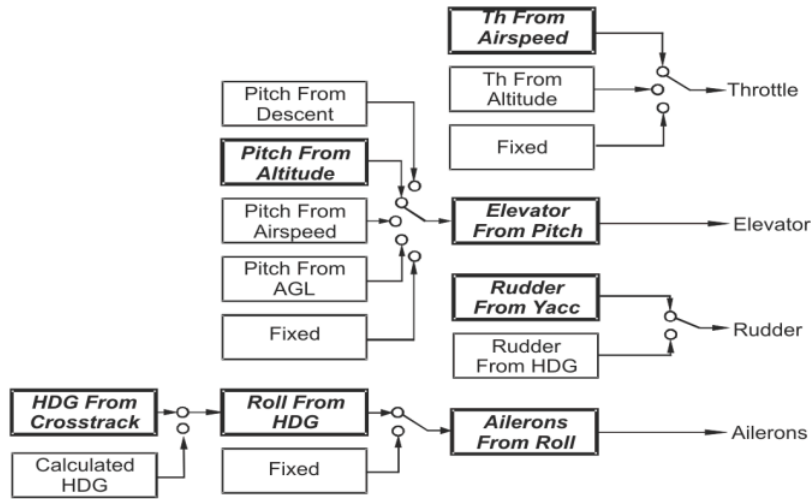


Figure 142: Level Flight AP

7.1.2 Flight Qualities

- Flying qualities are related to stability and control characteristics of an airplane and can be defined as those stability and control characteristics important in forming the pilot impression about the plane. Handling qualities are related to the ease/difficulty a pilot can fly an airplane and depend on:
 - Flying qualities
 - major contributor
 - Display and flight information in cockpit or ground control station
 - Primary flying control characteristics.

Airplanes are classified according to size and maneuverability:

- **Class I:** Small, light airplanes, such as light utility, primary trainer, and light observation craft.
- **Class II:** Medium weight, low-to-medium maneuverability airplanes, such as heavy utility/search and rescue, light or medium transport/cargo/tanker, reconnaissance, tactical bomber, heavy attack and trainer.
- **Class III:** Large, heavy, low-to-medium maneuverability airplanes, such as heavy transport/cargo/tanker, heavy bomber and trainer.
- **Class IV:** High maneuverability airplanes, such as fighter/interceptor, attack, tactical reconnaissance, observation and trainer.

The Different Flight Phases are:

- **Category A:** Nonterminal flight phase that requires rapid maneuvering, precise tracking, or precise flight path control. Mostly for military aircrafts.
- **Category B:** Nonterminal flight phase that are normally accomplished using gradual maneuvers and without precise tracking, although accurate flight patch control may be required. For example, cruise stage in flight.
- **Category C:** Terminal flight phase are normally accomplished using gradual maneuvers and usually require accurate flight path control. For example, landing/take-off.

For our aircraft Boeing 747 flight condition 6: we have a constraint for the ζ to be 0.0266 to 0.473 according to this , the overshoot % ranges according to the following table

ζ	O.S.%
0.0266	91.98 %
0.473	18.51 %

Figure 143: damping and % O.S.

7.1.3 Thrust from Airspeed:

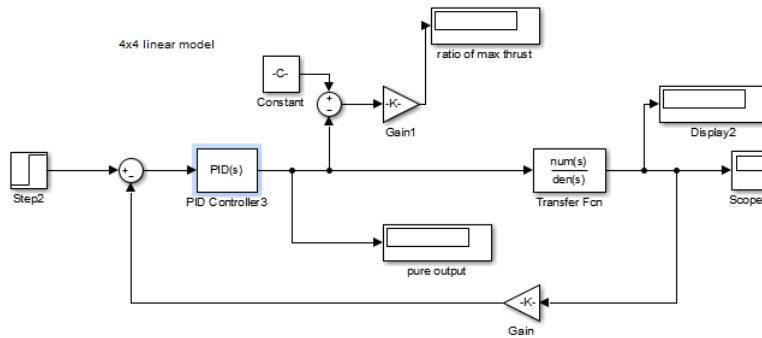


Figure 144: Thrust from airspeed

where the transfer function is as follows:

$$\frac{5.05e-05 s^3 + 5.303e-05 s^2 + 3.186e-05 s - 1.684e-06}{s^4 + 1.109 s^3 + 0.6708 s^2 + 0.004738 s + 0.001547}$$

After the tuning we have got the following PID controller:

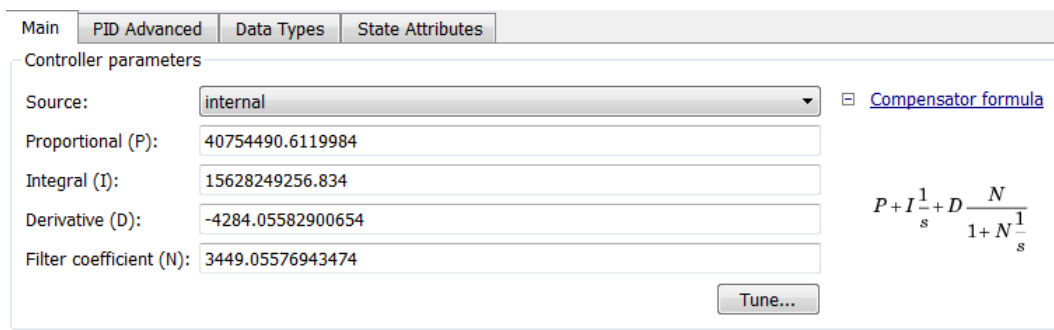


Figure 145: PID Controller

which gave us the following response:

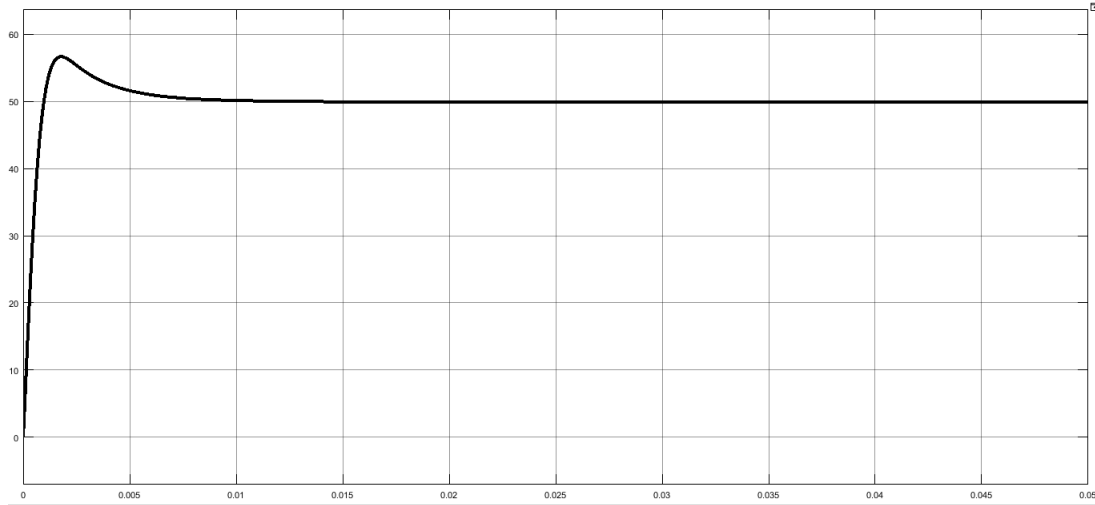


Figure 146: Thrust from Airspeed Response

where the following characteristics have been achieved:

Performance and Robustness	
	Tuned
Rise time	0.000713 seconds
Settling time	0.0061 seconds
Overshoot	13.5 %
Peak	1.13
Gain margin	Inf dB @ NaN rad/s
Phase margin	69 deg @ 2e+03 rad/s
Closed-loop stability	Stable

Figure 147: Thrust from Airspeed characteristics

7.1.4 Elevator from pitch and pitch from Altitude:

We used two nested loops to control the elevator from pitch , one to calculate the $\theta_{desired}$ and another one to control the elevator h, to satisfy the flying qualities mentioned above, this is shown below in the following block diagram.

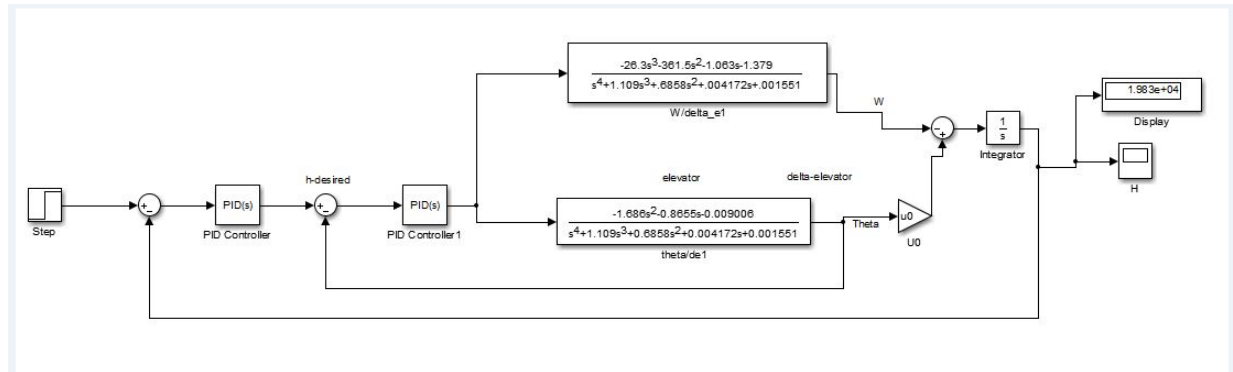


Figure 148: Elevator from pitch and pitch from Altitude control loop

we used an external loop to calculate the PID for the θ loop , which is shown below:

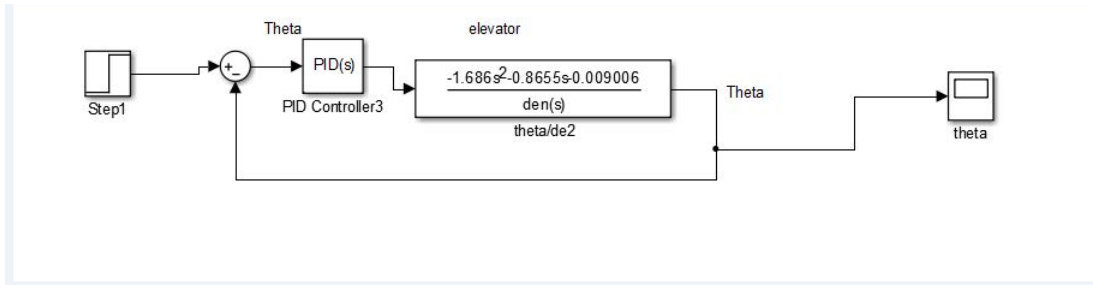


Figure 149: Calculating PID for the θ loop

the PID for this loop is as shown below:

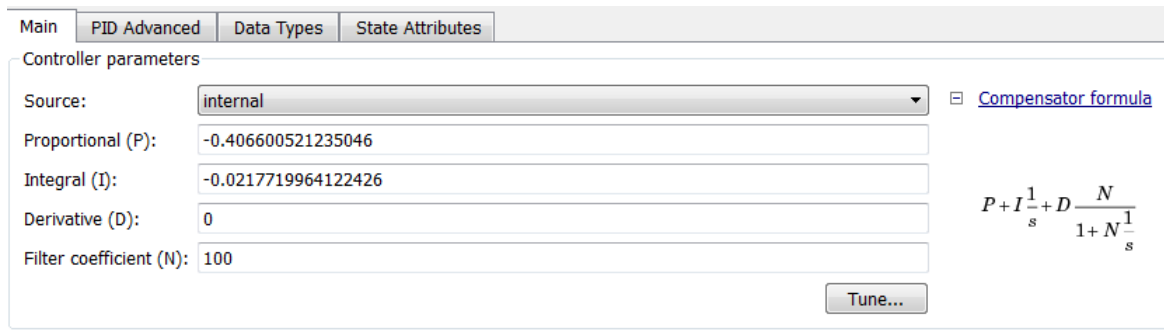


Figure 150: θ loop PID gains

and the response is as shown below:

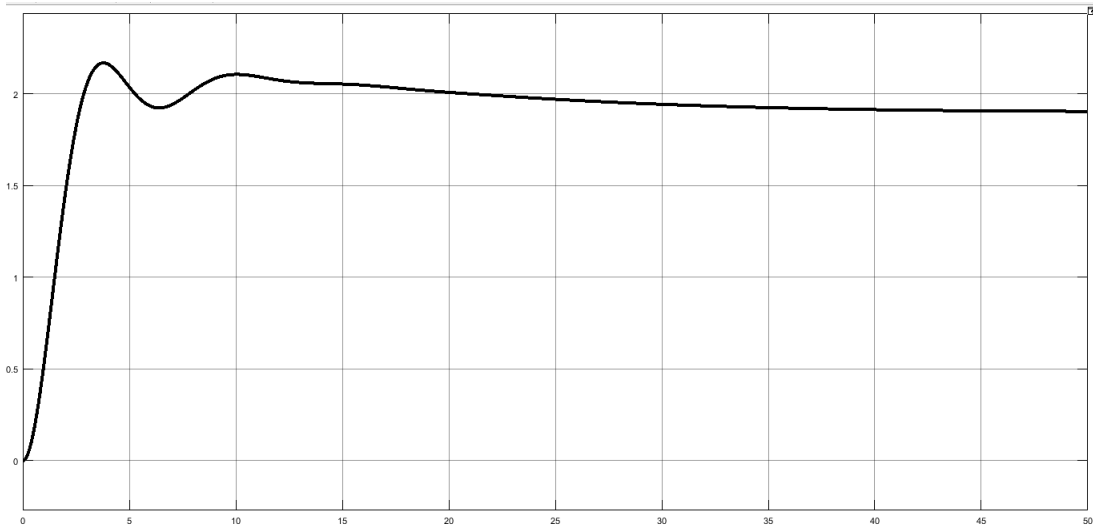


Figure 151: θ loop response

then for the whole loop the PID controller gains is as shown:

Main	PID Advanced	Data Types	State Attributes
Controller parameters			
Source:	internal	<input type="checkbox"/> Compensator formula	
Proportional (P):	0.00192107603996945		
Integral (I):	6.94146577282067e-06		
Derivative (D):	0.00459154395345001		
Filter coefficient (N):	47.6067825428897		
<input type="button" value="Tune..."/>			

$$P + I \frac{1}{s} + D \frac{N}{1 + N \frac{1}{s}}$$

Figure 152: Outer loop PID gains

and the outer loop response is as shown:

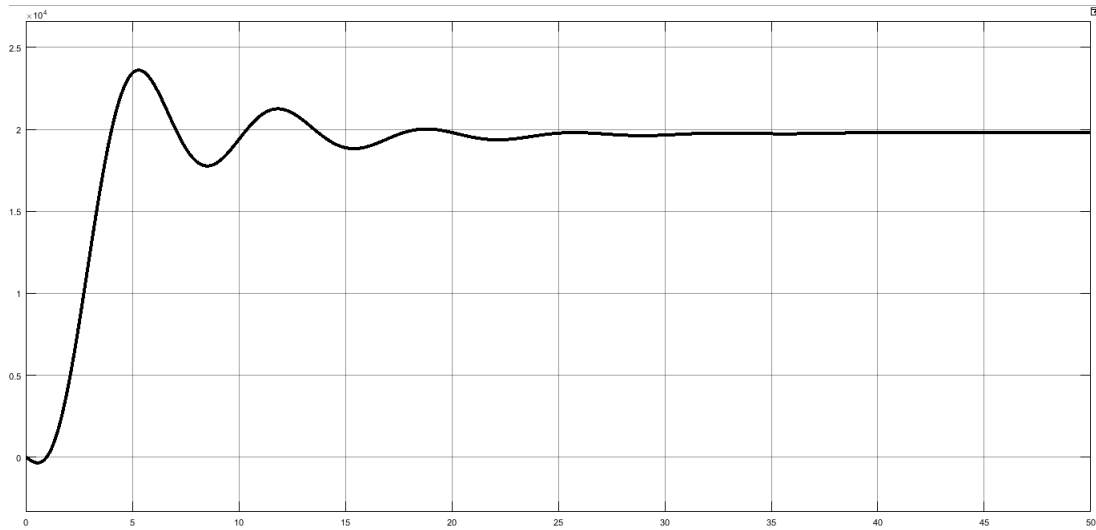


Figure 153: Outer loop PID response

where the outer loop response characteristics are as shown:

Performance and Robustness	
	Block
Rise time	2.15 seconds
Settling time	23.9 seconds
Overshoot	18 %
Peak	1.18
Gain margin	5.23 dB @ 0.965 rad/s
Phase margin	59 deg @ 0.417 rad/s
Closed-loop stability	Stable

Figure 154: Outer loop response characteristics

7.2 1- Re design the controller implemented before:

$u/\delta\theta$ Transfer Function : It's required to control the Thrsut from airspeed, we will work with the " $u/\delta\theta$ " Transfer function as follows;

$$\frac{5.05e-05s^3 + 5.303e-05s^2 + 3.186e-05s - 1.684e-06}{s^4 + 1.109s^3 + 0.6708s^2 + 0.004738s + 0.001547}$$

we are working on the 4x4 linearized Model to design our controller, but first we need to find the dominant poles to work on. First, the eigen values of the A matrix is

$$\begin{aligned} & -0.5527 + 0.5995i \\ & -0.5527 - 0.5995i \\ & -0.0016 + 0.0482i \\ & -0.0016 - 0.0482i \end{aligned}$$

and the step response of the 4X4 model and the root locus are as follow:

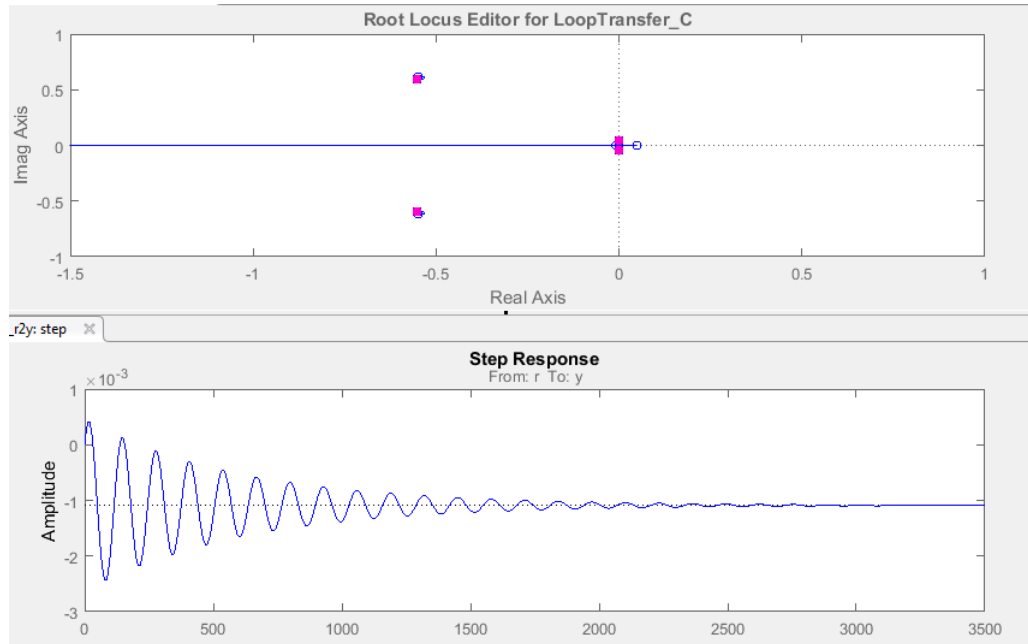


Figure 155

while the eigen values of the 2x2 Long period model is,

$$\begin{aligned} & -0.0014 + 0.0643i \\ & -0.0014 - 0.0643i \end{aligned}$$

Also, the step response and the root locus are as follow:

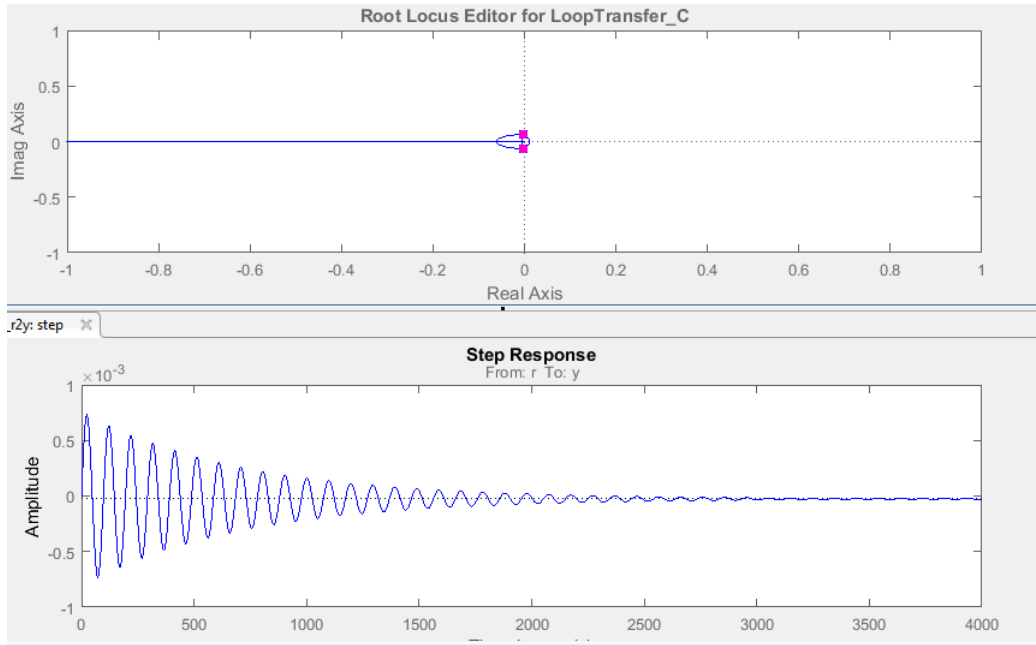


Figure 156

where we can deduce that we will work on the poles of the long period, we will assume that the long period poles are the dominant poles, thus we will try different ζ values to implement our controller, and observe the control action, till we get a better controller that is too comfortable for the pilot, and that's our goal.

Trial no.1

working for the Range of ζ obtained from Nelson that for the longintudant Long period, $\zeta \geq 0.04$

we have moved the root locus long period poles to intersect the lines of $\zeta = 0.1$, Thus The root locus figure is shown below;

First for $\zeta = 0.1$

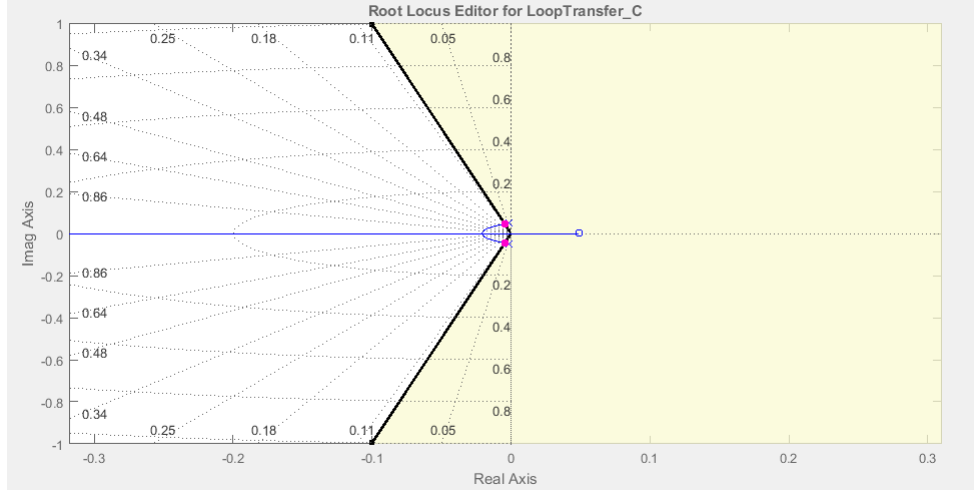


Figure 157

The Step response is as follows;

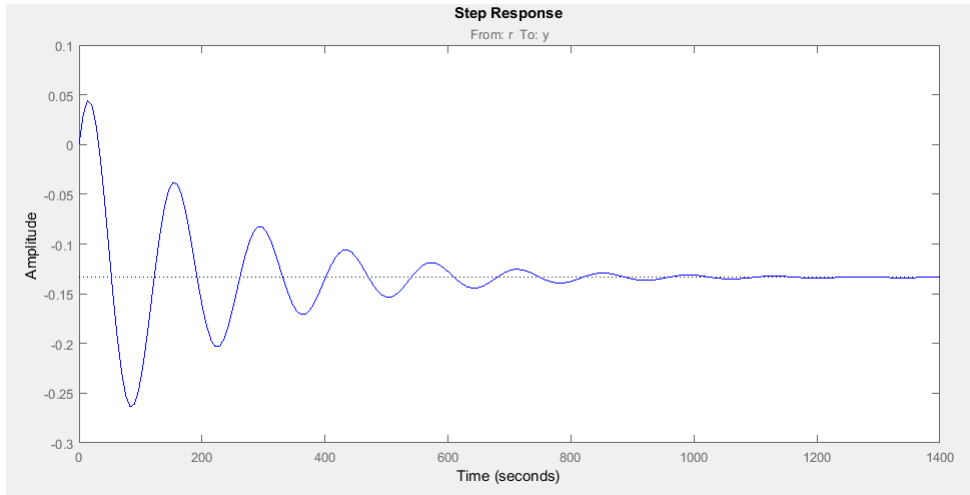


Figure 158

There we found that the Open loop gain "C"=110.56

In order to check that the results of the controller is applicable to the real life model. we need to check the Control action and the step response on our Model and controller, In the following steps;

Working on Simulink:

The model is as follows;

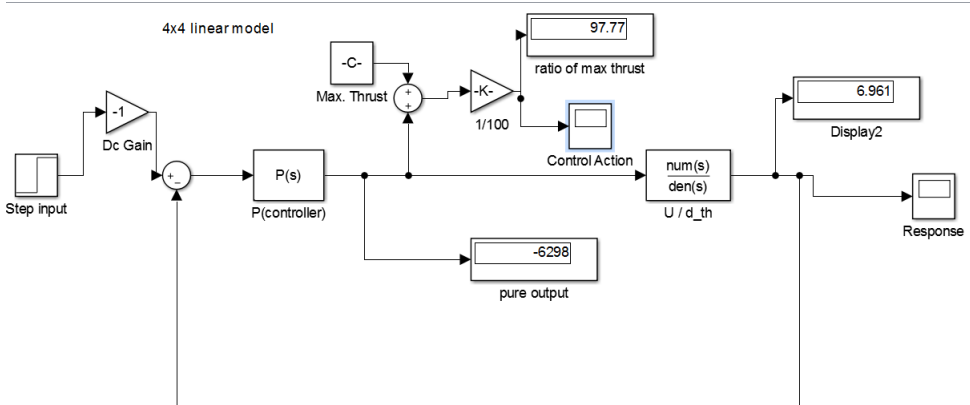


Figure 159

where we can see that the controller, K is a Proportional only, with the value of 110.56

Thus it can achieve the following response when given a final value for the step input of 50
The response is

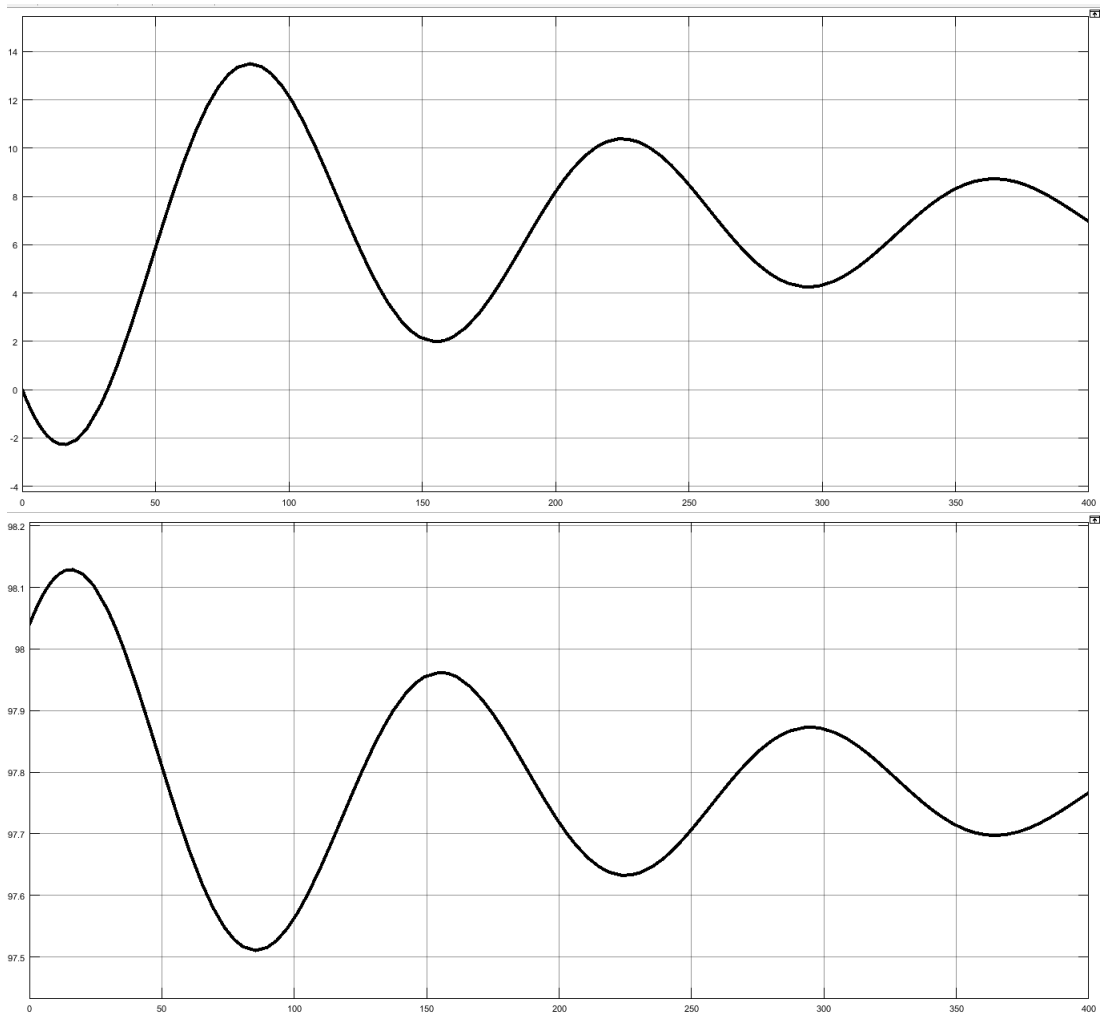


Figure 160

Trial no.2

working for the Range of ζ obtained from Nelson that for the longintudant Long period, $\zeta \geq 0.04$

For $\zeta = 0.4$

we have moved the root locus long period poles to intersect the lines of $\zeta = 0.4$, Thus The root locus figure is shown below;

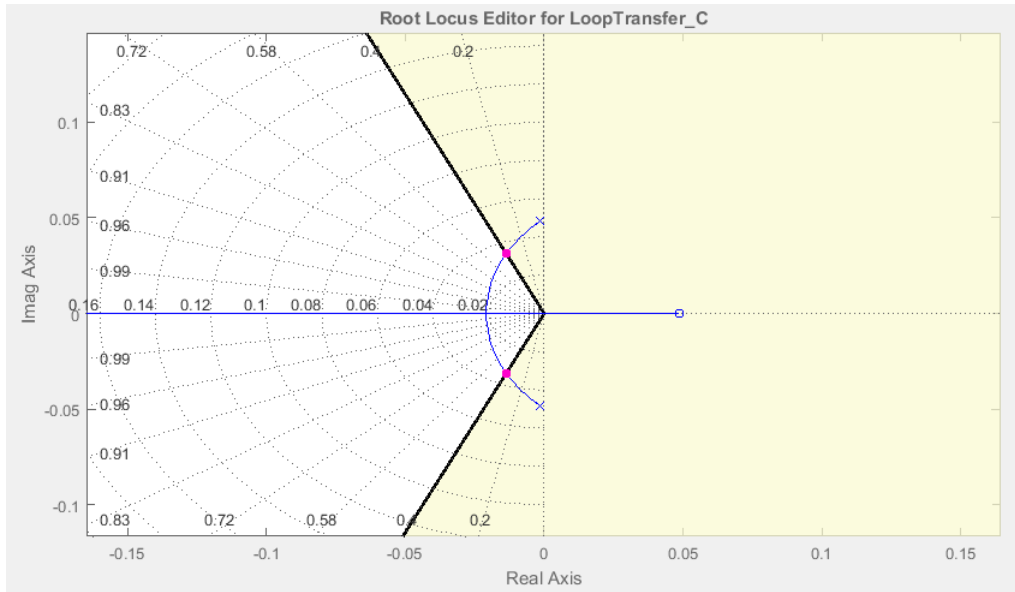


Figure 161

The Step response is as follows;

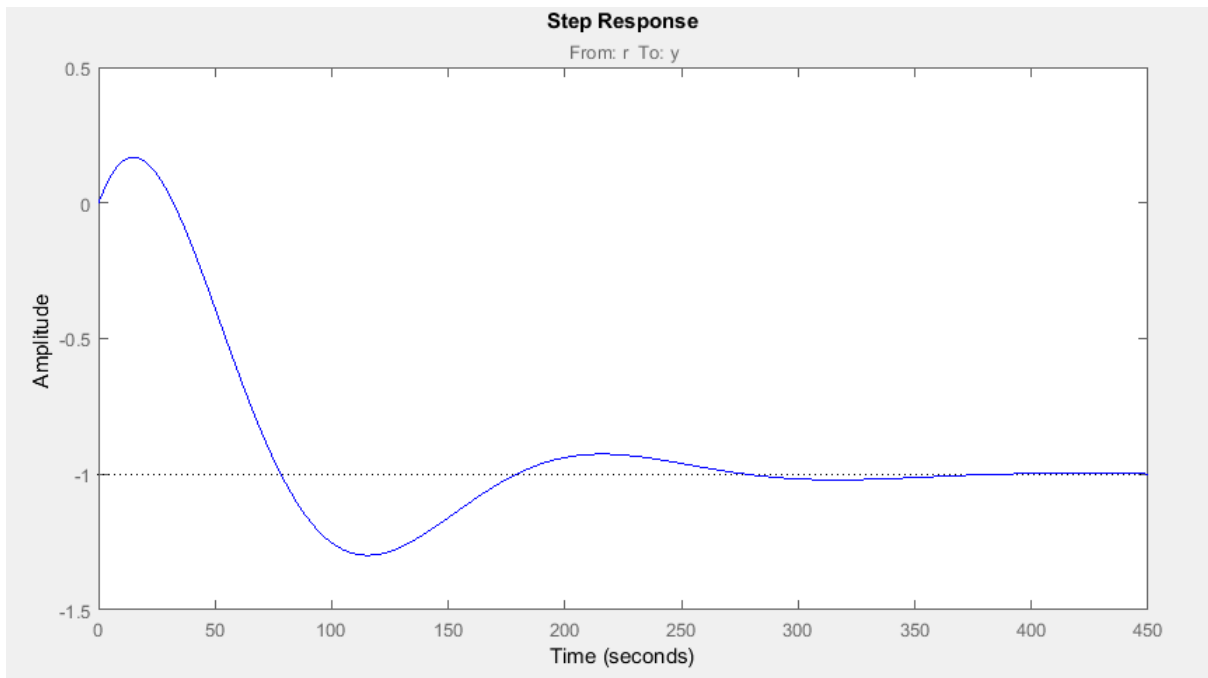


Figure 162

There we found that the Open loop gain "C"=459.79

In order to check that the results of the controller is applicable to the real life model. we need to check the Control action and the step response on our Model and controller, In the following steps;

Working on Simulink:

The model is as follows;

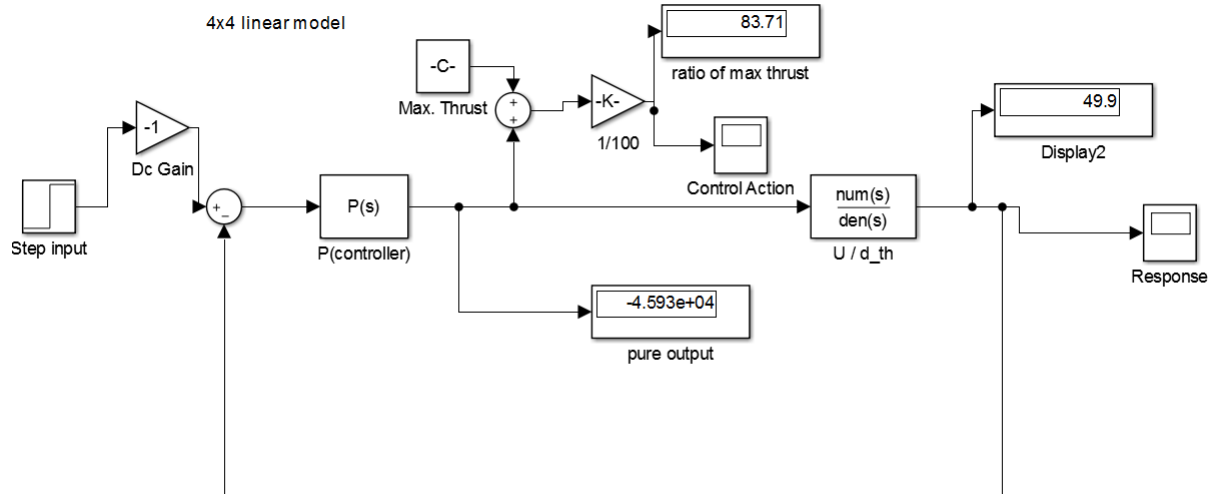


Figure 163

where we can see that the controller, K is a Proportional only, with the value of 459.79
Thus it can achieve the following response when given a final value for the step input of 50

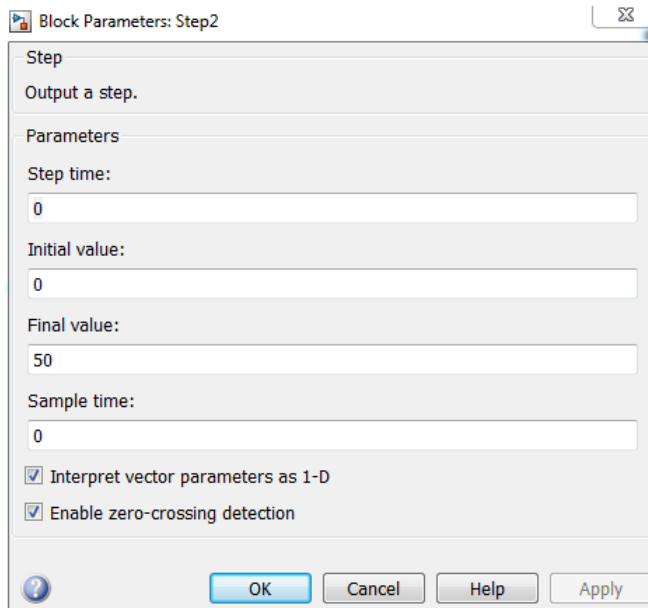
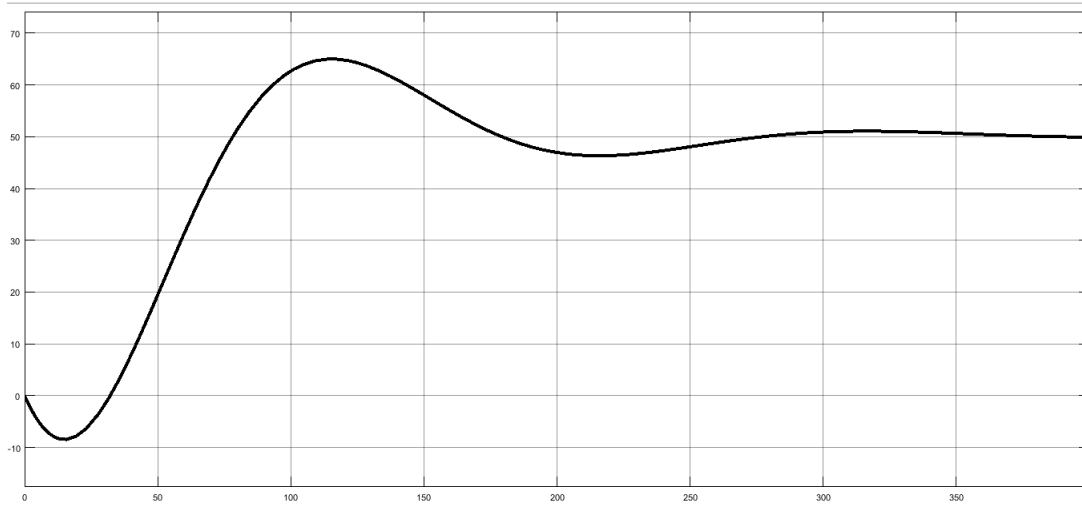


Figure 164

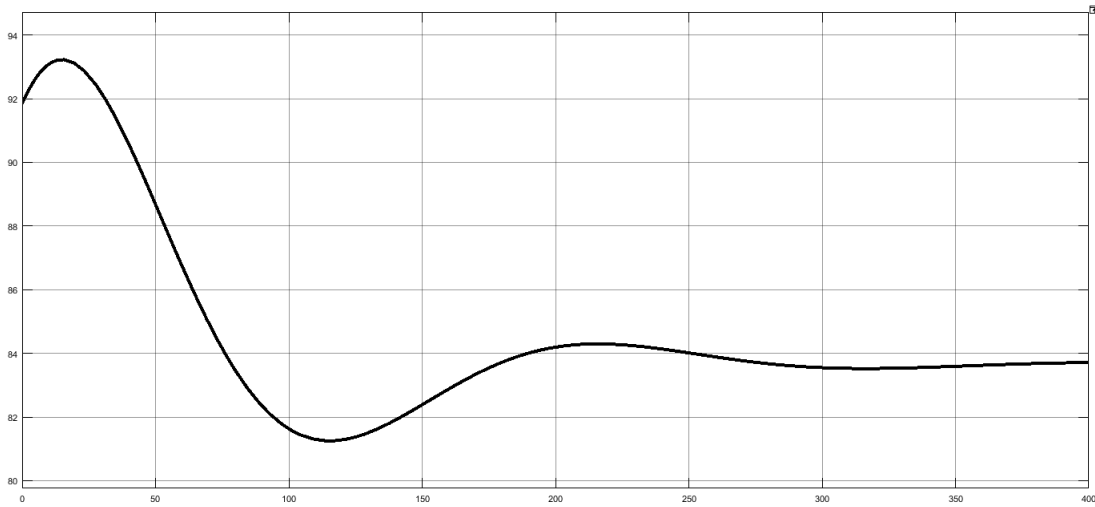
The step response is as follows:



we can notice that, the step response is almost the same as the response from the sisotool, It only differes in the sign of the settling value, that's why we multiplied the input in a DC gain equal to -1

We still need to check the control action, where the control action is 83.69 % of the maximum thrust, which is an acceptable value for us.

The control action is as follows:



Which is totally un-acceptable that the control action is 97.9 % that would be too-hard for the autopilot to be done

7.3 Re-design of the pitch from altitude :

The Transfer function is as follows for the internal loop of $q/\delta e$

$$\frac{-1.686s^3 - 0.8655s^2 - 0.009006s}{s^4 + 1.109s^3 + 0.6708s^2 + 0.004738s + 0.001547}$$

Using the same procedure shown above, and we resulted to the following simulink, the control action values is acceptable for us to be 55.38 % of the maximum input.

where the controller is as follows;

our requirements are to implement $\zeta = 0.433$ which is in the acceptable range of $0.3 < \zeta < 2$

we have made a second trial to design a controller, our aim is to make a velocity feedback controller to control q hence controlling θ and this will be the inner loop , the outer loop will be controlling altitude through θ . taking into consideration our requirement which is $0.3 < \zeta < 2$.

we have noticed that using a velocity feedback controller has reduced gains required to control altitude.and since q has negative open loop transfer function,we used unversed servo to get negative feedback.

servo dynamics $\frac{-10}{s+10}$

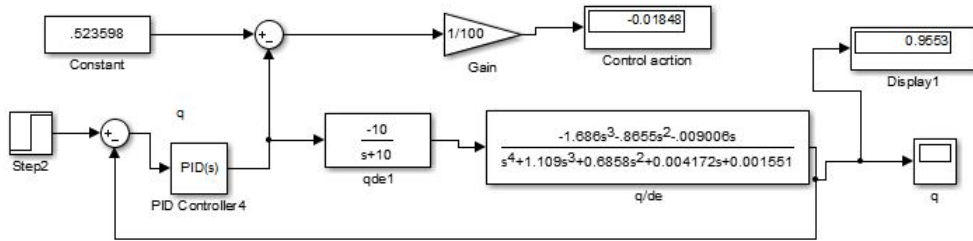


Figure 165

inner loop we get the following response

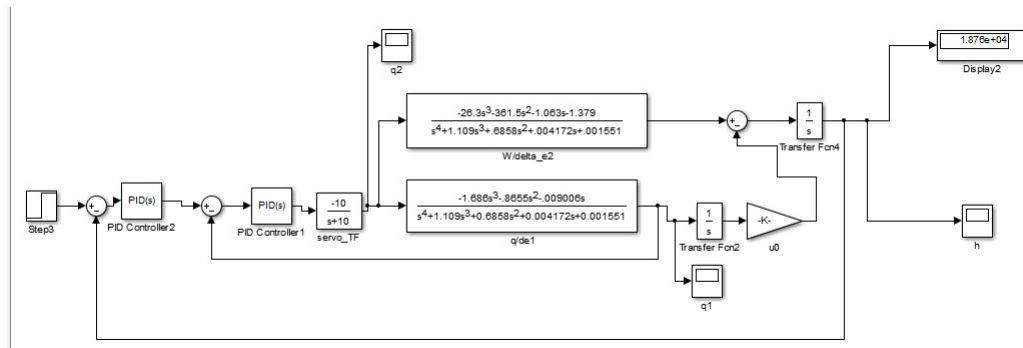
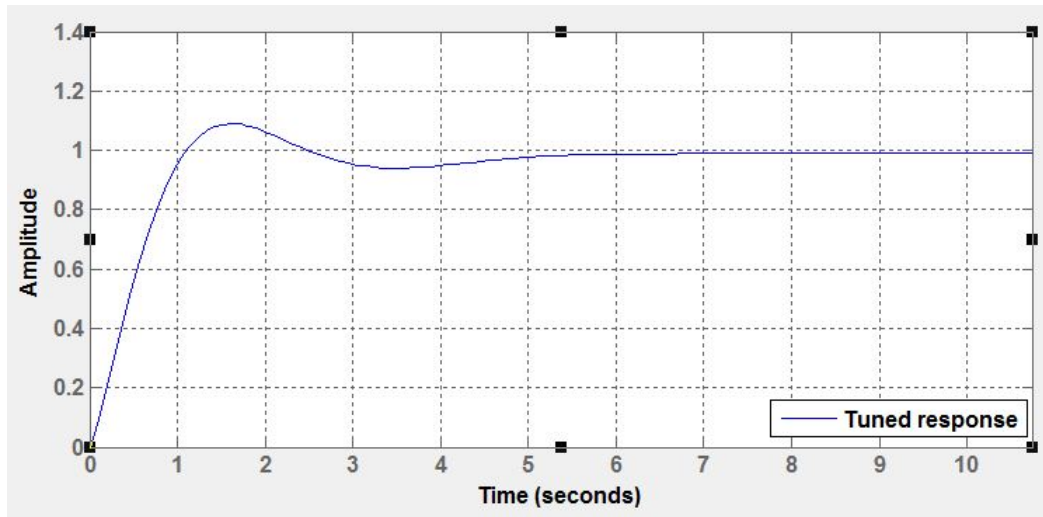


Figure 166

outer loop we get the following response

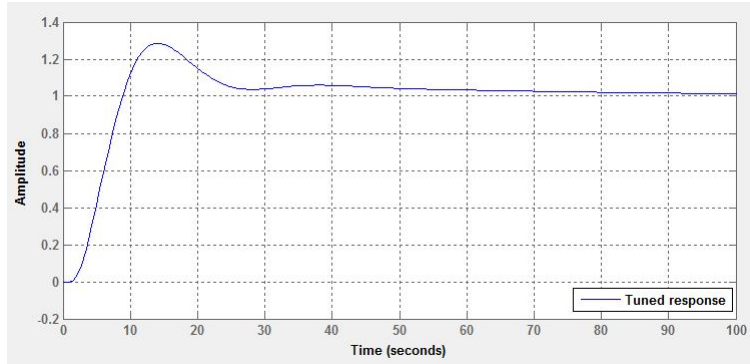


Figure 167

7.4 Re-design of the pitch from altitude (using SISO tool):

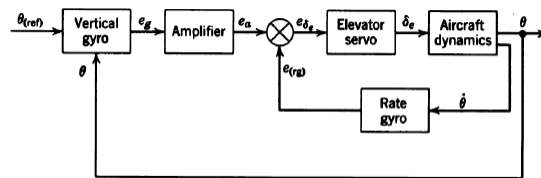


Figure 168: The displacement Autopilot using the velocity feedback

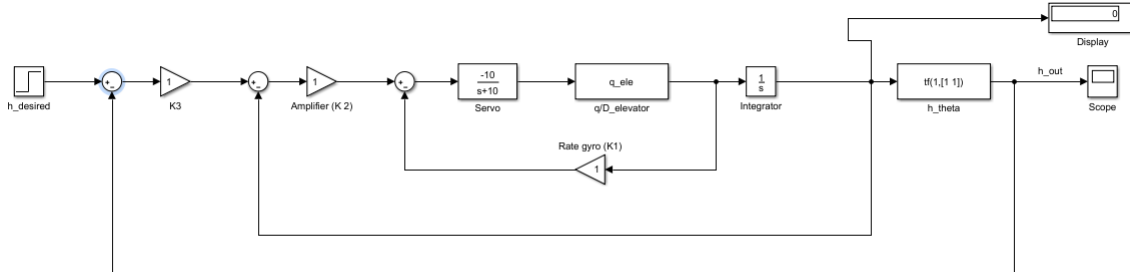


Figure 169: Simulink new full-model

$$\text{Where } \frac{h}{\theta} = \left(\frac{\dot{h}}{\delta_e} x \frac{1}{s} \right) * \left(\frac{1}{\frac{\theta}{\delta_e}} \right)$$

Where $\frac{\dot{h}}{\delta_e} = -\frac{u}{\delta_e} \sin(\theta_0) + \frac{w}{\delta_e} \cos(\theta_0) - \frac{\theta}{\delta_e} (w_0 \sin(\theta_0) + u_0 \cos(\theta_0))$, $q = \dot{\theta}$
Taking into consideration the ζ design limit mentioned before.

The inner most loop The inner most loop gain to achieve $\zeta \approx 0.96 \Rightarrow K_{inner} = 1.4204$

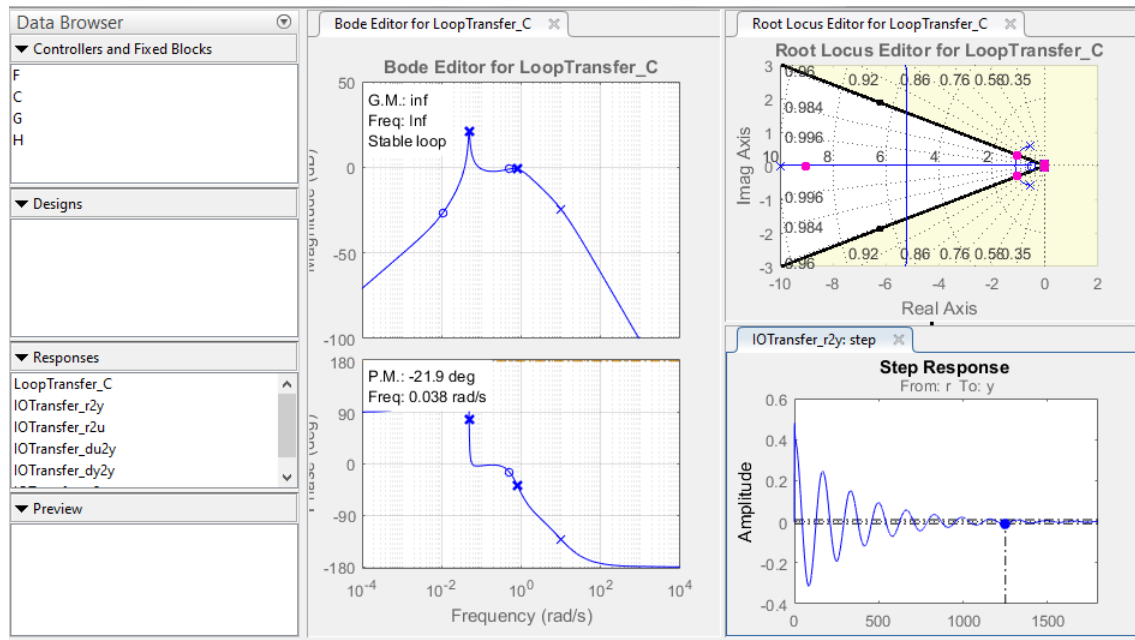


Figure 170: SISO on inner most loop

Now the open loop transfer function of the inner loop =

$$\frac{8.359 s^3 + 4.291 s^2 + 0.04465 s}{s^5 + 11.11 s^4 + 11.71 s^3 + 6.453 s^2 + 0.04727 s + 0.01547}$$

and the closed loop transfer function of the inner loop after adding the gain =

$$\frac{5.885 s^3 + 3.021 s^2 + 0.03144 s}{s^5 + 11.11 s^4 + 20.07 s^3 + 10.74 s^2 + 0.09192 s + 0.01547}$$

The second inner loop We will find that it is marginally stable as shown in the figure below:

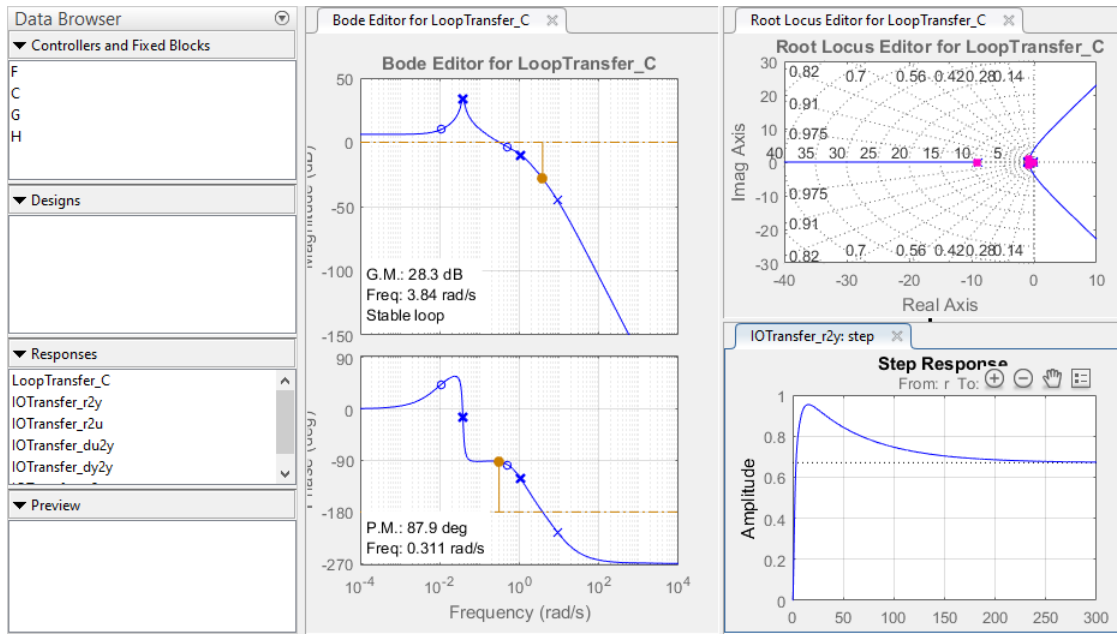


Figure 171: SISO second inner loop

Therefore, it is not enough to add a gain (to ensure stability of the next outer loop), so we have put to complex poles in the left hand sign : $(s = -19.65+10.72)$, $(s = -19.65-10.72)$

The root locus will be as shown

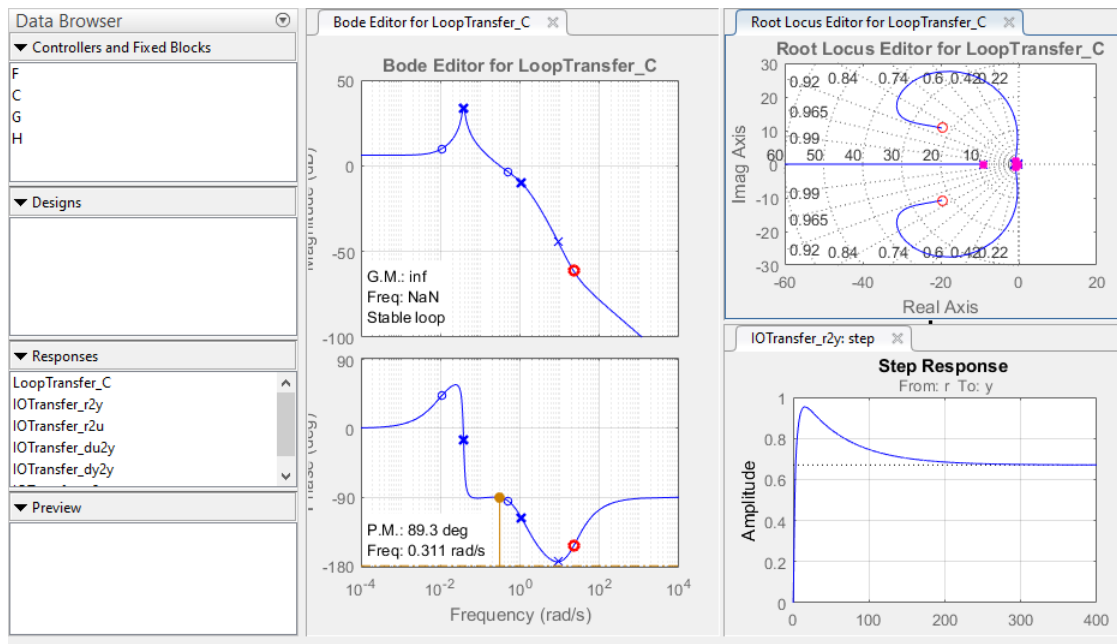


Figure 172: SISO second inner loop after adding complex zeros

, and to achieve $\zeta \approx 0.3$ we need a gain, so it will be shown below

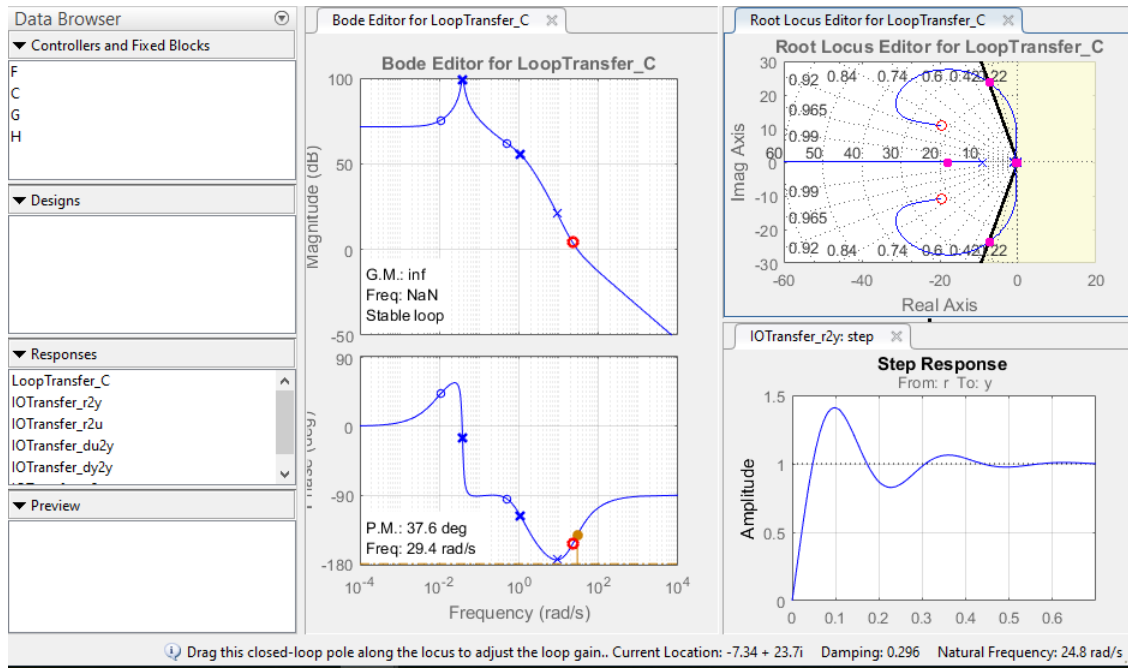


Figure 173: SISO second inner loop after adding complex zeros and gain

The effect of the two complex poles, and the added gain is as if we have added a feed back = $1870.8x(1 + 0.078s + (0.045s)^2)$ to the open-loop transfer function

finally the closed loop transfer function of this system with the new mentioned feedback will be =

$$5.885 s^2 + 3.021 s + 0.03144$$

$$-----$$

$$s^5 + 33.4 s^4 + 890.3 s^3 + 1.146e4 s^2 + 5656 s + 58.83$$

The outer loop Now, the root locus if the outer loop open loop transfer function will be as shown in figure

$$\begin{aligned} & -2235.4 s^{18} - 1.237604 s^{17} - 3.237604 s^{16} - 4.465154 s^{15} - 2.044840 s^{14} + 1.157604 s^{13} + 4.093840 s^{12} + 4.122940 s^{11} + 2.337464 s^{10} \\ & + 7705.4 s^9 + 1316.4 s^8 + 74.58 s^7 + 0.466 s^6 + 0.2558 s^5 + 0.02022 s^4 + 0.000334 s^3 + 1.078e-05 s^2 + 1.455e-07 s \\ & \dots \\ & + 4.429e-11 \\ & \dots \\ & s^{22} + 37.49 s^{21} + 1089 s^{20} + 1.324404 s^{19} + 3.187454 s^{18} + 8.122460 s^{17} + 16.313803 s^{16} + 1.097458 s^{15} + 3.777003 s^{14} \\ & + 1.613605 s^{13} - 9.947405 s^{12} - 4.137673 s^{11} - 1.053605 s^{10} - 1.154605 s^9 - 1.066 s^8 - 93.74 s^7 - 3.284 s^6 - 0.2549 s^5 \\ & - 0.000884 s^4 - 0.000387 s^3 - 0.1339e-05 s^2 - 1.3339e-06 s \end{aligned}$$

below =

it is so big because of the $\frac{h}{\theta}$ big transfer function, mentioned before.

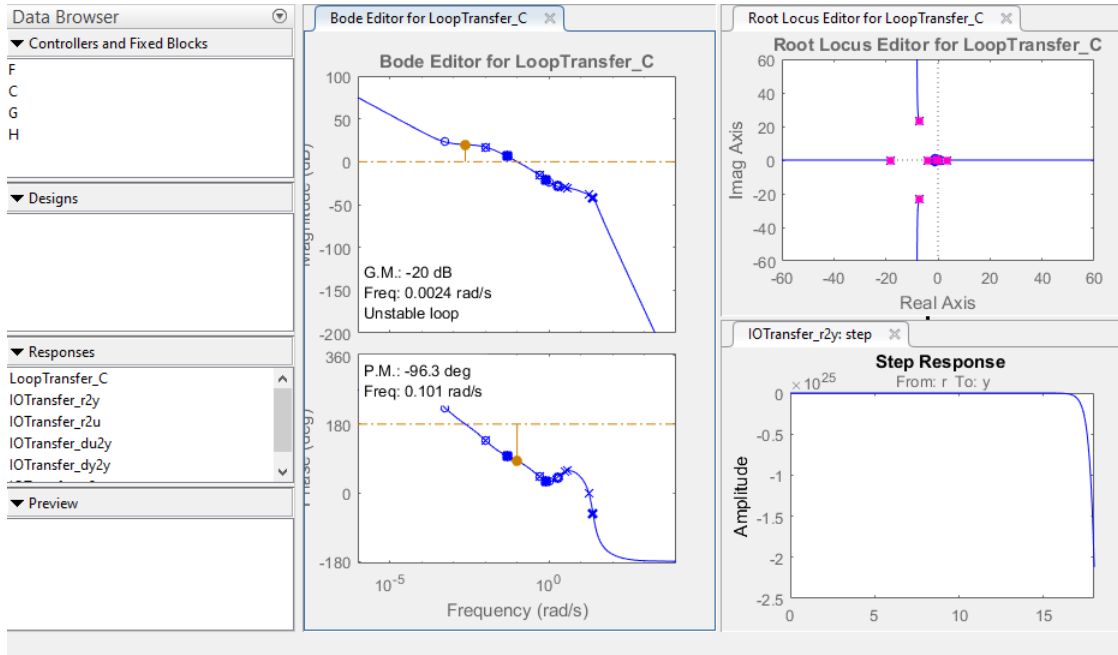


Figure 174: SISO outer open loop

it is unstable, and we couldn't control it but here is a trial, but it didn't work because I don't know how to deal with this unstable pole

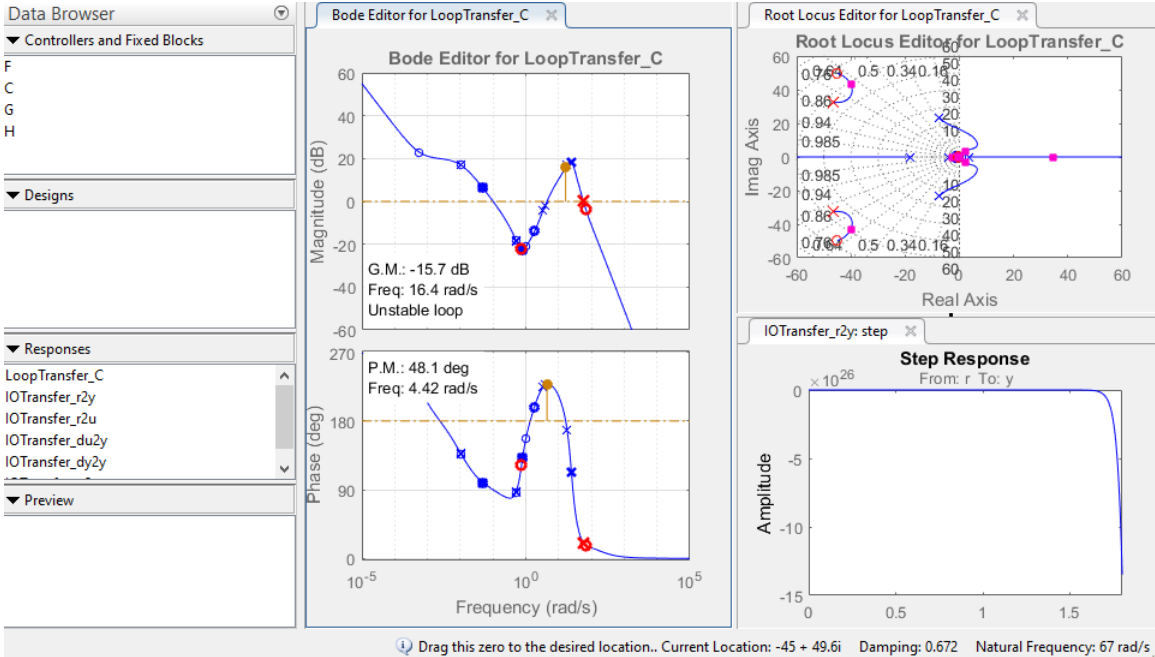


Figure 175: SISO second inner loop after adding complex zeros and gain

7.5 Implementing controller on nonlinear model

since the main used controller is a PID controller we have implement it on the 12 equation of motion using the following formula

$$\theta = K_p e(t) + K_i \int e(t) dt + K_d \frac{de}{dt}$$

The following response for u

The following response for q

The following response for h

Discretization: 1- $u/\delta t$ Controller discretization:

The controller is only a Gain with the value “ 459.79” , which is the same as in the Z-domain.

2- $q/\delta t$ Controller discretization:

The Internal loop controller is as shown below:

$$\frac{-0.009886s^2 - 8.222s - 14.21}{s^2 + 10s}$$

which is as follows, in the z-domain:

$$\frac{-0.009886z^2 - 0.5522z + 0.4723}{z^2 - 1.368z + 0.3679}$$

The outer loop, we couldn't obtain a controller for it to be discretized, the problem which prevented us was that the number of poles are more than the number of zeros.

8 References

1. Flight Stability and Automatic, Robert _ Nelson

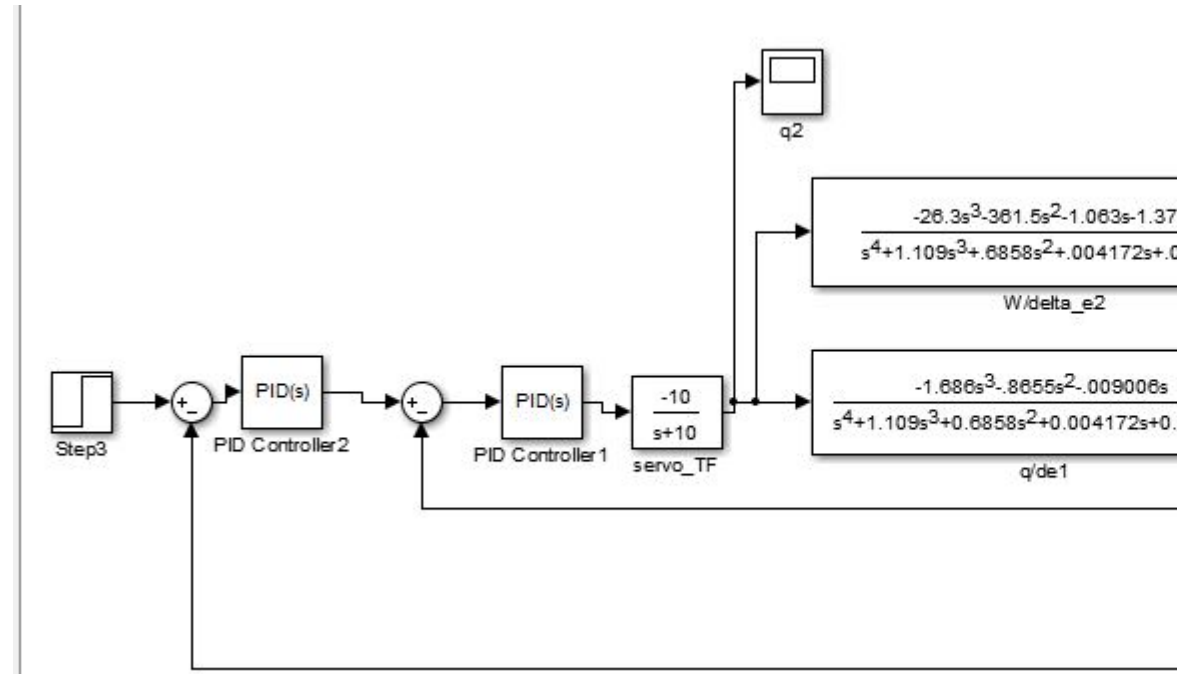


Figure 1:

Lateral Autopilot

The lateral Autopilot is divided into three Stages, because it differes from take-off to landing, ...etc.

Thus we need to implement 3 different autopilot controllers for each stage.

Level Flight:

We will implement the autopilot controller through 3 different block diagrams, one of them is longitudanl and have been implemeneted before, which is,

with the following control design loop from the lateral motion,

where we could implement the controllers above, following the design requirements of $T_s \leq 30$ for the inner loop and for $\zeta = 0.7$

with the following Transfer functions,

$$r/\delta_r = \frac{-0.6125s^3 - 0.7168s^2 - 0.1737s - 0.07785}{s^4 + 1.337s^3 + 1.379s^2 + 1.098s + 0.01332}$$

$$\phi/\delta_r = \frac{0.1784s^2 - 0.09379s - 1.683}{s^4 + 1.337s^3 + 1.379s^2 + 1.098s + 0.01332}$$

$$\phi/\delta_a = \frac{0.2113s^2 + 0.1193s + 0.2691}{s^4 + 1.337s^3 + 1.379s^2 + 1.098s + 0.01332}$$

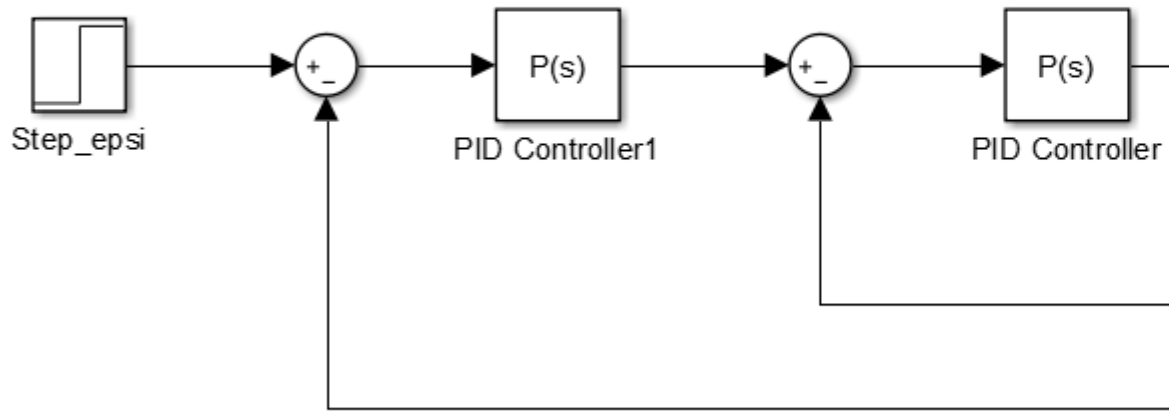
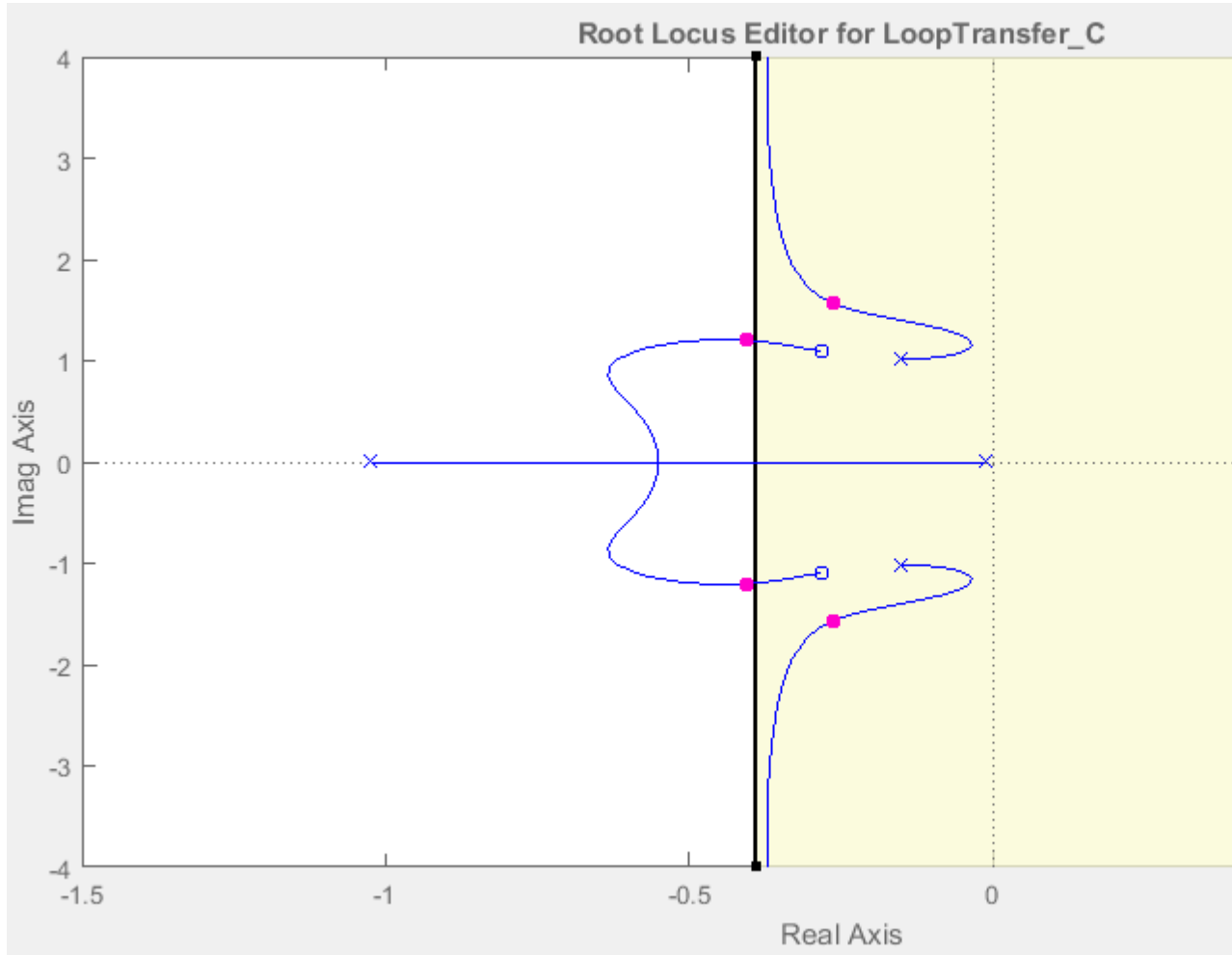
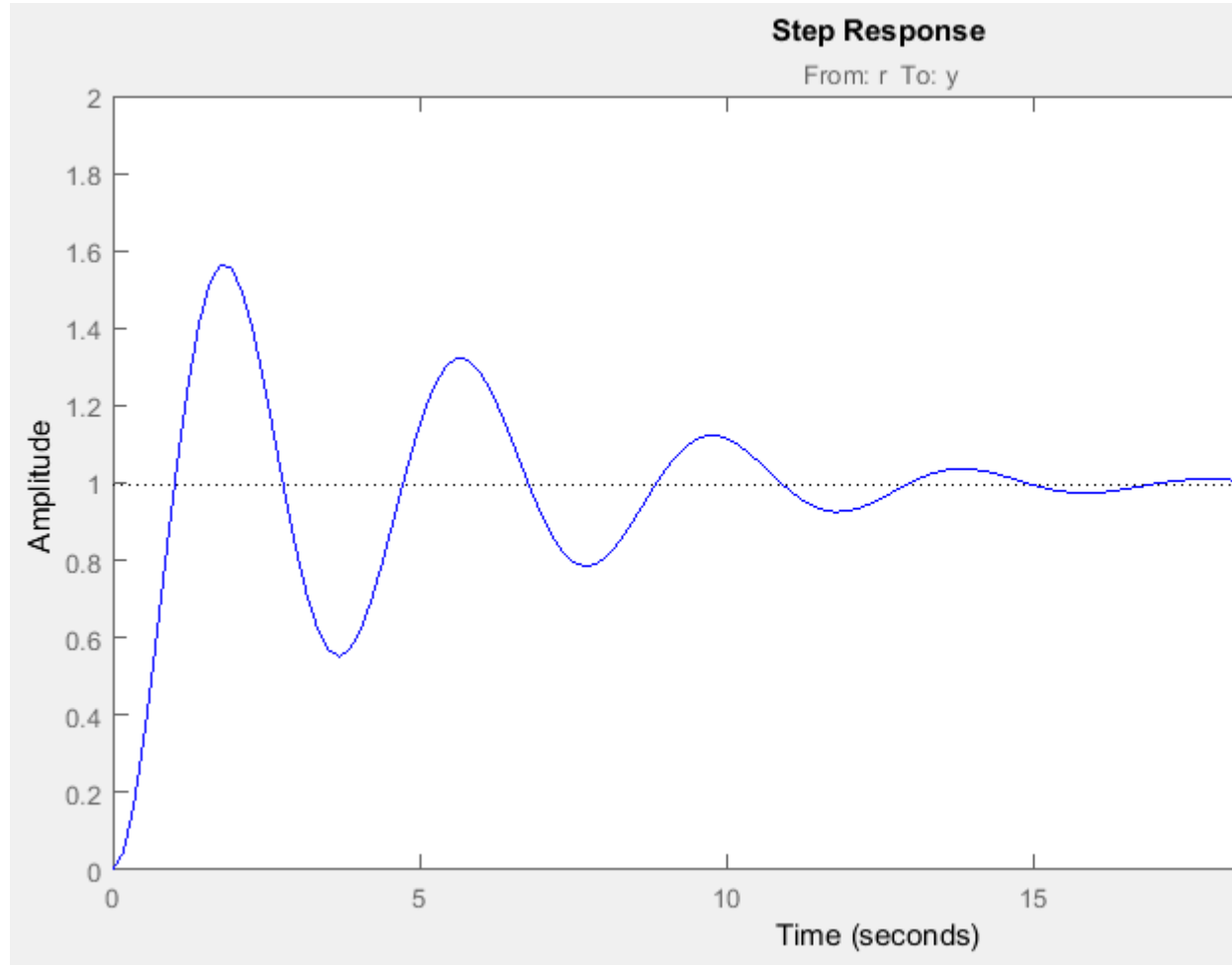


Figure 2:

For the internal loop, the root locus is as shown with $T_s \leq 30$.



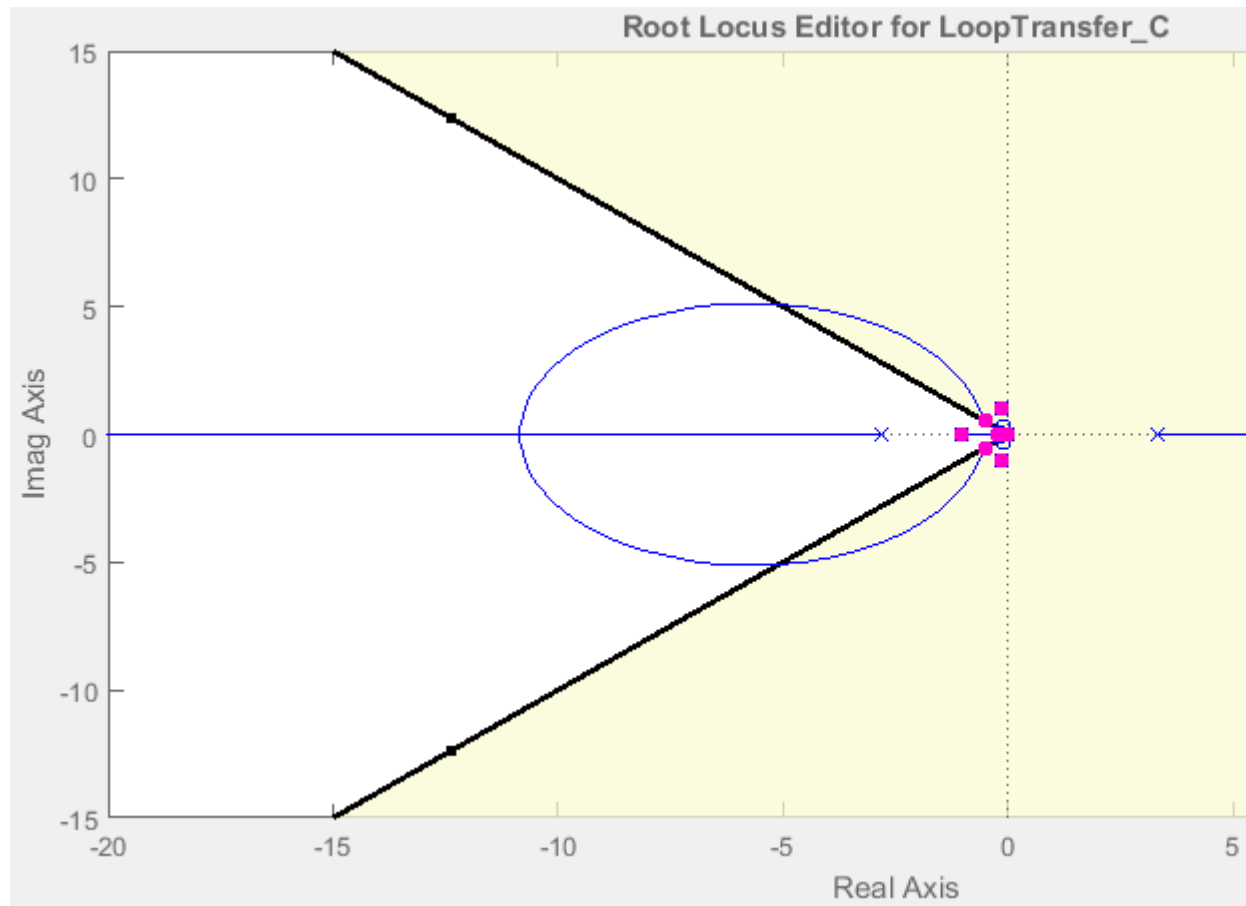
Hence, we can implement the controller, $C=15.082$, only P controller needed to give the following response,



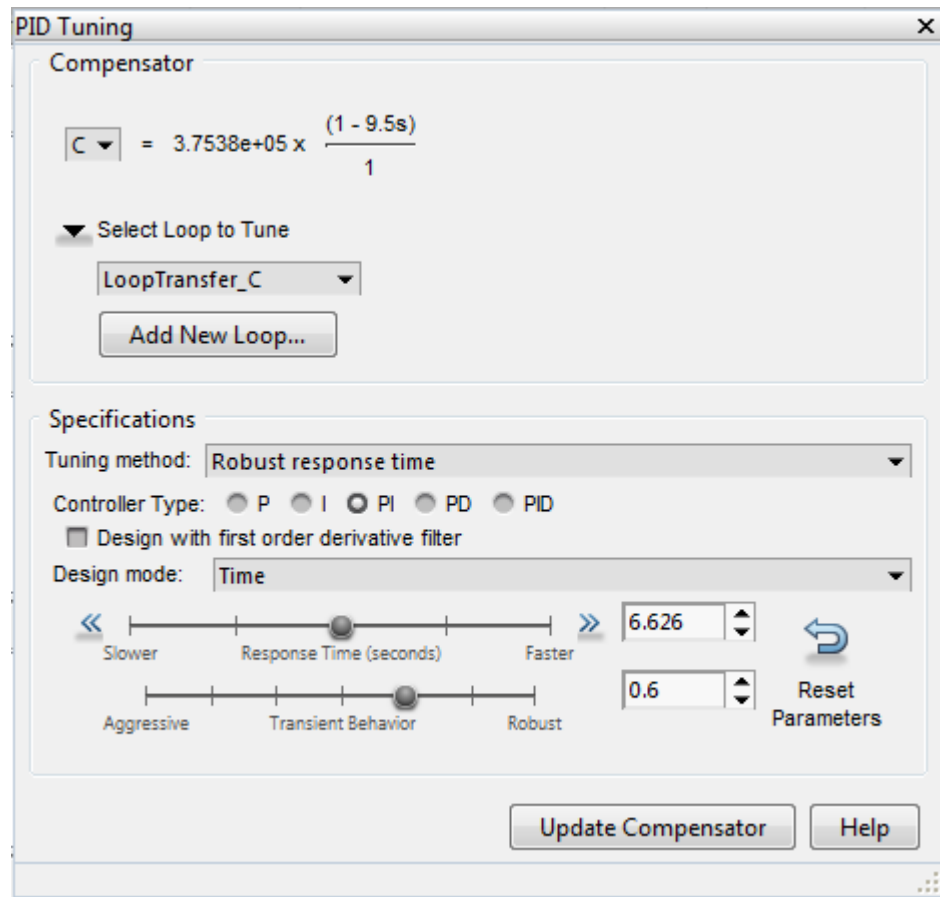
For the outer loop:

The following compensator were implemented, after so many trials and using the old compensator as a block.

implementing for $\zeta = 0.7$ the following root locus is given.



Hence, the following compensator is used,



$c = 3.7538e5 * \frac{1-9.5s}{1}$
which gives the following step response,

